1998

Identification and Characterization of Mlp1p and Mlp2p : Molecular Components of Filaments Localized at the Interface between the Nuclear Pore Complex and Nuclear Interior

Caterina Strambio-De-Castillia

Identification and Characterization of Mlp1p and Mlp2p: Molecular Components of Filaments Localized at the Interface Between the Nuclear Pore Complex and the Nuclear Interior

A thesis presented to the faculty of

The Rockefeller University

in partial fulfillment of the requirements for

the degree of Doctor of Philosophy

by

Caterina Strambio de Castillia

Acknowledgments

My deepest gratitude goes to Günter Blobel and Mike Rout for help advice and support throughout the course of this work. I am also very grateful to J. Aitchison, C. Akey, R. Beckmann, P. Bernstein, N. Bonifaci, Y. Chook, E. Coutavas, U. O'Doherty, C. Enenkel, R. Erdmann, B. Fontoura, J. Helmers, M. Hurwitz, E. Johnson, J. Kilmartin, M. Matunis, C. Nicchitta, L. Pemberton, M. Rexach, N. Schulke, S. Smith, H. Takashima and J. Waters for many helpful suggestions and discussions throughout the course of this study. I am deeply indebted to J. Aris, D. Goldfarb, E. Johnson, J. Kilmartin, M. Lewis, J. Loper, L. Pemberton, R. Schekman, M. Sogaard, J. Warner and R. Wozniak, for providing me with antibodies and other reagents without which this work would not have been possible. I thank J. Aitchison, C. Akey, R. Beckmann, Y. Chook, M. Hurwitz, E. Johnson, J. Kilmartin, J. Luban, M. Matunis, L. Pemberton, M. Rout and S. Smith for critical reading of this dissertation in whole or in part.

Thanks go to E. Sphicas and H. Shio for excellent technical assistance in the electron microscopic studies. I am very grateful to K. Levine for helpful advice in using the Coulter counter and in the analysis of the data. In addition I would like to thank F. Isdell and L. Oehlen for help in performing the FACS analyses. My sincerest thanks go to E. Ellison, H. Ijikata and Y. Oh for invaluable and skillful technical support that was essential for the completion of various parts of the work presented in this dissertation.

On a more personal level, many many thanks go to my parents Adriana Redaelli and Giovanni Strambio de Castillia for allowing me to be here in the first place, for helping me and supporting me throughout my life and for helping

me be who I am. I am also grateful to my brother Vincenzo Strambio de Castillia and to my many friends for much needed moral support, patience and friendship throughout my professional career and otherwise. In particular I would like to thank the following: Anna Redaelli, Alessandra Della Porta, Mauro Traversa, Fabio Re, Sidarta Ribeiro, Lucia and Claudio Mello, Silvia and Guillermo Cecchi, Amy and Roy Crist, Evette and Basil Ellison and Perla and Pepe Reyes.

Many thanks go to my parents, my mother in law, Shirley Luban, Lucia Mello and the skillful and caring staff of the Yellow room at The Rockefeller University Child and Family Center, Daril Browning, Alice Cruz, Dawn Foster and Carol Zeavin, for helping me taking care of my daughter and thereby allowing me to be a productive working-mother. In particular millions of thanks to Ursula and Perla Gonzales for giving Maria so much love and attention in the past few months and therefore allowing me the pace of mind necessary for the final efforts towards the completion of this dissertation.

All my gratitude of course to my husband, Jeremy Luban for all his love and support in bad as well as in good times. Finally, I am also very grateful to my daughter, Maria Luban for allowing to keep my feet on the ground and always remember what is "really important" and for giving me much unconditional love and a lot of happy moments.

Table Of Contents

List Of Figures

Tables

Abbreviations

CM	Crude Microsome
CSR	Central Spoke Ring
ECL	Enhanced Chemiluminescence
EM	Electron Microscopy
ER	Endoplasmic Reticulum
GFP	Green Fluorescent Protein
gpαF	glycosylated pro-α-Factor
H-NE	Heparin-extracted NE
HAT	Hypoxanthine, Aminopterin, Thymidine
HRP	Horse Radish Peroxydase
IEM	Immuno Electron Microscopy
IF	Immunofluorescence
INM	Inner Nuclear Membrane
ISR	Inner Spoke Ring
LSR	Lumenal Spoke Ring
mAb	Monoclonal Antibody
MLP	Myosin Like Protein
MPF	Matrix Protein Filament
MT	Microtubules
NE	Nuclear Envelope
NES	Nuclear Export Sequence
NL	Nuclear Lamina
NLS	Nuclear Localization Signal

NM	Nuclear Matrix
NPC	Nuclear Pore Complex
NUP	Nucleoporin
ONM	Outer Nuclear Membrane
ORF	Open Reading Frame
PAGE	Polyacrylamide gel electrophoresis
PEG	Polyethylene glycol
POM	Pore Membrane Protein
ppαF	prepro-α-Factor
PVP	Polyvinylpyrrolidone
SPB	Spindle Pole Body

Abstract

In eukaryotic cells the segregation of the genome in a closed organelle requires an efficient mechanism to ensure the constant exchange of material between the nucleus and the cytoplasm. Nuclear pore complexes (NPCs) provide the only known sites for exchange of material across the nuclear envelope (NE). A wealth of evidence has accumulated throughout the years that strongly suggest that the NPCs are structurally linked to the nuclear interior. It has long been proposed that this structural continuity is essential for the efficient exchange of material between the nuclear interior and the cytoplasm. Unfortunately, the understanding of the molecular basis of such functional and structural connections has lagged behind. This dissertation describes a combined biochemical and immunological approach aimed at the identification of novel yeast proteins that could be involved in providing such link. The first step of this approach was the development of a large scale enrichment procedure to prepare yeast nuclear envelopes (NEs). These NEs can be stripped of peripheral proteins to produce a heparin-extracted NE (H-NE) fraction highly enriched in integral membrane proteins. Extraction of H-NEs with detergents revealed previously uncharacterized ring structures associated with the NE that apparently stabilize the grommets of the nuclear pore complexes (NPCs). The high yields obtained throughout the fractionation procedure allowed balance-sheet tabulation of the subcellular distribution of various NE and non-NE associated proteins. As the second step of the approach described here, three different highly enriched NE-derived fractions were used to generate a panel of 114 monoclonal antibodies (mAbs) against NE-associated antigens. Finally, this panel of anti-NE mAbs were subjected to a novel NPC-clustering

screen aimed at the identification of NE-associated antigens that were only peripherally associated with the NPC. Two mAbs were isolated using this screen (MAb148G11 and MAb215B9). Both of these mAbs were found to recognize the same ~220 kD protein (p220) on immunoblots of highly enriched NE fractions. The gene encoding p220 was cloned and was found to be the previously identified gene of unknown function, *MLP1*. Disruptions of *MLP1* and its homologue *MLP2* (the uncharacterized yeast ORF, YIL149C), were found to be non lethal either separately or in combination. Though both Mlp1p and Mlp2p largely cofractionated with isolated NEs, neither cofractionated with isolated NPCs. Ultrastructural localization demonstrated that both Mlp1p and Mlp2p are localized to filaments that appear to connect the NPC to the nuclear interior. Functional studies performed using yeast strains harboring a double deletion of *MLP1* and *MLP2* suggested that these proteins could be involved in facilitating nuclear import and led to the proposal of a model for the possible role of these proteins in nuclear transport.

Chapter I: Introduction

The Structure and Function of the NE

The presence of a cell nucleus is a characteristic of eukaryotic cells and its development may represent one of the essential steps that allowed the progression from unicellular organisms to more complex life forms.

The nuclear envelope (NE; see list of Abbreviations) is a complex membrane system that defines the boundary between the nucleus and the cytoplasm. The NE is involved in several important functions. They include transport of both small molecules and macromolecules between the cytoplasm and the nucleus, nuclear division, maintenance of the nuclear architecture, higher level chromosome organization both during interphase and at mitosis, regulation of gene expression, and RNA processing.

The NE is composed of two distinct but continuous membranes enclosing a lumenal (perinuclear) space. Towards the cytoplasm is the outer nuclear membrane (ONM) which is continuous with the endoplasmic reticulum (ER) membranes and is thought to perform rough ER functions (Fawcett, 1966; Baba and Osumi, 1987; Preuss, et al., 1991). Facing the nucleoplasm is the inner nuclear membrane (INM), which contains distinct protein components that are not present in the ER.

In higher eukaryotes, the INM is often lined by a filamentous network called the nuclear lamina (NL) (Gerace, et al., 1978; for a review see, Moir, et al., 1995). The NL is thought to provide structural stability to the NE and it may also be essential for the maintenance of the internal nuclear architecture and as an anchoring site for the interphase chromosomes. The NL has also been

implicated in the regulation of various nuclear processes such as DNA replication (Goldberg, et al., 1995; Spann, et al., 1997). In vertebrates the NL consists primarily of intermediate filaments-type proteins called the lamins. The lamins can be classified into A and B subgroups based on their primary sequence and their biochemical properties, and four lamins (A, B1, B2 and C) are commonly found in mammalian somatic cells. Lamins A and B are attached to the INM with the help of an isoprenyl anchor (Beck, et al., 1988) and via the interaction with various integral membrane proteins that include p58 \ lamin-B receptor (LBR; Worman, et al., 1988; Worman, et al., 1990), the lamina associated polypeptides (LAPs) 1 and 2 (Senior and Gerace, 1988; Foisner and Gerace, 1993), and a recently identified protein of 18 kD that is part of the LBR complex (Simos, et al., 1996).

The INM and the ONM join to form specialized circular apertures of ~100 nm diameter containing the nuclear pore complexes (NPCs). The latter are macromolecular structures with a mass of ~125 $x10^6$ D in vertebrates (Reichelt, et al., 1990) and ~66 $x10^6$ D in yeast (Rout and Blobel, 1993; Yang, et al., 1998) that regulate the exchange of material between the nucleus and cytoplasm. Metabolites, ions and small macromolecules (relative molecular mass less than 40 kD) can passively diffuse through aqueous channels of 9 nm in the NPC. In contrast, large macromolecular particles with a diameter of up to 25-28 nm are selectively transported to and from the nucleus across the NPC via a highly regulated energy-dependent process (see below).

An important property of the NE of higher eukaryotes that is not shared by the budding yeast is that it disassembles early in mitosis to allow the chromosomes to interact with the cytoplasmic spindle and it reassembles to form a new cell nucleus in each of the two daughter cells at the end of cell division (see Marshall and Wilson, 1997, and references therein). The initial

event that takes place during late prophase is the fragmentation of the NE into small vesicles. The NL depolymerizes yielding soluble lamin A/C monomers or dimers and NE vesicle-associated B-type lamins (Gerace and Blobel, 1980). The NPCs are also dismantled at this time and many of its components sever their association with the pore membrane. The sequence of events that accompanies NE re-assembly is more controversial. It is clear that vesicles need to associate with the surface of late anaphase chromosomes and to fuse laterally to give rise to a continuous NE. In addition, NPCs need to reassemble and the NL has to reform underneath the INM. The controversy lies in the order in which these events occur, and the two main models that have been proposed differ in the role that each ascribes to the lamins in the interaction of chromatin and the vesicles that will give rise to the reformed NE.

There is now a general consensus that protein phosphorylation constitutes the major regulatory element of nuclear breakdown in mitosis. The cyclin B dependent mitotic kinase $p34^{cdc2}$ is directly responsible for many of the phosphorylation events, but other kinases may also contribute (Nigg, 1993; Pfaller and Newport, 1995). Hyperphosphorylation at mitosis-specific sites causes the lamin to depolymerize (for a review see, Moir, et al., 1995). Moreover, it appears that the interaction of the lamina with the INM is also regulated by phosphorylation of the proteins that have been implicated in anchoring it to the nuclear membrane (see above). The NPCs are also believed to disassemble in response to mitosis-specific phosphorylation of individual nucleoporins by $p34^{cdc2}$. The cell-cycle dependent phosphorylation of several nucleoporins including Nup98, gp210, Nup153, Nup214/CAN and Nup358 has recently been established experimentally (Macaulay, et al., 1995; Favreau, et al., 1996). The mechanism of disassembly of the nuclear membrane may be more complex. It is certain that the phosphorylation of NE components by

$p34^{cdc2}$ may not be sufficient to achieve complete breakdown and that additional kinases and cytoplasmic factors might be required (Newport and Spann, 1987; Peter, et al., 1990).

The NE in Budding Yeast

Generally, the yeast *Saccharomyces* represents a particularly advantageous experimental system for the study of complex cellular events because of the powerful genetics techniques that are available to study the *in vivo* properties of gene products of interest. It is widely accepted that many of the NE functions are conserved between higher and lower eukaryotes suggesting that the key components of these processes are also evolutionary conserved. Nevertheless, the budding yeast *Saccharomyces* presents some unique features that are not shared by higher eukaryotic cells.

Arguably, the most striking difference concerning NE biology is that the members of the yeast genus *Saccharomyces* divide by budding and undergo what is called a "closed mitotic division". As demonstrated by electron microscopic (EM) analysis and subsequently confirmed by indirect immunofluorescence (Robinow and Marak, 1966; Davis and Fink, 1990), the yeast NE does not break down during mitosis. At the beginning of the cell cycle, a bud starts forming on the parental cell and as it grows the NE invades it as a long narrow structure. The intrusion of the NE into the bud is closely followed by chromatin migration, and soon after that the nucleus divides in two daughter nuclei. After karyokinesis, cytokinesis quickly ensues.

In budding yeast, the microtubules (MTs) that constitute the mitotic spindle emanate from two dense plaques, the spindle pole bodies (SPBs), which are

embedded in the NE and are analogous to the centrosomes of animal cells (for reviews see, Masuda, 1994; Snyder, 1994; Marschall and Stearns, 1997). The SPB duplicates at the beginning of the cell cycle and initially the two SPBs remain juxtaposed in the plane of the NE and connected by a bridge structure. Later, the spindle MTs start to assemble at each of the two SPBs. When the two half spindles interdigitate, the bundle of polar MTs starts elongating and pushes the two SPBs further apart from each other. Two other types of MTs are also formed at the SPB giving the spindle its final organization. They are: 1) chromosomal MTs that interact with each of the chromosomes at the centromeres; and 2) astral MTs that arise from the outer surface of the SPB and project into the cytoplasm. While the chromosomal MTs are responsible for the accurate segregation of the pairs of sister chromatids to the opposite poles of the nucleus, the astral MTs appear to have a role in the migration of the dividing nucleus to the neck of the nascent bud and in its appropriate positioning relative to the plane of cytokinesis. SPB duplication is believed to be an important "check-point" in the process of cell division and some mutants blocked in SPB replication are unable to form a bud. It is worth noting that the SPB also has an essential role in the process of karyogamy that takes place during mating.

Several SPB molecular components have been recently identified using a variety of methods including genetic screenings that looked for cell division or karyogamy mutants, and biochemical approaches that entailed the partial purification of yeast SPBs and the generation of monoclonal antibodies (mAbs) to the protein constituents of the enriched fraction (reviewed in, Kilmartin, 1994). Particularly interesting is the identification of a mutant blocked in SPB duplication called *ndc1* (Goh and Kilmartin, 1993; Winey, et al., 1993). Isolation and analysis of the *NDC1* gene has revealed a gene product of 74 kD. Antibody staining locate the Ndc1p protein at the nuclear periphery in

association with both SBPs and NPCs (M. Winey and M. P. Rout, personal communication). It is possible that Ndc1p is a novel constituent of the NE that is involved in the insertion of both nascent SPBs and NPCs in the NE.

A second important peculiarity of the yeast system is that no NL has been found in this system. The presence of a NL in yeast was suggested by a variety of morphological, biochemical (Allen and Douglas, 1989) and immunological studies (Georgatos, et al., 1989), but so far none of the proteins that were initially identified as putative yeast lamins homologues have been further characterized. With the completion of the *Saccharomyces cerevisiae* sequencing project (Clayton, et al., 1997 and references therein), the existence of a lamin in yeast has been brought into further question since no putative homologues of the lamin proteins have been found in this organism.

NPC: Structure, Molecular Composition and Dynamics

NPCs provide the only known port for the exchange of material across the NE. The three-dimensional structure of the vertebrate NPC has been elucidated using a variety of EM techniques (Unwin and Milligan, 1982; Hinshaw, et al., 1992; Akey and Radermacher, 1993). The favored source of NPCs for these analyses has been amphibian oocytes but many aspects of the structure appear to be conserved in other vertebrates. These studies have provided a low resolution model (6-10 nm) for the architecture of the transport machinery. The membrane spanning portion of the NPC consists primarily of a cylindrical assembly of eight identical spoke structures symmetrically arranged around an 8-fold axis. The spokes form three concentric rings called the inner spoke ring (ISR), the central spoke ring (CSR) and the lumenal spoke ring

(LSR). The ISR encircles a central channel complex called "transporter" or "plug" that is believed to be the primary site for active transport (Akey and Radermacher, 1993). The LSR penetrates into the lumen of the NE and is therefore presumed to have transmembrane components that help anchor the NPC to the pore membrane. On both cytoplasmic and nuclear sides of the spoke ring assembly are two peripheral annular structures that are similar but not identical to each other and are called the cytoplasmic and nuclear rings. The cytoplasmic ring serves as the attachment site for eight cytoplasmic particles each of which is connected to a cytoplasmic filament that extends at least 30-50 nm into the cytosol. The nuclear ring is connected to eight fibers ~75-100 nm long that are joined at the terminal end by a smaller ring to form a structure called the nuclear "basket", "cage" or "fishtrap" (Ris, 1989; Jarnik and Aebi, 1991; Ris, 1991; Goldberg and Allen, 1992).

Both nuclear import and export utilize the central NPC transporter (Feldherr, et al., 1984; Dworetzky and Feldherr, 1988; Akey and Goldfarb, 1989). The currently available images of the transporter suggest that it is a hour-glass shaped gated structure (Akey, 1990; Akey and Radermacher, 1993; Goldberg and Allen, 1996). Ultrastructural studies of Balbiani ring mRNPs caught traversing the NPC suggest that the transporter provides a channel that can stretch to a 26 nm diameter and is 50-60 nm long (Stevens and Swift, 1966; Feldherr, et al., 1984; Kiseleva, et al., 1998). Recently, Feldherr and Akin (Feldherr and Akin, 1997) followed the passive diffusion of PEG-coated gold particles that lacked a specific targeting signal after microinjection into the nucleus or the cytoplasm of *Xenopus* oocytes. This study concluded that the transporter contains a single barrier that blocks the free diffusion of macromolecules in and out of the nucleus (i.e. a single gate) and that this

diffusion barrier is located in the middle of the NPC parallel to the mid-plane of the NE.

The NPCs of *Saccharomyces* share many common features with their vertebrates counterparts. However they are significantly smaller both in mass and in volume than the NPCs found in vertebrates (see above). The recent elucidation of the low-resolution three-dimensional structure of isolated NPCs from yeast has helped clarify the level of evolutionary conservation of this multi-molecular complex between distantly related species with important functional implications (Yang, et al., 1998). The most important conclusion of this study is that the difference in size and mass of the NPC between yeast and vertebrates can be accounted for by a concomitant simplification of the structure. In substance the yeast NPC appears to comprise only the central core of the vertebrate NPC and lacks many of the peripheral attachments including the LSR, the nuclear ring and the cytoplasmic ring with its attached cytoplasmic particles. Interestingly, the cytoplasmic fibers and nuclear basket appear to be conserved but are anchored to more central domains of the spoke-ring assembly. Consistent with a general reduction in size, the central transporter is also smaller and appears to be missing a central cylinder that gave the vertebrate transporter its hour-glass shape. The results of this study suggest that the yeast NPC are likely to have retained or recapitulated the features that characterize what a "minimal" functioning NPC should look like. Accordingly, the yeast NPC is able to ensure efficient exchange of material between the nucleus and the cytoplasm but lacks higher order structures necessary in multi-cellular organisms.

Approximately 30 proteins are estimated to constitute the NPC as inferred from studies of highly enriched yeast and mammalian pore preparations (Rout and Blobel, 1993; M. J. Matunis and G. Blobel, personal communication). A

variety of immunological, biochemical and genetic techniques have been successfully employed in the past few years to identify NPC-specific proteins (nucleoporins). The criteria commonly used to demonstrate that a novel protein is a *bona fide* nucleoporin are the following: 1) the protein must immunolocalize to the NPC by IF microscopy or better by immunoelectron microscopy (IEM); 2) the protein has to cofractionate with the NPC in subcellular fractionation procedures; 3) the proteins should interact genetically and or biochemically with other known nucleoporins; and 4) the polypeptide sequence of the protein might be similar to the sequence of other NPC constituents. To date ~30 yeast proteins and 15 vertebrate proteins have been identified that meet at least two of the above mentioned criteria for a nucleoporin (reviewed in, Rout and Wente, 1994; Bastos, et al., 1995; Doye and Hurt, 1997; Fabre and Hurt, 1997). Most nucleoporins are unrelated to non-NPC polypeptides in the databases. Nevertheless, a large number of yeast and vertebrate nucleoporins contains at least one region with characteristic repeat motifs that end in the dipeptide FG (reviewed in, Rout and Wente, 1994). There are at least three general types of repeat motifs regions that are generally referred to by the consensus sequence of the core of the repeat. These are the tetrapeptides GLFG (single letter AA code for gly-leu-phe-gly) and FXFG (single letter AA code for phe-any AA-phe-gly) and a third class containing a variety of different tetrapeptides such as PAFG (single letter AA code for pro-ala-phe-gly), SAFG (single letter AA code for ser-ala-phe-gly) or PASG (single letter AA code for pro-ala-ser-gly) commonly referred to as FG repeats. The spacer sequences between the FXFG and the FG repeats are generally highly charged and rich in serine and threonine residues. The GLFG spacers are generally devoid of acidic residues and have a prevalence of asparagine and glutamine residues. Most of the repeat containing nucleporins are believed to play a direct role in the nuclear

transport mechanism and indeed sequences containing these motifs have been found to directly interact with soluble transport factors (see below; Belanger, et al., 1994; Kraemer, et al., 1995; Moroianu, et al., 1995; Radu, et al., 1995; Aitchison, et al., 1996; Pemberton, et al., 1997; Rosenblum, et al., 1997; Rout, et al., 1997). In vertebrates, many of the repeat containing nucleoporins also contain numerous sites for the post-translational cytosolic addition of O-linked N-acetylglucosamine (GlcNAc) residues but the functional significance of this modification is presently not known (Holt, et al., 1987). Similarly unknown is whether yeast has similar modifications. Another common feature of nucleoporins is the presence of coiled-coil domains which may be involved in the homo- or hetero-polymerization of the protein (Buss and Stewart, 1995; Grandi, et al., 1995; Grandi, et al., 1995; Hu, et al., 1996). Some nucleoporins also exhibit other conserved structural elements such as cysteine-rich zinc-fingers thought to promote protein-nucleic acid or protein-protein interactions [for example vertebrate Nup153 and Nup 358 (Sukegawa and Blobel, 1993; Wu, et al., 1995; Yokoyama, et al., 1995)]; Ran binding sites thought to have a role in nuclear transport [for example Nup358 and yeast Nup36p and Nup2p (Loeb, et al., 1993; Dingwall, et al., 1995; Wu, et al., 1995; Yokoyama, et al., 1995; Nehrbass and Blobel, 1996); see below]; octapeptide motifs also found in RNA-binding proteins [for example yeast Nup100p, Nup116p and Nup145p (Fabre, et al., 1994)]; and leucine-rich regions thought to be responsible for protein-protein interactions [for example, vertebrate Nup358, Nup107 and Nup214/CAN (Kraemer, et al., 1994; Radu, et al., 1994; Wu, et al., 1995; Yokoyama, et al., 1995)]. In addition, Nup358 also contains a domain homologous to the prolyl-isomerase Cyclophilin A whose functional significance is not clear (Wu, et al., 1995; Yokoyama, et al., 1995).

The presence of distinct structural elements within the NPC architecture suggest the existence of defined NPC subcomplexes. Some of these subcomplexes have been identified and have shed considerable light on the functional organization of the NPC. The first of such subcomplexes to be identified was the vertebrate p62-complex (Guan, et al., 1995; Hu, et al., 1996; and references therein). This complex is composed of the repeat containing nucleoporins p62, p58 and p54 (in rat this complex contains also p45 which is absent in *Xenopus*) that interact with each other via their carboxy-terminal coiled-coil domains (Buss and Stewart, 1995; Hu, et al., 1996). The p62-complex is localized on both faces of the NPC at or near the center of the central transporter. Recently the biochemical interaction of p62 with a variety of soluble transport factors via its repeat-containing domain has been established experimentally (Paschal and Gerace, 1995; Percipalle, et al., 1997; Yaseen and Blobel, 1997). These observations, together with the results of *in vitro* functional studies (Finlay and Forbes, 1990; Finlay, et al., 1991), suggest a role in the recognition or the translocation of the transport substrates (see below). Interestingly, an analogous complex may exist in yeast. This complex includes Nsp1p (Hurt, 1988; Nehrbass, et al., 1990) which shares AA sequence similarity with p62 and is generally thought to be its homologue and two additional repeats-containing nucleoporins Nup57p (similar to p58; Grandi, et al., 1995) and Nup49p (similar to p54/p45; Wente, et al., 1992; Wimmer, et al., 1992). As with their vertebrate counterparts, these proteins also have a bipartite structure with a repeats-containing region at or near the amino-terminus that interacts with various known transport factors and a coiled-coil domain at the carboxy-terminus that is responsible for the formation of the complex (Grandi, et al., 1993; Grandi, et al., 1995; Schlaich, et al., 1997). Similarly to p62, Nsp1p has also been localized to both sides of the NPC (Nehrbass, et al., 1990). In

addition, *in vivo* functional data obtained with mutant forms of these proteins confirm the possibility of a direct involvement of Nup49p and Nsp1p in transport across the NPC (Mutvei, et al., 1992; Nehrbass, et al., 1993; Doye, et al., 1994). Taken together these results argue that the p62(Nsp1p)-complex represent a highly conserved subcomplex of the NPC that is most likely involved in the essential function of regulating or directly facilitating active nucleocytoplasmic transport.

Among the nucleoporins that do not contain obvious repeat sequences, Nic96p, Nup157p, Nup170p, Nup188p, Nup192p and the pore membrane protein Pom152p, are the most abundant constituents of biochemically isolated NPCs and are estimated to comprise ~25% of the total mass of the NPC (Aitchison, et al., 1995). Three of these proteins, Nic96p, Nup188p and Pom152p interact both biochemically and genetically (Aitchison, et al., 1995; Nehrbass, et al., 1996; Zabel, et al., 1996). Of these proteins, Nup188p and Pom152p have been localized in close proximity to the middle plane of the NPC (Wozniak, et al., 1994; Nehrbass, et al., 1996). Furthermore, Pom152p interacts genetically with both Nup170p and Nup157p (Aitchison, et al., 1995). These findings taken together with the NE and NPCs structural abnormalities observed in mutant strains of *NIC96* and *NUP188* , have led to the suggestion that these nucleoporins may be part of the structural core of the NPC (Nehrbass, et al., 1996; Zabel, et al., 1996). The observation that Nic96p is found in association with components of the Nsp1p-complex (see above) and that Nup170p binds the repeat-containing nucleoporin Nup1p (Grandi, et al., 1993; Grandi, et al., 1995; Kenna, et al., 1996), further implies that the NPC-core structure may provide a framework on which to anchor and correctly position more peripherally located nucleoporins involved in transport processes. Extending the analogy between yeast and vertebrates, the *Xenopus* homologue of Nic96p

has been recently isolated and it has been found to interact with p62 (Grandi, et al., 1997).

Yeast strains harboring mutant versions of many nucleoporins exhibit various NE alterations such as clustered NPCs and NE seals over the NPCs in addition to other pleiotropic defects connected to nuclear and nucleolar organization (for reviews see, Doye and Hurt, 1995; Wente, et al., 1998). Strikingly, all of the nucleoporin mutant strains that are characterized by NPC-clustering also accumulate mRNA in the nucleus *in vivo* suggesting a possible role of these nucleoporins in nuclear export of mRNA (Doye, et al., 1994; Fabre, et al., 1994; Wente and Blobel, 1994; Aitchison, et al., 1995; Gorsch, et al., 1995; Li, et al., 1995; Pemberton, et al., 1995; Del Priore, et al., 1996; Goldstein, et al., 1996; Murphy, et al., 1996). Interestingly, several of these nucleoporins (Nup84p, Nup85p, Nup120p and the carboxy-terminal domain of Nup145p) have been recently found to form a stable biochemical complex that also contains Sec13p and its homologue Seh1p (Siniossoglou, et al., 1996; E. Fabre and E. Hurt, personal communication). Furthermore, other nucleoporins exhibiting the dual mRNA export / NPC clustering phenotype are known to interact either functionally or directly with one or more of the Nup84p-complex (Heath, et al., 1995; L. Pemberton, personal communication). The functional significance of this dual phenotype is not known. However the interaction of factors involved in membrane biogenesis and vesicular transport such as Sec13p and Seh1p, with nucleoporins that appear to be responsible for NE organization is extremely provocative. Furthermore, it is worth noting that all of the only two yeast nucleoporins functionally involved in mRNA export that have been ultralocalized to date are associated with the cytoplasmic fibers projecting from the NPC (Kraemer, et al., 1995; Hurwitz, 1997). This has led to the proposal that the cytoplasmic fibers may be involved in clearing the export

substrates *en route* to the cytoplasm from the vicinity of the pore (Hurwitz, 1997).

Another stable NPC-subcomplex has been found only in vertebrates and has no counterpart in yeast. This complex comprises a component of the NPC cytoplasmic filaments Nup214/CAN and Nup88 but does not contain the other known cytoplasmically exposed vertebrate nucleoporin Nup358 (Fornerod, et al., 1997). Interestingly, the complete yeast genome does not appear to contain any sequences that resemble Nup88 suggesting that this protein could be a component of structures of the vertebrate NPC that are not conserved in yeast, such as the vertical domains of the spoke-ring assembly or the cytoplasmic ring and particles (Yang, et al., 1998; see also above).

Heterogeneity in NPC spatial distribution on the surface of the NE has been observed both in wild type yeast and higher eukaryotes cells and appears to depend upon the cell cycle, a variety of growth conditions and the state of transcriptional activation of specific domains of the genome (Franke and Scheer, 1974, and references therein; Winey, et al., 1997). In addition, recent *in vivo* studies that employed green fluorescent protein (GFP)-labeled nucleoporins in combination with mating assays, have confirmed that NPCs are highly dynamic structures capable of freely moving around in the plane of the NE to form NPC-clusters or to disrupt them upon induction of wild type nucleoporins (Belgareh and Doye, 1997; Bucci and Wente, 1997). NPCs in all cell types have to be inserted in the plane of the NE upon their *de novo* biogenesis. Furthermore in cells with open mitosis (see above), NPCs have also to undergo multiple rounds of disassembly, reassembly and insertion in the NE. Recent advances in the elucidation of the mechanisms of NPC reassembly and insertion after mitosis have been obtained by use of *in vitro* nuclear reconstitution systems derived from amphibian oocytes cell-free extracts.

Multiple steps in the assembly process could be distinguished and ordered on the basis of their differential sensitivity to a variety of known assembly inhibitors opening the road to the biochemical dissection of these intermediates (Macaulay and Forbes, 1996). Furthermore, some intermediates could be imaged using scanning EM suggesting that NPCs assembly occurs at the NE in a step-by-step fashion (Goldberg, et al., 1997). The first intermediates to be visualized were depressions in the ONM called "dimples". "Dimples" became holes that perforated the NE called "empty" pores that in turn could serve as seeds for the subsequent formation of pre-NPC structures called "star rings" and "thin rings". Finally, completely assembled NPCs were observed.

In addition to these NPC reassembly steps after mitosis, more subtle alteration in the structure of the NPC have been observed in association with the transit of transport substrates through the NPC. An example is represented by the extensive rearrangements undergone by the nuclear basket during export of Balbiani ring mRNP particles through the NPC (Kiseleva, et al., 1996).

Nucleocytoplasmic Transport

The primary function of the NPC is to provide a gated channel for the exchange of material between the cytoplasm and the nucleus. In actively growing cells it is estimated that every minute hundreds of proteins and ribonucleoprotein particles (RNPs) traverse each NPC in both directions. The most prominent nuclear import cargo consists of proteins, but also small nuclear RNPs (snRNPs) are constantly reimported into the nucleus after the cytoplasmic assembly of uridine-rich small nuclear RNAs (U snRNAs) with their protein counterparts. On the other hand, nuclear export involves chiefly messenger

RNPs (mRNPs), transfer RNAs (tRNA), ribosomal RNAs (rRNAs) assembled in ribosomal subunits and U snRNAs. In addition, some proteins constantly shuttle between the cytoplasm and the nucleus as part of their function. Some, such as the nucleolar protein nucleolin, do so slowly (Borer, et al., 1989; Schmidt-Zachmann, et al., 1993) while others, such as heterogeneous nuclear RNP (hnRNP) proteins A1, E and K, shuttle very rapidly (Pinol-Roma and Dreyfuss, 1992).

Both biochemical and genetic studies confirm that the basic mechanisms of nuclear transport appear to be highly conserved across distantly related species. Current models to explain these mechanisms are based on premises that have been firmly established for nuclear import and appear to apply also to nuclear export. The first of these premises is that different classes of transport substrates contain molecular signals that allow their recognition by specific transport factors. The best understood of these signals are the nuclear localization signals (NLSs) responsible for targeting a variety of proteins to the nucleus. NLSs were defined by systematic deletions and transfer experiments using primarily the large T antigen of SV40 (reviewed in, Dingwall and Laskey, 1991). NLSs are characterized in general by the presence of basic residues in one or two clusters. Other known transport signals include the nuclear export sequence (NES) and M9. NESs have been found on proteins whose presence in the nucleus is subject to regulation (for example, the polypeptide inhibitor (PKI) of the c-AMP dependents protein kinase (PKA) involved in signal transduction; Wen, et al., 1995) and on proteins that have a role in the export of specific classes of RNA molecules (TFIIIA for example, thought to be responsible for 5SRNA export; Guddat, et al., 1990; Fridell, et al., 1996). The typical NESs are short and hydrophobic with a high content of leucine residues (Fischer, et al., 1995; Wen, et al., 1995). M9 is a 38 AA sequence present on

the hnRNP shuttling protein A1 (Siomi and Dreyfuss, 1995; Weighardt, et al., 1995). M9 is required for the transport of A1 in both directions and functions as an NLS when transferred to reporter proteins. M9 does not bear any obvious similarity to either classical NLSs or NESs. RNA export signals have proven more difficult to define probably due in part to the close coupling of RNA post-translational modification and processing with transport. In addition, multiple signals may be required for the export of a single RNA molecule, making matters even more complicated. One of the RNA export signals that has been characterized is the monomethylated guanosine (m^7G) cap structure. The m^7G cap is recognized by a protein complex termed the cap binding complex (CBC) and it is one of the signals important for export of U snRNAs (Izaurralde, et al., 1992; Terns, et al., 1993; Jarmolowski, et al., 1994; Izaurralde, et al., 1995). Although this cap is definitely involved in pre-mRNA processing and mRNA translation it is not essential for mRNA export. Nevertheless, the m^7G cap could be important for ensuring that the 5' end of the transcript takes the lead at the NPC and it is exported first (see also below; Visa, et al., 1996). The other two tenets of nuclear transport are that signal-dependent transport of cargo is mediated by soluble carriers; and that transport processes depend upon the small GTPase Ran (Melchior, et al., 1993; Moore and Blobel, 1993; there are two Ran homologues in yeast, Gsp1p/Cnr1p and Gsp2p/Cnr2p; Belhumeur, et al., 1993).

The general mechanism for nuclear import has been established using *in vitro* import systems that take advantage of digitonin to permeabilize cells while leaving the NE intact (Newmeyer and Forbes, 1988; Adam, et al., 1990). These systems have been employed to biochemically isolate several essential transport factors, the importance of which has been confirmed by *in vivo* studies in yeast. In addition, results obtained using semi-permeabilized cells are in

accordance with results that had been previously obtained by following the ultrastructural localization of various import-competent substrates after microinjection in the cytoplasm of vertebrate cells (Richardson, et al., 1988; Akey and Goldfarb, 1989). In summary, the nuclear import of NLS-containing proteins can be divided in three major steps (Newmeyer and Forbes, 1988; Newmeyer and Forbes, 1990; Moore and Blobel, 1992): 1) Targeting or docking of the cargo to the NPC that requires a heterodimeric carrier and can happen in the absence of energy. 2) Translocation through the NPC that requires energy and is dependent upon Ran and various Ran cofactors (see below). 3) Release of the NLS-substrate into the nucleoplasm that most likely requires the GTP-bound form of Ran found prevalently in the nucleus (see below).

Protein carrying an NLS are recognized by the α subunit of a soluble heterodimeric factor called karyopherin α-β1 [Moroianu, et al., 1995; Radu, et al., 1995; also called importin α-β (Gorlich, et al., 1994; Gorlich, et al., 1995); NLS receptor and p97 (Adam and Adam, 1994); pore targeting complex (PTAC) 58-97 (Imamoto, et al., 1995; Imamoto, et al., 1995); or Kap60p/Srp1p-Kap95p/Rsl1p in yeast (Enenkel, et al., 1995)]. This complex docks at the NPC via interactions of the β1 subunit with the repeats domains of cytoplasmically exposed nucleoporins (Radu, et al., 1995; Rexach and Blobel, 1995). As mentioned above, this step is energy-independent but is thought to require both the GDP-bound form of Ran and the Ran cofactor, NTF2/p10 (in yeast, Ntf2p; Melchior, et al., 1993; Moore and Blobel, 1993; Moore and Blobel, 1994; Paschal and Gerace, 1995; Nehrbass and Blobel, 1996). Various models have been proposed to explain how this docked complex is actively translocated across the 50-60 nm long NPC transporter and is subsequently released into the nucleoplasm and the matter is still highly controversial (Melchior, et al., 1995; Radu, et al., 1995). All models agree in attributing a crucial importance to

Ran in maintaining vectorial cargo transport and regulating the binding and release steps that take place during translocation (Melchior, et al., 1993; Moore and Blobel, 1993; Richards, et al., 1997; reviewed in, Goldfarb, 1997). As for all small GTPases, Ran exists within the cell in a GDP-bound and in a GTP-bound form. The intrinsic GTPase activity of Ran is extremely low (Bischoff, et al., 1994) and is drastically stimulated by a GTPase activating protein termed RanGAP1/Fug1 (Rna1p in yeast; Bischoff, et al., 1994; Becker, et al., 1995; Bischoff, et al., 1995; Corbett, et al., 1995). Conversely, the replacement of the Ran-bound GDP with GTP is promoted by a guanine nucleotide exchange factor (GEF) termed RCC1 (in yeast Prp20p/Mtr1p/Srm1p; Ohtsubo, et al., 1987; Bischoff and Ponstingl, 1991; Bischoff and Ponstingl, 1991; Lee, et al., 1993; Tachibana, et al., 1994). Other Ran cofactors also have been described and are equally essential for nuclear import. These include a RanGAP stimulator called Ran binding protein (RanBP1) (in yeast, Yrb1p; Coutavas, et al., 1993; Schlenstedt, et al., 1995; Chi, et al., 1996; Floer and Blobel, 1996) and the above mentioned NTF2/p10. These cofactors of Ran are asymmetrically distributed within the cell and as a consequence cytoplasmic Ran is thought to exist prevalently in the GDP-bound form, while Ran-GTP is thought to predominate in the nucleus (Ohtsubo, et al., 1989; Schlenstedt, et al., 1995). This differential distribution of Ran-GTP *versus* Ran-GDP is thought to establish directional transport by ensuring that transport complexes are formed in one compartment and disassembled in the other. Consistent with this idea the complex of karyopherin α-β1 with the NLS-substrate is stable in the presence of Ran-GDP (i.e. in the cytoplasm) while the presence of Ran-GTP (i.e. in the nucleus) promotes its disassembly . In addition it has also been proposed that Ran could also act more locally to promote the repeated rounds of assembly and disassembly (i.e. docking and undocking) of the transport complex that

would be necessary for the stepwise movement of the substrate across the NPC (Radu, et al., 1995; Rexach and Blobel, 1995). A prediction of this docking-undocking model would be that Ran cofactors capable of modifying the nucleotide-bound state of Ran should be localized at the NPC. Consistent with this model, it was recently established that RanGAP can be recruited to the cytoplasmic side of the NPC as a consequence of a novel ubiquitin-like modification (Matunis, et al., 1996; Mahajan, et al., 1997; Mahajan, et al., 1998; Matunis, et al., 1998). Similarly, the cytoplasmically exposed Nup358 has a RanBP1-like domain that could act in concert with the NPC-associated RanGAP to promote GTP hydrolysis at this site (Wu, et al., 1995; Yokoyama, et al., 1995).

As recently demonstrated, several karyopherin β1-related proteins exist both in yeast and in higher eukaryotes (reviewed in, Wozniak, et al., 1998). A direct role for some of these karyopherin β1-homologues in the nuclear transport of specific classes of macromolecules has been firmly established (see below), while others have been involved only indirectly in nuclear transport.

Nuclear export has been studied using primarily four lines of investigation. The first had been the morphological study of the *Chironomus tentans* Balbiani ring transcripts during their nuclear processing and transport across the NPC (reviewed in, Daneholt, 1997). The main conclusion of these studies has been that these large mRNP particles have to unravel substantially during translocation and that they must make multiple contacts with the NPC during such process. Furthermore it has been established that in most cases the 5' ends of these mRNA transcripts reach the cytoplasm first and that they are engaged by the translation machinery as soon as they do. The second experimental approach has been successfully employed to gain insight into the signals and factors involved in export has been the microinjection of RNAs and

proteins into the nucleus of *Xenopus* oocytes. This system has been used to demonstrate that nuclear export requires energy and is saturable and that the export of different classes of RNAs requires at least partially distinct carriers (Zasloff, 1983; Bataille, et al., 1990; Jarmolowski, et al., 1994; Pokrywka and Goldfarb, 1995). Third, the development of an *in vitro* export assay (Moroianu, et al., 1997) has allowed the demonstration that re-export of karyopherin α from the nucleus is dependent upon Ran-GTP (Moroianu, et al., 1997) and that the karyopherin β1 homologue CAS (Cse1p, in yeast; see below) appears to be the export factor involved in mediating this process (Kutay, et al., 1997). Finally, valuable information has also been gained by the isolation and characterization of yeast mutant impaired in RNA export (Amberg, et al., 1992; Kadowaki, et al., 1994).

Genetic and biochemical data concur in attributing to shuttling hnRNP proteins such as A1 (and their yeast homologues Nab2p, Hrp1p/Nab4p and Npl3p; Anderson, et al., 1993; Singleton, et al., 1995; Henry, et al., 1996) an important role in mRNA export (Michael, et al., 1995; Lee, et al., 1996; Visa, et al., 1996; Izaurralde, et al., 1997). Interestingly, the Kap95p homologue, Kap104p has been recently found to be directly responsible for the import of the yeast mRNA-binding proteins Nab2p and Hrp1p/Nab4p (Aitchison, et al., 1996). Similarly, another yeast karyopherin β1 homologue Mtr10p/Kap111p was implicated in Npl3p import (Pemberton, et al., 1997). This function appears to be conserved in vertebrates where two proteins closely related to Kap104p, karyopherin β2/transportin1 and transportin2 were found to be required for import of hnRNP proteins (Pollard, et al., 1996; Bonifaci, et al., 1997; Fridell, et al., 1997; Siomi, et al., 1997).

Important information regarding the export of proteins from the nucleus has emerged from studies of the HIV protein Rev. Rev is a rapidly shuttling protein

that is responsible for ensuring that unspliced viral mRNAs encoding the structural proteins Gag and Pol are exported to the cytoplasm (Fischer, et al., 1994; Kalland, et al., 1994; Meyer and Malim, 1994). Rev export is NES-dependent (Fischer, et al., 1995; Szilvay, et al., 1995). Accordingly, Rev is thought to function as an adapter for linking viral RNAs to a cellular export pathway that appear to be required for export of several NES-containing proteins as well as for 5SRNA and several U snRNPs (Fischer, et al., 1995; Fridell, et al., 1996; Fritz and Green, 1996). Recently, CRM1 (and its yeast homologue, Crm1p), a member of the extended karyopherin family of nuclear transport factors, has been directly implicated in the export of Rev (Fornerod, et al., 1997; Fukuda, et al., 1997; Kudo, et al., 1997; Neville, et al., 1997; Ossareh-Nazari, et al., 1997; Stade, et al., 1997). Another important element of the Rev-export pathway could be the putative nucleoporin Rip/RAP1 (with its yeast homologue, Rip1p/Nup42p; Bogerd, et al., 1995; Fritz, et al., 1995; Stutz, et al., 1995; Stutz, et al., 1996).

The Structural and Functional Organization of the Nuclear Interior and its Connections with Nucleocytoplasmic Transport

Several essential processes are known to occur in the nucleus including DNA packaging, DNA replication, RNA transcription, RNA post-transcriptional processing and modification and RNA export. While much is known about the molecular bases of these nuclear processes, our knowledge of how the genome is structurally and functionally organized as a whole is still extremely limited. A big step in this direction was represented by the isolation and characterization of the nuclear matrix (NM; reviewed in, Berezney, et al., 1995;

Nickerson, et al., 1995). The NM, also called nuclear scaffold, is an extensive non-chromatin fibrillogranular network that occupies the interchromatinic regions of the nucleus (Fawcett, 1966; Monneron and Bernhard, 1969) The ultrastructure of the NM can be preferentially visualized *in situ* using EDTA regressive staining procedures that are thought to selectively stain non-chromatin and especially RNA-containing structures (Bernhard, 1969; Monneron and Bernhard, 1969). On the basis of the structural organization the NM it has been proposed that it could be divided in two domains. The first of these functional domains is called the chromatin domain and is thought to be involved in the structural organization of active DNA replication and transcription complexes. The second domain or RNP domain appears to be involved in providing the architectural milieu for post-translational RNA processing, modification and transport towards the NPCs. Interestingly, using the EDTA regressive staining method the NPCs are particularly densely stained and appear to be connected to the nuclear interior via NM channels (Monneron and Bernhard, 1969; Franke and Falk, 1971). Furthermore, the results of *in situ* pulse-chase experiments support the idea that newly transcribed RNA molecules migrates through interchromatinic regions in their trip towards the nuclear periphery (Fakan and Bernhard, 1971; Fakan and Bernhard, 1973; Nash, et al., 1975; Fakan, et al., 1976). These and other observations have led to the speculation that the NPCs could be closely connected with active chromatin regions and that the NM channels that are observed radiating from the NPCs could represent "tracks" for the regulated transport of material to and from the nucleus (Blobel, 1985). Recently, this model has received support from a study in which the rate of movement of a specific pre-mRNA molecule from its site of synthesis to the nuclear surface was measured using fluorescent *in situ* hybridization (Zachar, et al., 1993). Strikingly, this transport rate was found to

be consistent with a model that advocates the "channeled diffusion" of pre-mRNA molecules within restricted nuclear interchromatinic subcompartments also referred to as "extrachromosomal channel network" that could correspond to the "tracks" mentioned above.

The NM can be isolated using a variety of techniques that are all derived from the original protocol of Berenzey and Coffey (Berezney and Coffey, 1974). What all of these methods have in common is a series of sequential nuclease, salt and detergent extraction procedures aimed at preferentially removing the nuclear membrane and the bulk of the chromatin while leaving behind a residual scaffold composed prevalently of proteins and RNA. When *in vitro* NM preparations are observed by whole mount resinless thick-section EM they appear to be structurally tripartite with NPC, NL and internal fibrillogranular domains clearly distinguishable (Staufenbiel and Deppert, 1984; Fey, et al., 1986; Nickerson, et al., 1990). The fibrillogranular structure of the isolated NM is similar to the one observed *in situ.* This include the appearance of discrete interchromatinic granules (ICGs) as well as filaments that depending upon the exact nature of the extraction procedure being used appear to be either 3-5 nm (called matrix protein filaments or MPFs; Berezney and Coffey, 1977); or 10 nm thick (called core filaments; Jackson and Cook, 1988; He, et al., 1990). The precise relationship between MPFs and core filaments has not been established and they could represent two forms of the same structure. Interestingly though, regardless of the technique employed and consistent with the *in situ* observations, these NM filaments are seen interconnecting ICGs, in association with the chromatin and radiating from the NPCs (Monneron and Bernhard, 1969). Intriguingly, these NM filaments could correspond to the 5-6 nm filaments that have been found in association with the inner ring of the nuclear basket using a variety of EM techniques by different groups in

amphibian oocytes (Franke, 1970; Franke and Scheer, 1970; Franke and Scheer, 1970; Kartenbeck, et al., 1971; Richardson, et al., 1988; Ris and Malecki, 1993). In one recent study, ~50 nm hollow cables composed of eight ~6 nm-thick filaments were seen projecting from the small ring of the nuclear basket towards the nucleoplasm and appeared to form "tunnels" continuous with the inside of the baskets (Ris, 1997). Strikingly, such cables appeared to have a characteristic 50 nm periodicity and were seen as forming extensive networks connecting multiple NPCs to the nuclear interior. In the absence of molecular or biochemical information conclusions drawn from these various reported morphologies remain uncertain.

As mentioned above, both *in vivo* and *in vitro* methods of investigation concur in strongly suggesting that the NPC and the NM are structurally continuous. From the functional point of view, it has been speculated such structural connections could facilitate various nucleocytoplasmic transport processes. Recently, the investigation of the molecular basis of such connections has received great impetus from the study of vertebrate Tpr ("Translocated Promoter Region") and of the Tpr-related *Drosophila* protein Bx34. The amino-terminal ~200 AA of human Tpr have been detected in various human tumors fused with the kinase domains of the three protooncogenes *met*, *trk* and *raf* (Park, et al., 1986; Soman, et al., 1991; Greco, et al., 1992; Mitchell and Cooper, 1992). The sequence of *Tpr* predicts a large protein (~265 kD) with a bipartite secondary structure (Byrd, et al., 1994; Bangs, et al., 1996). The amino-terminal 70% of the polypeptide sequence (~184 kD) has a high α-helical content and is predicted to give rise to a coiled-coil domain. In contrast, the remaining 30% of the protein (~81 kD) is predicted to be unstructured and acidic. While initially Tpr had been localized exclusively to the cytoplasmic filaments associated with the NPC (Byrd, et al., 1994), more recent

work has conclusively demonstrated that Tpr is a constitutive component of long nuclear filaments (up to ~300 nm in *Xenopus*) that appear to connect the distal ring of the nuclear basket with the nuclear interior and could correspond to the 5-6 nm filaments described by Ris and others (see above; Cordes, et al., 1997). The predicted filamentous structure of Tpr together with its localization led to the natural speculation that this protein could have a role in providing a structural framework for the transport of material from the nuclear periphery towards the interior and *vice versa*. This conclusion has received further support from results obtained with a Tpr-related protein in *Drosophila*, called Bx34. This protein was initially described as one of two novel classes of *Drosophila* NE antigens that had been identified using mAbs obtained against chromosomal protein fractions (Frasch, et al., 1988). Strikingly, Bx34 was recently found both at the nuclear periphery in association or near NPCs and in the nuclear interior in extrachromosomal and extranucleolar regions reminiscent of the "extrachromosomal channel network" described in relation to mRNA processing and transport (Zimowska, et al., 1997). Consistent with its localization pattern, Bx34 was found to cofractionate exclusively with biochemical preparations of the NM suggesting that it could represent a component of the NM filamentous network. Interestingly, Bx34 retains its association with the chromosomes until very late in mitosis leading to the suggestion that it could have a structural role in aiding chromosomal segregation in anaphase.

Three general non-mutually exclusive models of how a filamentous protein could facilitate nucleocytoplasmic transport processes have been proposed (Zachar, et al., 1993). In the first model, filamentous proteins could help maintain channels between chromosomes to allow diffusion of nuclear metabolites and macromolecular particles. In the second, filamentous proteins could give rise to a nucleoplasmic gel that would be susceptible to conditional

alterations and could thus regulate the diffusion of molecules within the channels. Finally, filamentous proteins could participate in facilitated diffusion by providing docking sites for various nuclear metabolites that would restrict their movements to one dimension. In conclusion, whereas the precise function of Tpr /Bx34 is not presently known, it is easy to speculate that it could participate in one of the above mentioned ways in keeping a constant connection between the NPC and the nuclear interior where the various essential nuclear processes must take place.

A Combined Biochemical and Immunological Approach to identify Yeast Proteins that May Provide a Link Between the NPC and the Nuclear Interior

While it is clear that the NPC is a major regulator of nucleocytoplasmic transport, the knowledge of how this essential superstructure is connected both structurally and functionally to the nuclear interior is still extremely limited. The yeast *Saccharomyces* present numerous advantages over higher eukaryotes as a system to study these problems. They have neither the complications of developmental regulation of nuclear processes, nor of nuclear disassembly, having a closed mitosis; in addition, the genetics and molecular biology of yeast are better understood than in any other eukaryote, and the DNA sequence of the entire yeast genome is now known (Clayton, et al., 1997). The main caveat of the use of yeast to study complex cellular systems is that the cell biological and biochemical characterization of cellular membranes and compartments in budding yeast is less complete than in vertebrates, and would benefit from the

development of rigorous cellular fractionation techniques comparable to the ones available for higher eukaryotes.

This dissertation describes work aimed at isolating and characterizing two possible kinds of novel yeast NE-associated components: 1) those that could constitute a link between the NPC translocation machinery and the nuclear interior and 2) proteins specifically associated with the nuclear membrane. A genetic approach was considered unlikely to yield the desired results because of the difficulty of predicting a specific phenotype associated either with the loss of a structural component connecting the NPC with the nuclear interior or with the loss of nuclear membrane proteins. A second possible way that can be used to identify novel components of a complex cellular system is the production of large quantities of a highly enriched subcellular fractions containing the desired proteins followed by the immunization of mice to produce mAbs against components of such fractions. This approach was considered preferable for the following reasons: 1) an antibody can be used to determine the localization of the antigen inside the cell and at the same time to clone the gene encoding the antigen from an expression library; 2) any protein can be potentially identified using this approach as long as it can be produced in large enough quantities and it is immunogenic. In this respect, yeast presented a particular advantage as compared to higher eukaryotes because large amounts of material can be produced with relative ease using this system; and because yeast proteins can be expected to be particularly immunogenic due to the large degree of interspecific divergence between the source and the recipient of the antigen; and 3) mAbs can be produced in unlimited quantities and have the advantage of being targeted against individual antigens. Furthermore, this approach had proven invaluable in similar circumstances to isolate novel components of complex macromolecular assemblies that had

escaped identification via genetic means (Rout and Kilmartin, 1990; Rout and Kilmartin, 1991).

This dissertation therefore describes a combined biochemical and immunological approach. The first step of such approach was the production of a highly enriched NE fraction from the yeast *Saccharomyces.* NEs were prepared from yeast nuclei on a large scale and in high yield. The fractionation pattern of representative markers throughout the procedure was used to asses the degree of enrichment of individual NE-associated proteins in the isolated NE fraction and at the same time to demonstrate the preferential depletion of "contaminating" proteins.

Three distinct NE-derived fractions were used to produce a panel of mAbs against NE associated components. A novel NPC-clustering assay was devised to specifically isolate anti-NE mAbs that recognized either antigens found at an interface between the NPCs and the nuclear interior or integral membrane proteins of the INM. This screen did not yield any putative nuclear membrane proteins. Nevertheless, two mAbs were isolated that recognized a ~220 kD NE antigen only partially associated to the NPCs. The gene encoding this antigen was molecularly cloned and was found to correspond to the previously isolated *MLP1* (Kolling, et al., 1993). This gene encodes a nuclear protein of unknown function that is the closest yeast relative of Tpr. Ultrastructural localization and functional studies strongly argue that Mlp1p and its yeast homologue Mlp2p could be involved in providing a structural link between the NPCs and the nuclear interior that is responsible for facilitating nucleocytoplasmic transport. In conclusion, evidence presented in this dissertation could open the road for much needed molecular investigation into an area of cell biology that is still in its infancy.

Chapter II: Materials And Methods

Yeast Subcellular Fractionation; Preparation of Enriched Nuclei and Highly Enriched NPCs

The yeast strains *Saccharomyces uvarum* (NCYC 74, ATCC 9080), considered a strain of *Saccharomyces cerevisiae* (Mortimer and Johnson, 1986), or *S. Cerevisiae* (W303; Thomas and Rothstein, 1989) were used throughout the procedure. Enriched nuclei were prepared as previously described (Rout and Kilmartin, 1990; Rout and Kilmartin, 1994). Briefly, 70-90 g of mid-logarithmic phase cells (~1 x 10^7 cells/ml for diploid cells and ~2 x 10^7 cells/ml for haploids) were obtained from a 36 liter yeast culture. Cells were harvested and converted to spheroplasts in 1.1 M sorbitol (Rout and Kilmartin, 1994). Spheroplasts were harvested by centrifugation and then lysed in 300 ml of PVP solution [8% polyvinylpyrrolidone (PVP); 20 mM potassium phosphate, pH 6.5; 0.75 mM $MgCl_2$]. The cell lysate (fraction 1) was separated by centrifugation (15 min at 10,000 *g*) into crude cytosol (fraction 2) and a crude nuclei pellet (fraction 3). The nuclei were resuspended in 144 ml of 1.7 M sucrose in PVP solution and this suspension was divided into 12 equal aliquots. Each aliquot was overlayered over a three step sucrose/PVP gradient (8 ml each of 2.01 M sucrose, 2.10 M sucrose and 2.30 M sucrose in PVP solution) in a SW28 tube (Beckman Instruments, Palo Alto, CA). The gradients were centrifuged in a Beckman SW28 rotor at 28,000 RPM (103,000 *g*) for 4 h at 4°C. After centrifugation fractions were collected from the top. The load zone, including a thick layer at the top of the tube (fraction 4), and a thick yellowish band at the load/2.01 M interface (fraction 5), both contained intact

mitochondria, vesicles and microsomes (as judged by EM). Very little material was present in the third gradient fraction at the 2.01/2.10 M interface (fraction 6). A dense white band at the 2.10 M/2.30 M interface contained the bulk of the nuclei (fraction 7). The bottom of the gradient (fraction 8) included a pellet composed mainly of cells remnants.

Highly enriched NPCs were prepared from nuclei (fraction 7) exactly as described in Rout and Blobel (Rout and Blobel, 1993).

Yeast NE Preparation

NEs were prepared from the enriched nuclear fraction (fraction 7). The OD at 260 nm of the nuclear fraction was measured after 1 in 100 dilution in 1.0% SDS; approximately 1000-2000 OD_{260} nm were obtained from a 36 liter prep. The nuclear fraction was adjusted to a refractive index of 1.4340 with PVP solution and centrifuged at 145,000 *g* 1 h at 4°C. The supernatant was carefully but thoroughly removed by aspiration, and the tubes placed on ice. Typically, 20 ml of freshly prepared, ice cold bt-DMSO [bt buffer (10 mM bisTris-Cl, pH 6.5; 0.1 mM $MgCl_2$) containing 20% (v/v) DMSO] in the presence of 20 µg/ml DNase I-EP (Sigma, St. Louis, MO) and 1% (v/v) solution P (90 mg/ml PMSF, 0.3 mg/ml pepstatin A in absolute ethanol), were added to 2000 OD_{260} nm of nuclei. This was followed immediately by vigorous vortexing at 4°C until the pellet was completely resuspended. The suspension was then incubated at room temperature (~25°C) for 5-10 min. After incubation, the lysed nuclei were placed back on ice and 60 ml of 2.1 M sucrose, 20% Nycodenz (Accudenz; Accurate Chemical and Scientific, Westbury, NY) in bt buffer in the presence of 0.1% (v/v) solution P, were added and thoroughly mixed. The suspension was

divided into 6 Beckman SW28 tubes and overlayered with 12 ml of 2.0 M sucrose (R.I. = 1.4295) and 12 ml of 1.5 M sucrose (R.I. = 1.4055) in bt buffer containing 0.1% (v/v) solution P. The tubes were centrifuged in a Beckman SW28 rotor at 28,000 rpm (103,000 *g*) for 24 h at 4°C. The tubes were unloaded from the top using a hand-held pipette. A faint white band at the top of the tube was completely removed (~6.0 ml collected per tube; fraction 9). The NEs were found at the 1.5 M/2.0 M interface, appearing as a broad, white, slightly flocculent band (~12.0 ml collected per tube; fraction 10). Next was a dense, sharp yellowish/white band containing a few NEs, chromatin and cell remnants (~12.0 ml collected per tube; fraction 11). The final ~7.0 ml collected (fraction 12), including a dense brownish/white pellet, contained soluble and particulate matter mainly derived from chromatin.

For the preparation of isolated nuclei and highly enriched NEs from *S. cerevisiae* , the procedures described above were modified exactly as described (Rout and Strambio-de-Castillia, 1998).

Extraction of Yeast NEs

For heparin extraction, 0.6 ml (~0.4 mg of protein) of the yeast NE fraction were mixed with 2.4 ml of a solution containing 10 mg/ml heparin (Sigma, St. Louis, MO), 0.1 mM DTT and 0.5% (v/v) solution P in bt buffer. After 1 h on ice, 50 µg/ml RNase A was added and the incubation was continued for 15 min at 10°C. The sample was over layered onto two 1-ml layers of 1.0 and 2.0 M sucrose in bt buffer containing 0.1% (v/v) solution P, and centrifuged in a Beckman SW55 rotor at 45,000 RPM (~192,000 *g*) for 30 min at 4°C. The tube was unloaded from the top using a hand-held pipette. The first fraction (~2 ml;

fraction 13) contained the bulk of the solubilized proteins. The next fraction (~1.8 ml; fraction 14) contained some of the soluble proteins together with a few of the NE membranes. The bulk of H-NE membranes was recovered at the 1.0 M/2.0 M sucrose interface and appeared as a tight white band (~0.4 ml; fraction 15). The last fraction (~0.8 ml; fraction 16) sometimes contained small amounts of H-NEs.

The yeast NE fraction was extracted with sodium carbonate using a previously described method (Wozniak, et al., 1994).

Post-Translational Translocation Assay

The procedures for the preparation of yeast nuclei and NEs described above were modified to maintain the ER-translocation activity throughout the fractionation procedure. Firstly, yeast spheroplasts were allowed to recover in YPD medium (1% yeast extract, 2% peptone, 2% dextrose) containing 1.0 M sorbitol for 30 min at room temperature before lysis. Secondly, all the solutions starting from the lysis buffer and including all the gradient solutions were supplemented with 2 mM DTT. Finally, the $MgCl_2$ concentration in the nuclear lysis buffer and in the solutions used for the NE flotation gradient (fractions 9-12) was raised from 0.1 to 0.5 mM. The degree of enrichment of "active" NEs was shown to be similar to that obtained with the original method (data not shown). Just before the *in vitro* protein translocation reaction the "active" NE fraction was concentrated 20-fold by pelleting at 70,000 *g* for 30 min, and gently resuspending in solution A (20 mM Hepes-KOH, pH 7.4; 100 mM KOAc, 2 mM $Mg(OAc)_2$; 2 mM DTT) containing 0.25 M sucrose. The heparin extraction of the "active" NE fraction was carried out as described above except that 2 mM

DTT was added to all solutions and gradients, the RNase A digestion step was omitted and the H-NEs were pelleted through a 1.0 M sucrose cushion [1.0 M sucrose, 2 mM DTT, 0.5 mM $MgCl_2$, 0.5% (v/v) solution P in bt buffer] instead of being recovered over 2.0 M sucrose. Heparin traces were removed by resuspending the "active" H-NEs pellet obtained from 2.4 ml of NEs, in 2.4 ml of 0.5 M KCl, 2 mM DTT, 0.25 M sucrose, 0.5% (v/v) solution P and incubating the suspension for 1 h on ice. The membranes were recovered by centrifugation through a 0.5 ml, 0.6 M sucrose cushion [0.6 M sucrose; 10 mM bisTris-Cl, pH 6.5; 0.5 mM $MgCl_2$; 0.1% (v/v) solution P], at 39,000 RPM (~100,000 *g*) in a TLS-55 Beckman rotor for 1 h. The supernatant from the 0.5 M KCl wash was shown not to contain significant amounts of extracted proteins (data not shown). Finally, the sample was resuspended in a volume of 0.25 M sucrose in solution A equal to roughly 2.5% of the initial NEs volume.

Yeast crude microsomes (CMs), used as a positive control for the ER translocation reaction, and yeast crude cytosol were prepared as described (Waters and Blobel, 1986; Waters, et al., 1986). [^{35}S]-methionine labeled prepro-α-Factor (ppαF) was synthesized using a wheat germ *in vitro* translation kit (Promega, Madison, WI) following the specifications of the manufacturer. Immediately before use, the translation mixture containing ppαF was diluted with 3 volumes of 8 M urea and incubated for 10 min at 20°C. The translocation reaction and the protease protection assays were performed as described (Waters and Blobel, 1986; Chirico, et al., 1988). Typically, the translocation mix (total volume 150 µl) consisted of the following: 43.6 µl of "master mix" [14.4 mM Hepes-KOH, pH 7.4; 276 mM KOAc; 1.0 mM $Mg(OAc)_2$; 1.0 mM DTT; 1.7 mM ATP; 86 mM creatine phosphate; 0.7 mg/ml creatine kinase; 0.07 mM GDP-mannose; 0.07 mM UDP-glucose; 0.07 mM UDP-N-acetylglucosamine; 1.4% (v/v) glycerol], 90 µl of yeast crude cytosol in solution A containing 1.0 mM Mg-

ATP, and 14 µl of CM, NE or H-NE membranes in solution A containing 0.25 M sucrose. This mixture was pre-incubated at 20°C for 5 min and the import reaction was then started by the addition of 2.4 µl of urea-denatured translation product. At the end of the reaction the sample was divided in 3 equal aliquots. 30 µl of water were added to the first aliquot. 10 µl of 8 mM $CaCl_2$, 10 µl of water and 10 µl of 800 µg/ml trypsin were added to the second aliquot. The third aliquot was treated as the second except that 10 µl of water were substituted with 10 µl of 8% (v/v) Triton X-100. All aliquots were incubated on ice for 30 min and the reactions were stopped by the addition of 10 µl of 50 mM PMSF. After an additional 10 min on ice, the samples were TCA precipitated and analyzed by SDS-polyacrylamide gel electrophoresis (PAGE) and fluorography.

Fractionation of NE Proteins by Ion-exchange Chromatography

Proteins contained in 30 ml of the highly enriched NE fraction described above (Fraction 10), were harvested by methanol precipitation as described below (see "Miscellaneous" section). The methanol pellet was solubilized in 4 ml of 10 mM MES, pH 6.5, 100 mM DTT, 1% SDS at 90° C for 10 min. The resuspended proteins were mixed with 36 ml of 20 mM MES, pH 6.5, 7 M Urea, 1% (v/v) Triton X-100, 0.1% SDS, 1 mM DTT (buffer 7). In the meantime, 16 ml of a 1:1 suspension of the cation-exchange S-Sepharose resin (8 ml of resin bed) were loaded on a broad base, 50 ml column and washed three times with 20 ml of buffer 7. The NE sample was loaded onto the column and was allowed to absorb onto the resin by incubating 1 hr at 25° C with gentle rocking. After the binding step, the flow-through from the column was harvested and pooled

with a 20 ml wash in buffer 7 (this pooled material was termed "unbound fraction"). The column was eluted 2 times with 30 ml each of 1 M NaCl in buffer 7. Proteins from both bound and unbound fractions were harvested by methanol precipitation. Aliquots were separated on SDS-PAGE. After electrophoresis, the fractionation pattern of known NPC-components was analyzed by immunoblotting using MAb414 (Davis and Blobel, 1986). The unbound fraction (termed S-NE), was found to be selectively depleted of most nucleoporins recognized by MAb414. Proteins from this fraction were harvested by methanol precipitation, resuspended in PBS and used to immunize mice.

Immunization of Mice and Production of mAbs

Native NEs and H-NEs were harvested by ultracentrifugation and resuspended in PBS. S-Sepharose fractionated NEs (S-NEs) were prepared as described above. For the initial immunization, BALB/c mice were immunized sub-cutaneously with 0.5-0.74 mg of antigen per mouse per injection emulsified with Freund's complete adjuvant. Each mouse received up to 4 booster sub-cutaneous injections in incomplete Freund's adjuvant at 4-6 weeks intervals. 3-5 days prior to fusion, the mouse received a final intra-peritoneal injection of antigen without adjuvant. The production of hybridomas from B-lymphocytes derived from mice spleens was as previously described (Galfre and Milstein, 1981; Rout and Kilmartin, 1990). Supernatants were screened by indirect IF microscopy of whole yeast cells. *S. uvarum* cells were fixed in 4% (v/v) formaldehyde and 10% (v/v) methanol in phosphate buffer pH 6.5, for 3, 6 and 12 min (Kilmartin and Adams, 1984; Wente, et al., 1992). An equal proportion of

cells from each fixation time was mixed together and applied to 15-wells slides, followed by fixation in methanol for 5 min at -20° C and acetone for 30 sec at 25° C. Slides were stained with the hybridoma supernatants essentially as described (Rout and Kilmartin, 1990; Wente, et al., 1992; Kilmartin, et al., 1993). Positive supernatants were also screened by immunoblotting of enriched NEs. Proteins from this fraction were separated by SDS-PAGE after loading on a large preparative well spanning the entire width of the gel. After electrophoresis the proteins were transferred on nitrocellulose and the blot was sandwiched between the two plates of a multi-lane apparatus (Miniblotter 27, Immunetics, Cambridge, MA). This allowed the incubation of up to 26 hybridoma supernatants at the same time without cross-contamination. Bound antibodies were visualized using a secondary HRP-conjugated rabbit anti-mouse antibody followed by ECL. Cells from positive lines were cloned up to four times by limiting dilution using a standard protocol. The IgG subclass of the monoclonal was established using a mouse mAb isotyping kit from Amersham (Amersham Life Science inc., Arlington Heights, IL). All the mAb immunostaining experiments described in this thesis were performed using tissue culture supernatants.

Molecular Cloning of the *MLP1* Gene

A *S. cerevisiae* genomic expression library was screened using MAb148G11. The library was acquired from Clonetech (Clonetech Laboratories Inc., Palo Alto, CA) and contained an estimated 1.5 x 10^6 independent clones. The library consisted of yeast genomic DNA fragments ranging between 0.8 - 5.0 kb (average size 1.8 kb) inserted in the EcoRI site of

λgt11. The library was screened by immunoblotting following the specifications of the manufacturer. 3 positive λ clones were obtained and purified to homogeneity by four consecutive rounds of screening. The DNA from these λ clones was purified using standard protocols and subjected to restriction analysis. This demonstrated that the three clones contained an identical insert of ~1.8 kb. The insert from one of the positive λ clones was subcloned in pBluescript SK(+/-) and sequenced from both ends using the T3 and the T7 standard primers. DNA sequences comparisons were performed using the BLAST algorithm (Altschul, et al., 1990). Deducted AA sequences were compared to sequences in the SGD (*Saccharomyces* Genome Database), GenBank and EMBL databases using the FASTA algorithm (Parson and Lipman, 1988). AA sequence alignments were performed using FASTA and CLUSTALW v 1.6 (Higgins D., et al., 1994). AA sequences were analyzed using Protean v. 1.08 (DNAStar Inc., Madison, WI) and MacStripe 1.3.1 (Lupas, et al., 1991).

Gene Disruption and Protein A tagging of *MLP1* and *MLP2*

All yeast strains were derived from W303 (Thomas and Rothstein, 1989; Table I). Procedures for yeast manipulation were as previously described (Sherman, et al., 1986). Gene replacement and protein A tagging of *MLP1* and *MLP2* were accomplished using published methods (Rothstein, 1990; Aitchison, et al., 1995; Aitchison, et al., 1995). *MLP1* was replaced with *URA3* by generating a PCR product containing the entire *URA3* gene flanked by 75 nucleotides directly upstream and 75 directly downstream of the *MLP1* coding region. This PCR product was transformed into diploid yeast cells by

electroporation and Ura$^+$ transformants were selected on SM Ura$^-$ plates. A similar procedure was followed to disrupt *MLP2* except in this case the coding region of the gene was replaced with *HIS3* and transformants were selected on SM His$^-$ plates. In both cases correct integration was verified by PCR analysis of the genomic DNA. Heterozygous diploid cell carrying individual deletions of *MLP1* and *MLP2* respectively (*mlp1::URA3/MLP1*, CSDC01a/α; *mlp2::HIS3/MLP2*, CSDC04a/α), were sporulated and tetrads were dissected to generate *mlp1::URA3* (CSDC03α) and *mlp2::HIS3* (CSDC05a) haploid strains. A heterozygous diploid carrying disrupted copies of both *MLP1* and *MLP2* (*mlp1::URA3/MLP1, mlp2::HIS3/MLP2*; CSDC07a/α) was constructed by mating CSDC03α and CSDC05a. CSDC07a/α was sporulated and tetrads were dissected to generate haploids carrying both deletions (*mlp1::URA3, mlp2::HIS3*; CSDC09α, *mlp1Δ, mlp2Δ*). PCR was used to verify the 2:2 segregation of the copy of each disrupted gene (*mlp1* and *mlp2*) with the appropriate selectable marker (*URA3* and *HIS3*, respectively). Haploid strains of opposite mating types carrying the double deletion of *MLP1* and *MLP2* were mated to generate a homozygous diploid strain (*mlp1::URA3/ mlp1::URA3, mlp2::HIS3/ mlp2::HIS3*; CSDC13a/α, *mlp1Δ, mlp2Δhd*). In all cases the expression of Mlp1p in wild type and mutant strains was analyzed by immunoblotting of whole yeast cell lysates and by indirect IF microscopy using MAb148G11 and MAb215B9.

For protein A tagging of Mlp1p and Mlp2p, PCR products were generated that contained the coding region for four and a half IgG-binding repeats of protein A followed by a *HIS3, URA3* cassette flanked by 75 nucleotides immediately upstream and 75 nucleotides immediately downstream of the stop codon (i.e. excluding the stop codon itself) of each gene. These PCR products were transformed into diploid yeast cells as above. The heterozygous diploids

harboring tagged versions of *MLP1* and *MLP2* respectively were sporulated and tetrads were dissected to generate tagged haploid strains. In both cases, 2:2 segregation of the HIS^+, URA^+ phenotype with the expression of Mlp1p-pA or of Mlp2p-pA was verified by immunoblot of whole yeast cell lysates.

Table I. Yeast Strains

Strain Name[a]	Genotype	Derivation
W303	*MATa/MATα, leu2-3,112/ leu2-3,112, his3-11,15/ his3-11,15, trp1-1/trp1-1, can1-100/can1-100, ade2-1/ade2-1, ura3-1/ura3-1*	[Thomas, 1989 #452]
CSDC01a/α	*W303 Mata/Matα, mlp1::URA3/MLP1*	This Study
CSDS02a	*W303 Mata, mlp1::URA3*	This Study
CSDC03α	*W303 Matα, mlp1::URA3*	This Study
CSDC04a/α	*W303 Mata/Matα, mlp2::HIS3/MLP2*	This Study
CSDC05a	*W303 Mata, mlp2::HIS3*	This Study
CSDC06α	*W303 Matα, mlp2::HIS3*	This Study

Table I. Yeast Strains (continued)

Strain Name	Genotype	Derivation
CSDC07a/α	*W303 Mata/Matα, mlp1::URA3/MLP1, mlp2::HIS3/MLP2*	This Study
CSDC08α, **mlp2Δ**	*W303 Matα, MLP1, mlp2::HIS3*	This Study
CSDC09α, **mlp1Δ, mlp2Δ**	*W303 Matα, mlp1::URA3, mlp2::HIS3*	This Study
CDSC10a, **mlp1Δ**	*W303 Mata, mlp1::URA3, MLP2*	This Study
CSDC11a, **wt**	*W303 Mata, MLP1, MLP2*	This Study
CSDC12a	*W303 Mata, mlp1::URA3, mlp2::HIS3*	This Study
CSDC13a/α, **mlp1Δ,mlp2Δ hd**	*W303 Mata/Matα, mlp1::URA3/mlp1::URA3, mlp2::HIS3/mlp2::HIS3*	This Study

Table I. Yeast Strains (continued)

Strain Name	Genotype	Derivation
CDSC14a/α	*W303 Mata/Matα, mlp1-proteinA::HIS3, URA3/MLP1*	This Study
CSCD15a, **mlp1-pA**	*W303 Mata, mlp1- proteinA::HIS3, URA3*	This Study
CSDC17a/α	*W303 Mata/Matα, mlp2- proteinA::HIS3, URA3/MLP2*	This Study
CSDC18a, **mlp2-pA**	*W303 Mata, mlp2- proteinA::HIS3, URA3*	This Study
W303/pGALMLP1	*W303 Mata/Matα, pGALMLP1::URA3*	This Study

Footnotes:

[a] All strains are isogenic to W303. The most important strains for the experiments described in this thesis dissertation were given a second, more descriptive name that is used in the text and in the figure legends. This designation is indicated in bold characters.

Growth Competition Assay

The growth competition experiment was performed following published procedures (Smith, et al., 1996; Rout, et al., 1997; Thatcher, et al., 1998). Briefly, wild type and mutant cells were grown to mid-logarithmic phase before diluting them into fresh YPD. Initially, wild type and mutant cells were mixed at a 2:1 ratio to a total concentration of 3×10^5 cells/ml. Cells were grown at 30° C and maintained in logarithmic phase at all times. At each time point 10 µl aliquots of neat and 10-fold dilutions were spotted on YPD and the appropriate selective plates. Cells were diluted back to the original concentration and the incubation was continued until the next time point. Data are presented as the percentage of mutant cells present in the population as a function of time. The natural logarithm of the genotype ratio (% mutant/% wild type) at each time point was plotted to produce a line extrapolated using the least squares fit (KaleidaGraph v 3.02; Synergy Software, Reading, PA). The slope of each line used to estimate the selection coefficient of each mutant relative to wild type (Thatcher, et al., 1998).

Ultrastructural Studies

EM of whole yeast cells was performed as follows. Logarithmically growing yeast cells were harvested by centrifugation and fixed in 2% (v/v) formaldehyde, 2% (v/v) glutaraldehyde in pc buffer (170 mM KH_2PO_4, 0.1 mM $MgCl_2$, 30 mM sodium citrate, pH 5.8), for 60 min at 25° C. After fixation cells were washed twice in pc buffer. Cells were resuspended in a minimal volume of 100 mM Tris-Cl, pH 9.4, 10 mM DTT and incubated at 30° C for 10 min. Cells

were washed once in pc buffer and then resuspended in a minimal volume of pc buffer containing 100 µl of glusulase (NEE-154; NEN, Boston, MA), 20 µl of 1% mutanase (NovoZym 234; BiosPacific inc., Emeryville, CA) and 20 µl of 1% zymolyase 20-T per ml of final solution. The digestion of the cell wall was carried out for 2 hr at 30° C and the cells were washed two times in 100 mM sodium acetate, pH 6.1, and incubated in 0.6 M sorbitol, 100 mM sodium cacodylate, pH 7.0, overnight at 4° C Cells were then harvested by centrifugation, post-fixed with 1% (v/v) osmium in 100 mM sodium cacodylate, pH 7.0, for 30 min at 25° C, dehydrated with ethanol and embedded in Epon resin. Samples were thin-sectioned for visualization by transmission EM.

Transmission EM of highly enriched NE fractions was performed essentially as described (Rout and Blobel, 1993). Briefly, NEs and H-NEs (fractions 10 and 15 respectively) were diluted to 1.0 M sucrose with bt buffer and were centrifuged at 67,000 *g* for 15 min at 4° C. The pelleted samples were fixed in 1.0 M sucrose, bt buffer containing 2% (v/v) glutaraldehyde for 1 hr at 25° C. The fixative solution was gently removed and substituted with 2% (v/v) glutaraldehyde in 50 mM potassium phosphate, pH 7.0, and the incubation was continued overnight at 4° C. Samples were post-fixed with 1% (v/v) osmium in the same buffer, dehydrated and prepared for EM visualization as described above.

Transmission EM of isolated yeast nuclei was as follows. Nuclei (fraction 7) were diluted with 1 volume of 1.25 M sucrose in bt buffer and spun at 290,000 *g* for 10 min at 4° C. The nuclei pellet was fixed and prepared for transmission EM analysis as described above, with the exception that the first fixation was performed in 1.25 M sucrose-bt buffer.

Samples of isolated NEs and H-NEs were sedimented on EM grids and negatively stained as described (Rout and Blobel, 1993).

IEM analysis of isolated NEs was performed using a modification of a published procedure (Rout and Kilmartin, 1990; Kraemer, et al., 1995). Four wells were cut out from a 96-wells microtiter plate and were incubated with 2.5% (v/v) glutaraldehyde in water for 30 min at 25° C. The fixative was removed and the wells were washed briefly under flowing water. 100 µl of 1% poly-L-lysine in water were added to each well and the incubation was continued for 30 min at 25° C before washing the wells with water again. Isolated yeast NEs (fraction 10) were diluted with 1 volume of bt-DMSO, transferred to the pre-treated microtiter wells (100 µl of diluted sample per well) and centrifuged at 23,500 *g* for 2 hr at 4° C. The pellets were washed once with bt-DMSO. NE pellets were fixed with 4% (v/v) formaldehyde in bt-DMSO for 5 or 10 min at 25° C and then they were washed twice with bt-DMSO and once with IEM buffer [0.5% BSA, 0.5 x PBS-K (5 mM KH_2PO_4, 20 mM K_2HPO_4, 75 mM NaCl, pH 7.0), 1 mM $MgCl_2$, 10 µM $CaCl_2$, 10 µM $ZnCl_2$, 0.02% sodium azide, 0.2% (v/v) solution P]. The primary antibody was incubated overnight in IEM buffer at 4°C. Samples were washed three times for 30 min each with IEM buffer at 25° C, and incubated with 10 nm gold-labeled affinity purified goat anti-mouse antibody in IEM buffer overnight at 4° C. Samples were washed as above and then twice with 0.5 x PBS-K, 1 mM $MgCl_2$. Gold-labeled NEs were fixed in 1.25% (v/v) glutaraldehyde in 0.5 x PBS-K, 1 mM $MgCl_2$, at 25° C for 2 hr. Fixed samples were post-fixed with 1% osmium in the same buffer and prepared for transmission EM as described above.

IEM of isolated whole nuclei was as follows. Isolated yeast nuclei were subjected to mild osmotic shock by diluting them with 9 volumes of PVP solution. These "broken" nuclei were then transferred (100 µl of diluted sample per well) to microtiter wells that had been pre-treated as described above and centrifuged at 23,500 *g* for 30 min at 4° C. Nuclei pellets were washed twice

with PVP solution at 25° C followed by one wash each for 5 min with the following three solutions: 1) 25% (v/v) M buffer (5% dried milk in bt-DMSO), 75% (v/v) PVP solution; 2) 50% (v/v) M buffer, 50% (v/v) PVP solution; 3) 75% (v/v) M buffer, 25% (v/v) PVP solution. Finally, the nuclei pellets were washed once in M buffer for 5 min at 25° C. Incubations with the primary and the gold-labeled secondary antibodies were as described above with the exception that 5 nm instead of 10 nm gold was used and that IEM buffer was substituted with M buffer. Subsequent steps were also as described above with the following exceptions: 1) 0.5 x PBS-K, 1 mM $MgCl_2$ was substituted with bt-DMSO; and 2) after treatment with osmic acid, samples were post fixed with 1% tannic acid in 50 mM potassium phosphate, pH 7.0 for 30 min at 25° C.

Cell Volume Analysis

Logarithmically growing haploid yeast cells were sonicated for 10 sec to disperse the cell clumps using a Kontes Micro Ultrasonic sonicator (Baxter Healthcare Corporation, McGraw Park, IL) set at 55 output level, harvested by centrifugation and fixed with 4% formaldehyde in 0.1 mM potassium phosphate, pH 6.5, 0.1 mM $MgCl_2$, for 2 hr at 25° C. After fixation cells were washed once in the same buffer and sonicated again as above. Cells were subjected to cell volume analysis using a Coulter channelizer 256 (Coulter Electronics Inc., Hialeah, FL) following the specifications of the manufacturer.

Chromosome Segregation Assay

Determination of the rate of mitotic chromosome III loss was carried out as previously described (Chi and Shore, 1996; Wotton and Shore, 1997). Briefly, average sized single colonies of diploid wild type and mutant cells were resuspended in YPD and sonicated as described above to disperse cell clumps. · Dilutions were spread on YPD plates to determine the viable cell count. Half of each colony was mated with a 100-fold excess of cells from *MATa* and *MATα* haploid tester strains (KMY38α and KMY39a, respectively; generous gift of Erica Johnson) to select for colonies that arose from individual mating events. The chromosome loss rate (number of events per cell per generation) was calculated according to the following formula: rate = (0.4343 x F)/(logN - logN_0) where F = the median mating frequency, N = the number of cells in the colony and N_0 = the number of cells from which the colony arose (Drake, 1970).

Flow Cytometry of Yeast Cells

Logarithmically growing yeast cells (typically 5 ml) were sonicated to disperse cell clumps (as described above), harvested by centrifugation and dehydrated in 2 ml of 70% (v/v) ethanol at 25° C for 12 hr. Cells were washed twice with 1 ml of 50 mM Tris-Cl, pH 7.8 and then resuspended in 1 ml of the same buffer containing 2 mg/ml of DNase free-RNase A. RNA was digested at 37° C for 12 hr. At the end of the incubation, cells were pelleted and digested with 0.5 ml of 5 mg/ml pepsin in 55 mM HCl at 37° C for 30 min to remove the majority of the cellular proteins. Cells were washed once with 1 ml of 200 mM Tris-Cl, pH 7.5, 211 mM NaCl, 78 mM $MgCl_2$, and finally resuspended in 180

mM Tris-Cl, pH 7.5, 190 mM NaCl, 70 mM $MgCl_2$ containing 50 µg/ml of propidium iodide. Shortly after staining the DNA with propidium iodide, samples were analyzed by flow cytometry. 50 µl of each sample were transferred to a 3.5 ml Falcon tube (Falcon 2052; Beckton and Dickison, Franklyn Lakes, NJ), diluted with 2 ml of 50 mM Tris-Cl, pH 7.8 and immediately analyzed using a FacSort flow cytometer (Beckton and Dickinson, Franklyn Lakes, NJ). Data analysis was performed using the CellQuest v 3.1f software provided by the manufacturer of the instrument. Typically, 10,000 individual events were read per sample.

In vivo Import and Diffusion Assays

The *in vivo* import assay was performed essentially as described (Shulga, et al., 1996). Wild type W303 and *mlp1Δ*, *mlp2Δhd* cells were transformed with pGFP-LEU (generous gift from D. Goldfarb), which constitutively expresses GFP (Cody, et al., 1993) fused to the SV40 large T antigen NLS. Only freshly transformed cells were used for each experiment. Cells were grown in selective medium containing 2% dextrose to mid-logarithmic phase, harvested by centrifugation and washed once with sterile water. Washed cells were resuspended in dextrose-free selective medium containing 10 mM each of sodium azide and 2-deoxy-D-glucose (referred to from now on as deoxyglucose) and incubated at 30° C for 45 min to allow the diffusion of GFP out of the nucleus. At the end of this incubation, cells were harvested by centrifugation, washed once with sterile water and pellets were incubated at 4° C until use. The import assay was started by resuspending the pelleted cells in ~5 volumes of pre-warmed selective medium containing 2% dextrose and

placing them at 30° C. At each time point a small aliquot of the cell suspension was placed on a glass slide, mounted with a coverslip and observed at a Zeiss Axiophot fluorescent microscope using the FITC channel. The number of normal cells that showed a clear accumulation of GFP-NLS in the nucleus (nuclear cells) and the number of cells in which the reporter was cytoplasmic were counted at each time point. At least 40 independent cells were scored per time point. At least 4 independent sets of cells were counted to construct the graph presented in Fig. 24. The results are presented as the percentage of cells presenting nuclear signal as a function of time. Linear regression lines were drawn through the linear portion of each curve using KaleidaGraph and the slope of these straight lines were used to estimate the relative import rates.

Passive diffusion assays were performed as follows. pGFP-LEU transformed wild type and mutant cells were grown as described in the previous paragraph. Cells were harvested by centrifugation and resuspended in 1/5 of the initial volume of selective medium. Resuspended cells were held at 4° C until use. The diffusion assay was started by centrifuging the cells, washing them once in sterile water, resuspending them in 1 volume of 10 mM sodium azide and 10 mM deoxyglucose in dextrose-free selective medium and finally placing them at 30° C. Aliquots were taken at each time point and scored as described above. At least 3 independent sets of 40 cells were scored at each time point. The relative passive equilibration rates were estimated as described for the import rates.

Overexpression of *MLP1*

In order to achieve the overexpression of Mlp1p in yeast cells, the *MLP1* gene was inserted into the pYES2 yeast expression plasmid (Invitrogen Corporation, Carlsbad, CA) downstream of the *GAL1/10* inducible promoter. Briefly, the unique BspHI site located at nucleotide position 4958 of pYES2 was disrupted using the Klenow fragment of DNA polymerase I to generate pYES2-no BspHI. DNA from the λ clone λPM-5620 (Olson, et al., 1986; ATCC catalog number 70598; America Type Culture Collection, Rockville, MA) containing a yeast genomic fragment of ~16800 bp from chromosome XI (chromosome bp coordinates: 611843-628638), was used as the template to generate a ~650 bp PCR product containing the 5' region of *MLP1* from nucleotide position -12 (relative to the first bp of the coding region) to nucleotide position +634 flanked by a BamHI site at the 5' end. This PCR product was cut with BamHI and EcoRI (site located at nucleotide position +572 of the MLP1 coding region) and inserted into the BamHI and EcoRI sites of pYES2-no BspHI, to generate pYES2-570MLP1. Finally, a ~5900 bp BspHI fragment of λPM-5620 that contains the entire *MLP1* coding region except the first 8 bp, was inserted into pYES2-570MLP1 that had been linearized with BspHI (site located at nucleotide position +8 of the *MLP1* coding region) to generate pGALMLP1.

pGALMLP1 was transformed into W303 cells by electroporation and transformants were selected taking advantage of the *URA3* selectable marker present on the plasmid. Only freshly transformed cells were used for each experiment. In order to induce the expression of *MLP1*, W303/pGALMLP1 cells were grown to mid-logarithmic phase in selective medium containing 2% D(+)-raffinose (referred to as raffinose throughout the text), transferred to selective medium containing 1% raffinose and 2% galactose and incubated at 30° C for up to 4 hr. For repression of *MLP1* expression, W303/pGALMLP1 cells were

grown in raffinose as above, transferred to selective medium containing 1% raffinose and 2% dextrose and incubated for 4 hr at 30° C.

Miscellaneous

Protein concentrations were measured by either the modified Bradford assay of Pierce (Coomassie Plus; Pierce, Rockford, IL), or the amido-black assay (Rexach, et al., 1994), using BSA as a standard. SDS-PAGE and immunoblotting were performed essentially as described (Rout and Blobel, 1993). Proteins were precipitated with methanol as follows. Briefly, 9 volumes of methanol were added to the protein sample and the mixture was incubated at -20° C for 1 hr. At the end of the incubation, the sample was centrifuged at 15,000 *g* for 1-2 hr at 4° C. The supernatant was discarded by inversion and the remaining traces of methanol were removed by aspiration without disturbing the pellet. The pellet was air-dried very briefly and the protein sample was resuspended in an opportune amount of protein loading buffer for electrophoretic analysis.

Detergent extracted H-NEs were produced by a pretreatment of the sample on the EM grid in 1.5% (v/v) Triton X-100, 2.0% digitonin in bt buffer for 15 min at 25°C immediately prior to fixation. Highly enriched NPCs (Rout and Blobel, 1993) were extracted with heparin by mixing 5 ml of the sample with 20 ml of 10 mg/ml heparin in bt-DMSO and incubating on ice for 30 min. After the extraction, the heparin-resistant material was sedimented over a EM grid and negatively stained as previously described (Rout and Blobel, 1993).

The intensity of bands on immunoblots was quantified either using the ImageQuant v 1.1 software in the PhosphorImager system (Molecular

Dynamics, Sunnyvale, CA; Figs 8 and 16, *Nuclei Prep, NE Prep*). Occasionally, computer images of ECL signals on photographic films were quantified using the Gel plotting macro of NIHImage v 1.60 (Research Services Branch, National Institute of Health, Bethesda, MD).

Cells were prepared for indirect IF microscopy using the procedure of Kilmartin and Adams (Kilmartin and Adams, 1984) with the modifications of Wente et al. (Wente, et al., 1992) and Kilmartin et al. (Kilmartin, et al., 1993). Double labeling with the mouse MAb118C3 and a polyclonal rabbit anti-Sec61p antibody (Stirling, et al., 1992) was visualized using Cy3-labeled polyclonal donkey anti-mouse IgG (cross absorbed against rabbit IgG) and FITC-labeled polyclonal donkey anti-rabbit IgG (cross absorbed against mouse IgG) (Jackson ImmunoResearch Laboratories, West Grove, PA). Double labeling with MAb215B9 and a polyclonal rabbit anti-Nsp1p antibody (Nehrbass, et al., 1990) was visualized using the same procedure. In all single labeling experiments, the bound antibody was visualized using Cy3-labeled polyclonal donkey anti-mouse or anti-rabbit IgG (Jackson ImmunoResearch Laboratories, West Grove, PA). The staining and photomicrographic recording conditions were as described (Wente, et al., 1992).

Yeast genomic DNA preparations were as previously described (Hoffman and Winston, 1987). Yeast whole cell lysates were prepared as follows. Cells were grown to mid-logarithmic phase and harvested by centrifugation. Pellets were solubilized in 1.85 M NaOH, 7.4% (v/v) β-mercaptoethanol (BME) for 10 min at 4° C. An equal volume of 50% TCA was added to the samples and the incubation was continued for 10 min at the same temperature. Samples were spun at 15,000 *g* for 10 min at 4° C and the pellets were washed once with pre chilled acetone. Pelleted samples were solubilized in 5% SDS, 0.5 M Tris-base by sonication and were heated to 95° C for 10 min. An equal volume of 40%

glycerol, 200 mM DTT, 0.002% bromophenol blue was added and samples were heated again as above before SDS-PAGE analysis.

Chapter III: Isolation And Characterization Of Nuclear Envelopes From The Yeast *Saccharomyces*

Comments on the Procedure

An excellent starting point for the preparation of NE fractions was provided by the yeast nuclear isolation method described by Kilmartin. Thus fractions 1 to 8 of the procedure described here (Fig. 1), which included the nuclei (fraction 7), were prepared as reported (Kilmartin and Fogg, 1982; Rout and Kilmartin, 1990). To be useful as a more general assay for subfractionation, as well as a preparative method for NEs, the NE enrichment procedure needed to have a considerably higher yield and degree of enrichment than previous techniques (Kilmartin and Fogg, 1982; Mann and Mecke, 1982; Mann and Mecke, 1982). It was also of primary importance to retain, when possible, the morphological (and potentially functional) characteristics of intact NEs.

The mild buffer conditions previously determined to be favorable for nuclear fractionation were retained for the preparation of NEs (Kilmartin and Fogg, 1982; Rout and Kilmartin, 1990; Rout and Blobel, 1993). Nuclei were lysed in bt-DMSO in the presence of DNase. The presence of DMSO appeared to lessen the osmotic shock to the NEs during nuclear lysis in addition to its stabilizing effect on spindles and NPCs (Rout and Kilmartin, 1990; Rout and Blobel, 1993). By increasing the density of the nuclear lysate with sucrose and Nycodenz, the NEs could be made to float to their buoyant density on an equilibrium sedimentation gradient, away from denser protein and nucleoprotein contaminants. The presence of Nycodenz in the adjusting solution reduced the viscosity of the resulting adjusted lysate, increasing the

yield by ensuring the rapid egress of even the smaller NE fragments from the lysate. It also allowed a lower osmolarity, which reduced the osmotic shock to the NEs, especially when floating from the lysate into the lighter layer above. An appropriate step gradient was chosen to concentrate the NEs at a single step interface. The relatively narrow range of NE densities is evidenced by the high yield of NEs recovered in this layer (see below).

For the removal of the peripheral NE proteins and nucleoproteins, a heparin treatment was chosen instead of the more usually employed high pH treatments (Fujiki, et al., 1982) for two main reasons. First, the heparin treatment was performed in mild buffer conditions similar to those of the NE isolation procedure, lessening the chances of compromising membrane integrity or damaging membrane-bound complexes. Second, it proved especially efficient at removing the most significant peripheral NE "contaminants": chromatin (Courvalin, et al., 1982; Rout and Blobel, 1993) and ribosomes. Indeed, purified yeast ribosomes were reduced from their normal sedimentation coefficient of 80 S to < 6 S by this treatment (data not shown). It was also known that high heparin concentrations would disassemble NPCs (Rout and Blobel, 1993; see below). The heparin-extracted material was run on a 10-40% (w/v) sucrose gradient and the sedimentation profile of the nucleoporins recognized by MAb414 and MAb350 was analyzed (Davis and Fink, 1990; Rout and Blobel, 1993). As expected, all of the detectable extracted nucleoporins displayed a behavior consistent with a sedimentation coefficient of < 6 S (data not shown). A treatment with RNase was performed because although it did not have a significant effect on the protein composition of H-NEs, it was shown to effectively remove contaminating ribosomal RNA from this fraction (data not shown). This indicates that RNase digestion can be eliminated without significantly altering the efficiency of the heparin extraction

procedure. The great disparity in size between the extracted material and the remaining H-NE membranes allowed the latter to be sedimented away from the former by a rapid centrifugation step.

Figure 1. Schematic diagram of the yeast NE enrichment and NE heparin extraction procedures.

Numbers enclosed in circles represent the fraction numbers as described in Materials and Methods and in the text. The NE-containing fractions are indicated in bold type.

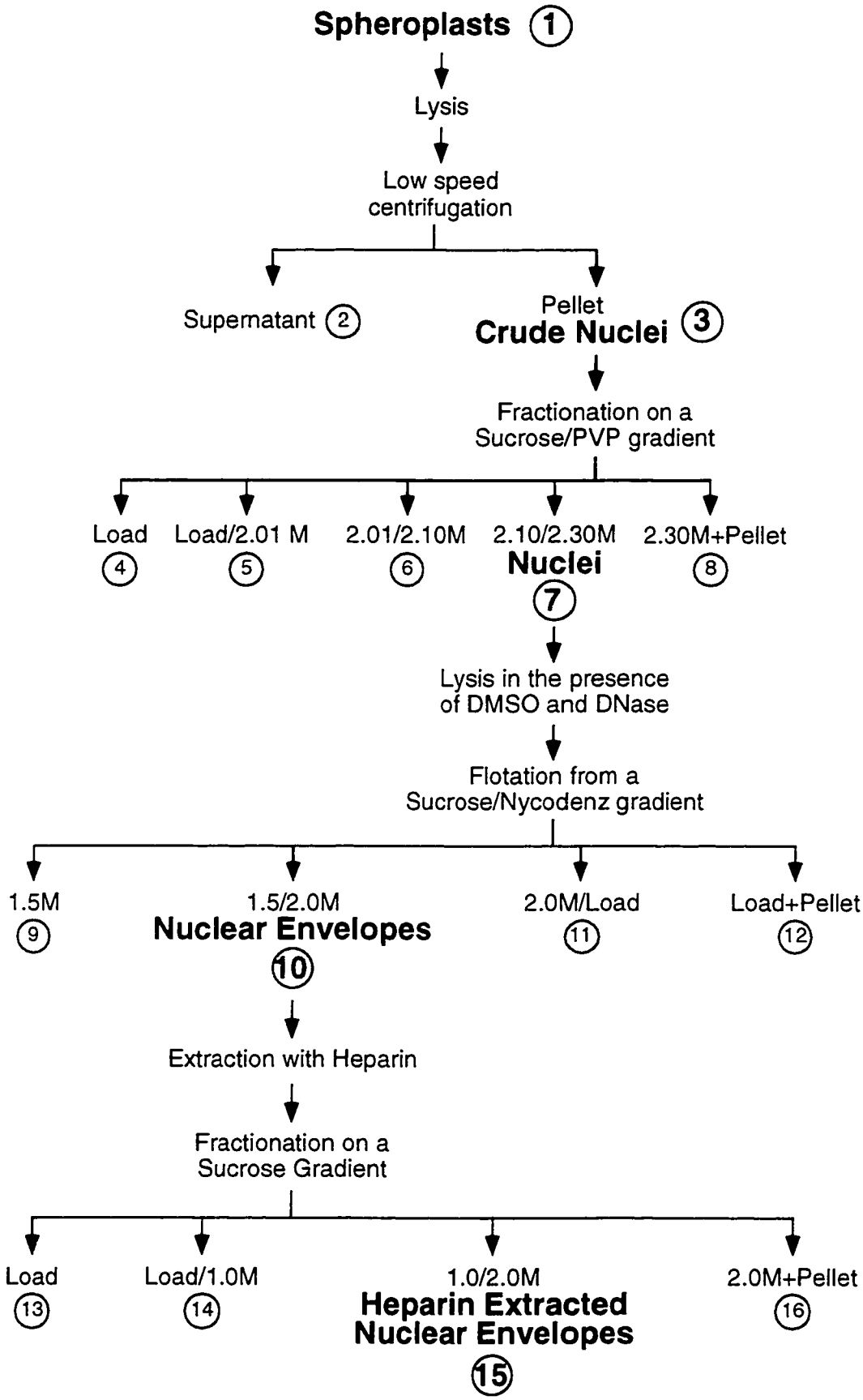

Electron Microscopy of the NE Fractions

The NE and H-NE fractions were examined in detail by transmission EM of both negatively stained spreads and thin sections of pelleted material (Fig. 2). The NE fraction (Fig. 2 *A* and *C*) consisted mainly of large sheets of double membranes. Significant regions of these had blebbed and ballooned (which is not generally seen in the NEs of thin sectioned whole cell preparations), probably as a result of osmotic shock during nuclear lysis. The sheets were interrupted by numerous grommets, and the holes formed by these contained thin disks of relatively dense material. These structures were morphologically recognizable as NPCs in both transverse and tangential sections and negatively stained preparations. No clear examples of ordered filamentous structures could be found on either side of the transversely sectioned NPCs. The NPCs were present at ~30/mm^2 in the negatively stained NEs (Fig. 2*C*), two to three times the figure estimated for intact nuclei (Mutvei, et al., 1992; Rout and Blobel, 1993). This considerable increase in density could be due to contraction of NEs no longer kept under elastic tension by underlying chromatin and associated structures, which might be exacerbated by osmotically induced swelling of the cisternal spaces between the NPCs. SPBs could also be found, still inserted in the NE and retaining many of their nuclear MTs, attesting to the mild isolation conditions used (Fig. 2 *A* and *C*). The presence of these MTs indicates that the NE fraction would be active in a MT nucleation assay (Kilmartin and Fogg, 1982; Rout and Kilmartin, 1990). The alignment of the asymmetric SPBs within the envelope unequivocally established the cellular orientation of the two membranes (reviewed in, Kilmartin, 1994). Many of the NEs retained their normal nuclear direction of curvature; concave on the nuclear (inner) side, convex on the cytoplasmic (outer) side. The exposed

surfaces of the inner membranes were largely devoid of any material, including chromatin and any recognizable lamina (Fig. 2 *A*). In sharp contrast, the outer membranes often had exposed surfaces densely studded with ribosomes (Fig. 2 *A*). These were present at ~800/mm^2 in the negatively stained NEs (Fig. 2 *C*), giving roughly 25 ribosomes per NPC (this latter figure should be independent of shrinkage or swelling of the NE and thus represent the *in vivo* figure more closely). The perinuclear cisternae generally contained low amounts of electron dense material, though some contained considerably more than others. The fraction contained no other recognizable organelles, except for occasional small remnants of undigested cell walls.

Many of the H-NEs were also recovered as large double-membraned sheets (Fig. 2 *B* and *D*). They appeared more ballooned and fragmented than the NE but their cisternae still contained electron dense material in thin sections (Fig. 2 *B*). However, they lacked any trace of ribosomes, by either thin section or negative stain (Fig. 2, *B* and *D*). The SPBs had apparently been removed from the envelopes, although by thin section occasional examples of heparin-extracted SPBs could be found free of membranes (Rout and Kilmartin, 1990). Thus, although many of the H-NEs were curved, there was no morphological marker left to tell whether they retained the native direction of curvature, like the NEs. Strikingly, the NPC grommets still remained, with the resulting holes being of approximately the same size and frequency as those found in the NEs, although the dense material comprising the morphologically recognizable NPC structure had been removed (Fig. 2 *B* and *D*). This indicates that despite the removal of the peripheral NPC components (see also below), integral and probably lumenal components of the NE that maintained the original circular architecture of the NPCs had been retained. The only recognizable

contaminants were occasional cell wall remnants, carried through from the NE fraction.

Figure 2. Morphological analysis of the NE and H-NE fractions.

(A and B) Transmission electron micrographs of pelleted, thin sectioned NEs (A) and H-NEs (B). (C and D) Transmission electron micrographs of negatively-stained NE (C) and H-NE (D) fractions. (A) The following structures are indicated: outer nuclear membrane (*open arrowhead*); inner nuclear membrane (*closed arrowhead*); longitudinal (*large open arrow*) and tangential (*large closed arrow*) sections of NPCs; SPBs and attached MTs (*small arrows*). (B, C and D) Circular apertures left by the extraction of NPCs are indicated (*large closed arrows*) as well as MTs (*small arrow*). Bar, 1 μm.

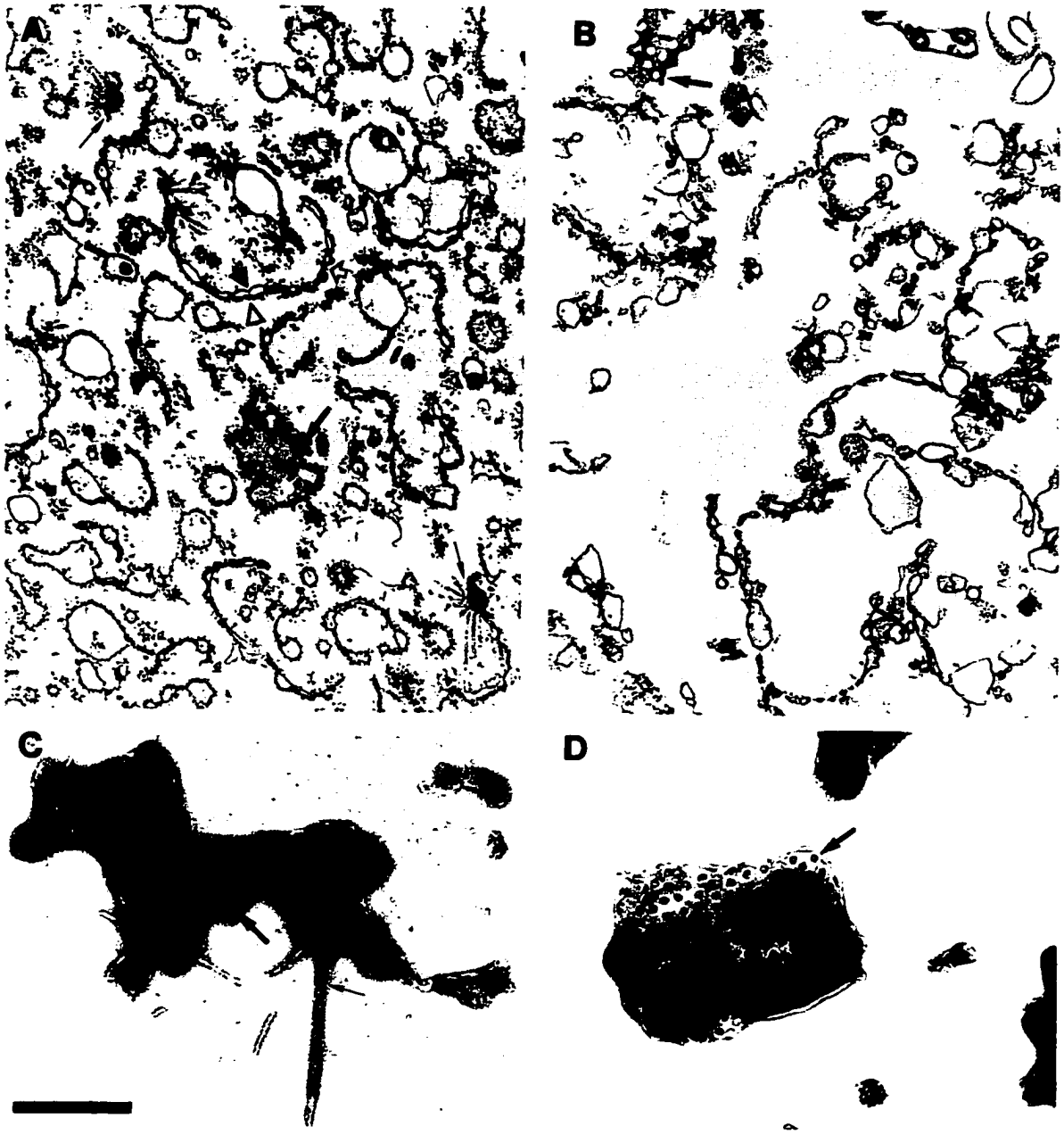

SDS-PAGE Analysis and Immunoblots

To determine the protein composition and purity of the NE and H-NE fractions, the enrichment procedure was subjected to biochemical and immunological analyses. Protein samples obtained from each of the fractions collected during the preparation of isolated NEs and H-NEs (Fig. 1) were resolved by SDS-PAGE. To compare the novel heparin stripping procedure with the standard carbonate extraction method (Fujiki, et al., 1982), yeast isolated NEs (fraction 10) were treated with sodium carbonate and the carbonate-resistant material (*Carbonate Extracted NEs*) was run side by side with H-NEs on a protein gel (Fig. 3).

Inspection of Fig. 3 reveals that the overall complexity and abundance of the proteins present in each of the enrichment steps decreased during fractionation. Furthermore, the fractionation behavior of specific supermolecular structures was followed by virtue of the characteristic banding pattern of certain of their components on SDS gels. Chromatin is represented by the four yeast histones (Fig. 3, *dots*) which were mainly lost after nuclear lysis and totally removed by heparin extraction. Characteristic ribosomal bands (Fig. 3, *asterisks*) were lost throughout the enrichment procedure and their complex behavior will be discussed below. Three bands are known to contain known NPC and pore membrane proteins (Fig. 3, *arrows*); all coenriched with the NEs but only one, containing Pom152p (a pore membrane specific integral membrane protein) was found in the H-NEs (Wozniak, et al., 1994; J. D. Aitchison, U. Nehrbass, M. P. Rout and R. W. Wozniak, unpublished observations). The comparison of carbonate-extracted NEs with H-NEs (Fig. 3) revealed that the protein composition of these two fractions was similar, suggesting that heparin is at least as efficient as carbonate in the removal of

peripheral proteins from the nuclear membranes. On the other hand, certain specific proteins that were quantitatively removed by carbonate were retained after heparin extraction and *vice versa*. For example, the ribosomal markers appeared to be stripped by heparin with greater efficacy than by carbonate.

In order to assess the degree of enrichment of isolated NEs and H-NEs, the percentage yields of cytoplasmic, nucleoplasmic, NE specific (peripheral and membrane-bound), ER-specific and ribosomal proteins were estimated by quantitative immunoblotting. The yields of the NE components were used together with measurements of the total amount of protein in each fractions to generate fold-enrichments for NE-containing fractions. These data allowed the construction of a balance-sheet of the distributions of various cellular proteins and their associated organelles in the different steps of the fractionation procedure (Figs. 4, 6 and 8).

Analysis of three non-NE proteins from the mitochondria, the Golgi apparatus and nucleolus demonstrated that potential cytoplasmic and nucleoplasmic contaminants were efficiently removed from the NE fractions. Mitochondria were followed by use of the integral membrane protein p32 (Pain, et al., 1990). As expected virtually all of the signal fractionates away from NE specific markers early in the procedure; most of this protein remains in the top two fractions of the nuclear gradient (Fig. 4*A*, fractions *4* and *5*). Quantitative immunoblotting showed that less of 0.04% of the total cellular amount of p32 remained associated with isolated NEs and that less than 0.01% of this signal was associated with the H-NE fraction (data not shown). The integral membrane protein of the Golgi, Sed5p (Hardwick and Pelham, 1992), was mainly found in the crude cytosol fraction (Figs. 4*B* and 8*D*, fraction *2*; 79% of the total cellular signal). Approximately 90% of the crude nuclei pool of Sed5p (19% of the total), remained at the top of the nuclear gradient (Figs. 4*B* and 8*D*,

fractions *4* and *5*). The small remaining amount fractionated with the nuclei, NEs and H-NEs (Figs. 4*B* and 8*D*, fractions *7*, *10* and *15*, respectively), consistent with this being an integral membrane protein that is involved in ER to Golgi transport and therefore can be expected to be present, at least in small quantities, also in the ER (Hardwick and Pelham, 1992; C. Hopkins, personal communication). The nucleolar protein Nop1p coenriches with the nuclei but was rapidly removed from the NE after nuclear lysis (Fig. 4*C*; Aris and Blobel, 1988). Quantification of the immunoblot presented in Fig. 4*C* demonstrated that only approximately 1.4% of Nop1p fractionated with the NEs and that Nop1p was undetectable in the H-NE fraction (data not shown).

Peripheral NE proteins, represented here by two SPB proteins p90 and Spc110p/Nuf1p, and various known NPC proteins (nucleoporins) detected by MAb350 and MAb414, cofractionate with the NE until they were lost after treatment with heparin (Figs. 4*D*, *E*, *F* and 8*A*; Rout and Kilmartin, 1990; Kilmartin, et al., 1993). An exception was represented by Nup2p (Fig. 4*F*, indicated by *white dots*), which falls off after DNase digestion of the nuclear fraction as it does in the NPC isolation procedure (Loeb, et al., 1993; Rout and Blobel, 1993). Spc110p/Nuf1p was partially retained (~10%) in the heparin stripped NE fraction. This could be a consequence of its localization within a heparin-resistant substructure of the SPB, that may be removed from the NE but not solubilized during the extraction procedure (Rout and Kilmartin, 1990; Rout and Kilmartin, 1991), a hypothesis supported by the EM data (above). The intensities of the signals generated by p90(SPB) (Fig. 4*D*), Spc110p/Nuf1p (Fig. 4*E*) and the 65 kD fragment of Nup145p (*p65(NPC)*, Fig. 4*F*; Wente and Blobel, 1994) were measured and averaged to estimate the overall percentage yield of peripheral membrane proteins of the NE (Fig. 8*A*). Approximately 80% of the total peripheral NE components was recovered in fraction *10* (isolated NEs),

representing a more than 90% yield as compared to the nuclear fraction (fraction *7*). The great majority of this signal was removed after heparin treatment (94% of the NE signal, totaling 95% of the original cellular signal). This may in fact underestimate the efficiency of the extraction of many proteins due to the somewhat unrepresentative behavior of Spc110p/Nuf1p (discussed above); for example, p65(NPC) was extracted with an efficiency greater than 98% (data not shown).

Since a NE specific membrane marker was not available, one was made by raising mAbs against the H-NE fraction (see Chapter IV). One of these was found to recognize a single band of ~150 kD in isolated NEs, H-NEs and highly enriched NPCs (Rout and Blobel, 1993). We used two approaches to demonstrate that this antibody, MAb118C3, specifically recognizes Pom152p (Fig. 5). First, MAb118C3 recognizes a single band of the expected mobility in both isolated nuclei and NEs prepared from wild type yeast cells and it fails to do so in NEs similarly prepared from a *POM152* knock-out strain (PM7AB; a diploid *S. cerevisiae* strain homozygous for *pom152-2::HIS3*; generous gift from R. W. Wozniak). Second, this same antibody reacts with a single band of 150 kD present in chromatographic fractions highly enriched for Pom152p (SDS-hydroxylapatite fraction 36 and HPLC fraction 69; Wozniak, et al., 1994). MAb118C3 was used to monitor the fractionation pattern of the wild type Pom152p protein throughout the various steps of the NE, H-NE and NPC preparations (Figs. 6 and 8*B*). As expected, Pom152p was shown to coenrich with both the NE and H-NE as well as the highly enriched NPC fraction. Surprisingly, a significant amount (29%) of the signal fractionates together with rough ER markers (fractions *4* and *5*). The majority (82%) of the nuclear associated Pom152p (42% of the total cellular amount) was recovered in the NE fraction similar to the behavior of the peripheral markers. Furthermore,

nearly 90% of this signal was resistant to heparin extraction in contrast with the peripheral NE components. To confirm that this result reflects the *in vivo* subcellular localization of Pom152p, logarithmically growing cells were stained with both MAb118C3 and a rabbit anti-Sec61p polyclonal antibody and viewed by indirect IF microscopy (Fig. 7). Indeed, this shows that whilst the majority of Pom152p was localized at the NE, a certain amount of this protein was found at the peripheral ER. A *POM152* knock-out strain (PM152-75; a haploid *S. cerevisiae* strain carrying *pom152-2::HIS3*; J. Aitchison, M. P. Rout, G. Blobel and R. W. Wozniak, unpublished results) was examined by indirect IF under conditions similar to the ones used for the experiment presented in Fig. 7. As predicted no signal was detected, either at the nuclear rim or at the cellular periphery where ER staining would have been expected (data not shown).

The behavior of ER proteins during the enrichment procedure was monitored using the ER markers Sec61p, Cytochrome P450 reductase and Kar2p/Bip (Figs. 4 *H*, *I*, *J* and 8*C*; Yabusaki, et al., 1988; Normington, et al., 1989; Rose, et al., 1989; Rothblatt, et al., 1989). As expected the majority of each ER marker was found in fractions *4* and *5*. However, approximately 20% of each ER marker was found associated with the nuclei (fraction *7*). Subfractionation of the nuclei showed that all three proteins coenriched absolutely with the NEs. The extent to which each of the ER markers cofractionated with the H-NE fraction correlated with their degree of association with the ER membrane. Hence, the integral membrane protein Sec61p coenriched absolutely with H-NEs (Fig. 4*J*). Cytochrome P-450 reductase was more easily extracted by heparin, consistent with previous observations (Black and Coon, 1982; Yabusaki, et al., 1988; Fig. 4*I*). Roughly half of the rough ER lumenal protein Kar2p/Bip (55%; data not shown) was resistant to heparin extraction (Fig. 4*H*). This could indicate that a substantial proportion of this

protein is protected from heparin because it is enclosed in intact membranous compartments (i.e. perinuclear cisternae). This explanation is unlikely since approximately 80% of Kar2p/Bip present in both NE fractions is sensitive to trypsin (data not shown), suggesting that the majority of the perinuclear cisternae is accessible to heparin but not efficiently extracted by it.

Ribosomes were followed using a mAb against the large subunit protein, L3 (Fried and Warner, 1981; Figs. 4*G* and 8*E*). The fractionation pattern was complex but as expected this ribosome marker was observed to associate with cytosolic ribosomes (fraction *2*) and ER-bound ribosomes (fractions *4* and *5*). The L3 cofractionating with the nucleus (fraction *7*) appeared to be associated with two different nuclear compartments, which were separated during the preparation of isolated NEs. 27% of the nuclear L3 was found in the ribosomes bound to the outer surface of the NE (fraction *10*). The remaining 73% (fractions *11* and *12*, 7% of the total) was found in fractions containing the nuclear and nucleolar remnants. As this antibody stains the cytoplasm and the nucleolus but not the rest of the nucleus by indirect IF microscopy (data not shown), the remaining signal is believed to represent the ribosomal proteins associated with nucleolar pre-ribosomal structures. Greater than 93% of the NE-bound protein was removed upon heparin extraction of the NE fraction, leaving only 0.2% of the total cellular ribosomal protein bound to the nuclear membrane after heparin treatment.

The removal of contaminating proteins was dramatically demonstrated in Fig. 8*F*, where less than 1% of the total cellular protein was present in the NE fraction (fraction *10*) while less than 0.2% was associated with the H-NE (fraction *15*). These data were used in combination with the numbers representing the percentage yield of nuclear membranes in fractions *1*, *3*, *7*, *10* and *15* [generated from the yields of peripheral NE proteins (fractions *1-12*) and

Pom152p (fractions *13-16*)] to calculate the approximate degree of enrichment of NEs throughout the fractionation procedure (Fig. 8*G*). As can be seen the enrichment of the NE and H-NE fractions was roughly 100-fold and 340-fold respectively, which represent a 68% overall recovery of nuclear membranes. The degree of enrichment of the NE and H-NE fractions described here was highly reproducible between preparations (data not shown). Similar preparations have been successfully made, with minor technical modifications, from numerous other *S. cerevisiae* strains (see for example Fig. 5)

Figure 3. SDS-PAGE profile of proteins in subcellular fractions obtained during the preparation of NEs and H-NEs showing the loss of a large amount of contaminating proteins and concomitant coenrichment of representative NE proteins.

(Left and Middle panels) Yeast cells were subjected to subcellular fractionation as described in Fig. 1 and in the text. (Right panel) NEs were treated with carbonate to remove peripheral membrane proteins and the carbonate-resistant material (Carbonate Extracted NEs) was directly compared with similar amounts H-NEs (Heparin-extracted NEs). Proteins present in each of these fractions were resolved on a 5-20% polyacrylamide SDS gel. The gel was first stained with Coomassie brilliant blue (Coomassie stain) and then stained with silver (Coomassie-Silver stain). The lane number at the top of the gels reflects the fraction number (Fig. 1). Total cell lysate (Spheroplasts) and subsequent fractions containing NEs are indicated. Fractions that belong to each of the four enrichment steps are grouped as indicated by brackets at the top and bottom of the gels. The figures below the bottom brackets (Loading equivalents) represent the number of cell equivalents (n) that were used as a starting material to prepare each of the fractions. This number had to be increased from left to right to allow the detection of single proteins in the final lanes. Histones (*dots*), three characteristic bands containing known nuclear pore proteins (*arrows*: the lowest band is Pom152p, a pore membrane protein) and three representative ribosomal markers (*asterisks*, right panel) are indicated. *Arrowheads* point to a band that is believed to be the RNase A introduced in the course of heparin extraction. Numbers at the side of the left panel indicated the position of the molecular weight standards.

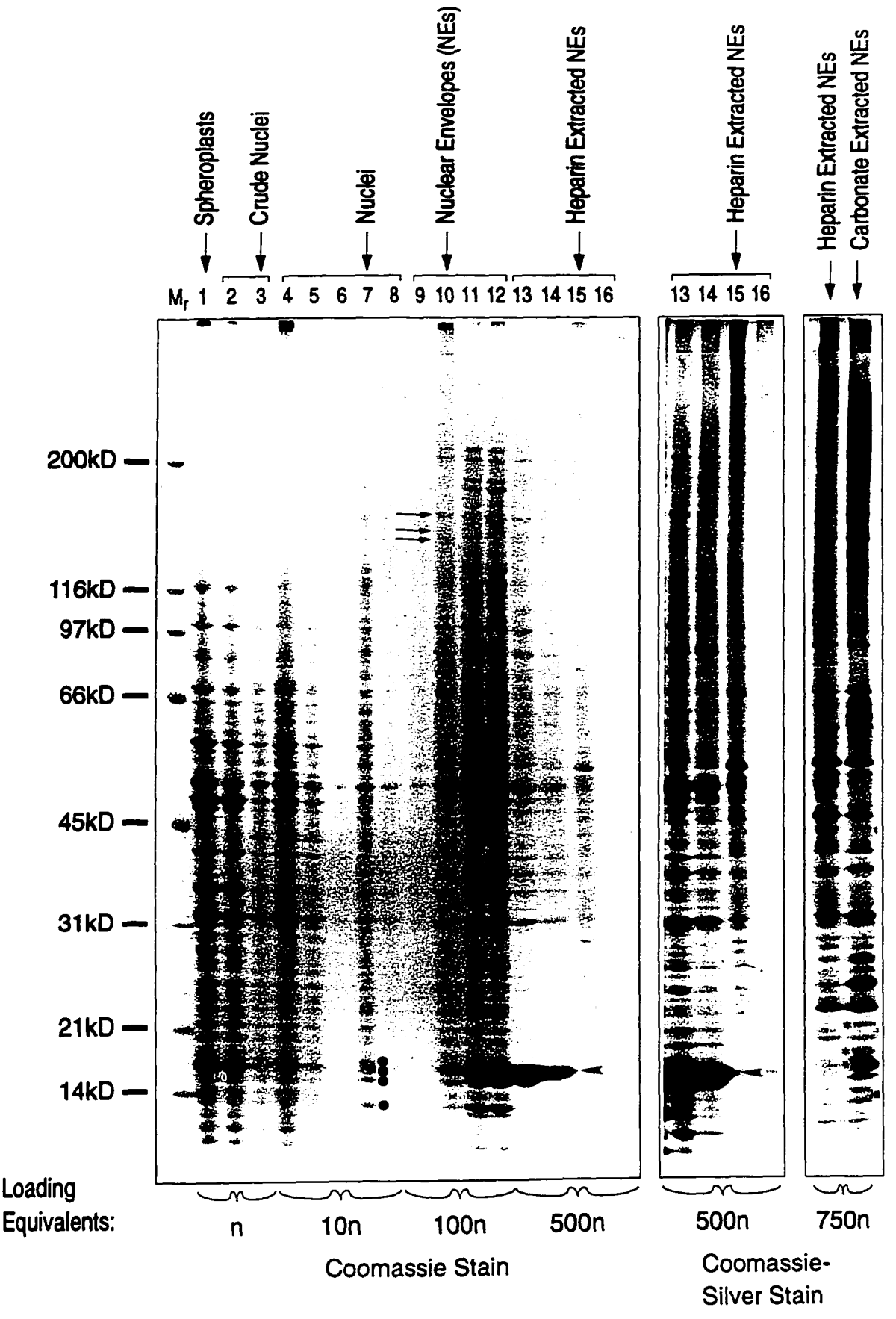

Figure 4. Immunoblot analysis of the enrichment procedure showing that the fractionation behavior of various cellular markers is consistent with high yields and low levels of contamination in the NE and H-NE fractions.

Fractions were prepared as described in Fig. 1 and in the text. Gels were exactly as described in Fig. 3. Blots were incubated in the presence of the various antibodies which were detected by incubation with a secondary rabbit anti-mouse antibody (in the case of the mAbs) and subsequently with [^{125}I]-conjugated protein A. (*A*) The integral membrane mitochondrial protein, p32, detected with a polyclonal rabbit serum (Pain, et al., 1990). (*B*) The integral membrane protein of the Golgi, Sed5p, detected with an affinity purified polyclonal rabbit serum (Sogaard, et al., 1994). (*C*) The nucleolar protein Nop1p, detected with the mAb D77 (Aris and Blobel, 1988; Henriquez, et al., 1990). (*D*) The SPB peripheral membrane protein, p90, detected by the use of the mAbs, 35B5 and 48B6 (Rout and Kilmartin, 1990). (*E*) The SPB component Spc110p/Nuf1p detected with a mix of the mAbs, 3D2, 45D10 and 35A11 (Rout and Kilmartin, 1990). (*F*) Various peripheral nuclear pore proteins revealed by utilizing MAb414 and MAb350. NUP1^{X}, indicates the overlapping signal of Nup1p (Davis and Fink, 1990) and Nup116p (Wente, et al., 1992). Similarly, NSP1^{X}, indicates Nsp1p (Nehrbass, et al., 1990) and Nup100p (Wente, et al., 1992). These mAbs also recognize Nup2p (*white dots*), p65 (a 65 kD breakdown product of Nup145p), Nup57p (Grandi, et al., 1995) and Nup49p (Wente, et al., 1992). Other non-specifically cross-reacting proteins are detected by this antibody and they were described elsewhere (Davis and Fink, 1990; Rout and Blobel, 1993). (*G*) The mAb, TCM1, was used to follow the ribosomal marker, L3 (generous gift of S. P. Johnson and J. R. Warner). (*H*) The lumenal heath-shock protein of the ER, Kar2p/Bip was detected using the mAb, 2E7 (Napier, et al., 1992). (*I*) A rabbit antiserum was used to recognize the ER membrane-associated protein, Cytochrome P450 reductase (Sutter and Loper, 1989). (*J*) The integral membrane protein of the ER, Sec61p, was detected with a rabbit anti-peptide serum (Stirling, et al., 1992). The lanes are

numbered as in Fig. 3. The NE containing fractions are indicated above the blots. *Loading Equivalents*, see legend of Fig. 3.

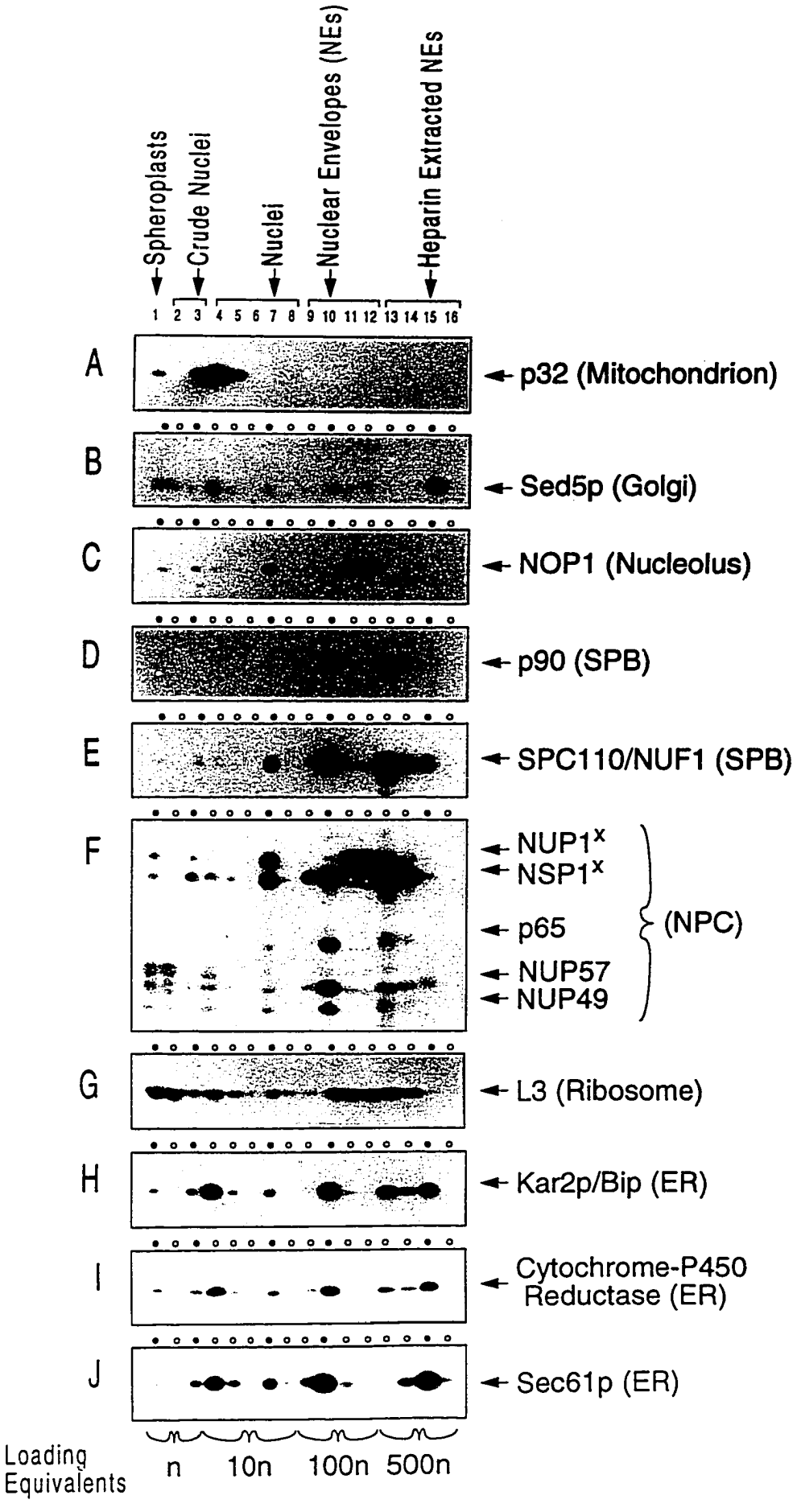

Figure 5. The mAb, MAb118C3, specifically recognizes the pore membrane protein, Pom152p.

Yeast nuclei (lane 1) and NEs (lane 2) were prepared following the procedure presented in Fig. 1 and in the text. NEs were also prepared from wild-type *S. cerevisiae* yeast cells (W303; lane 3) and from a *POM152* knock-out strain (PM7AB; lane 4), using the same method. S. uvarum cells were fractionated as described (Wozniak, et al., 1994), to produce chromatographic fractions highly enriched for Pom152p [SDS-hydroxylapatite fraction number 36 (lane 5) and HPLC fraction number 69 (lane 6)]. Equal protein amounts from the above mentioned fractions were resolved on SDS-PAGE and transferred to a nitrocellulose filter. The blot was incubated with MAb118C3 and bound immunoglobulin was detected by ECL (Amersham Life Science, Arlington Heights, IL), following the instructions of the manufacturer. The position of Pom152p (*POM152*) is indicated. Numbers on the right of the gel denote the position of molecular weight standards.

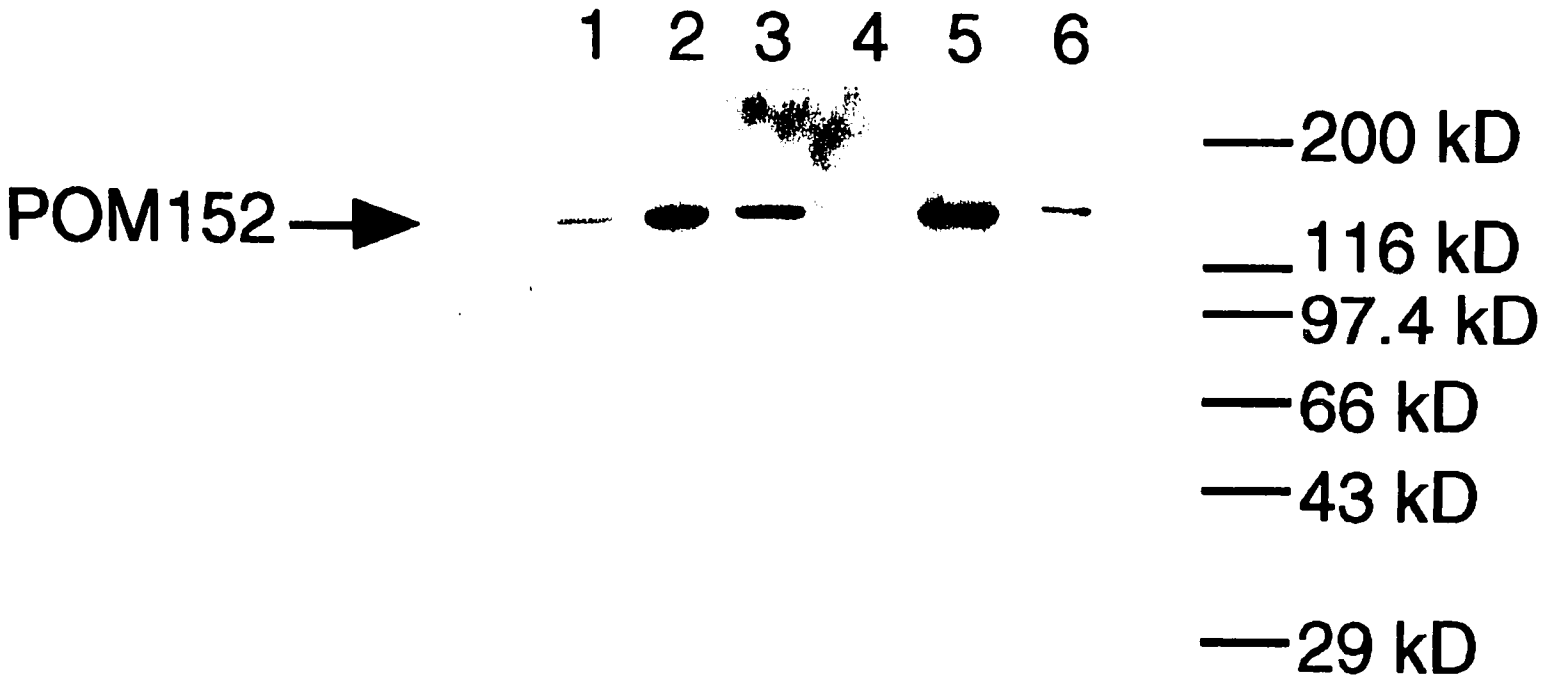

Figure 6. The pore membrane protein, Pom152p, coenriches with both a highly-enriched NPC fraction and with nuclear membranes.

Yeast nuclei (*Nuclear Prep*; Rout and Kilmartin, 1990) were used as the starting point for the preparation of either the NE and H-NE fractions (*NE Prep*) or of a highly enriched NPC fraction (*NPC Prep*; Rout and Blobel, 1993). Blots similar to the ones used in Fig. 4 and the ones described by Rout and Blobel (Rout and Blobel, 1993) were probed with MAb118C3 that reacts against Pom152p.

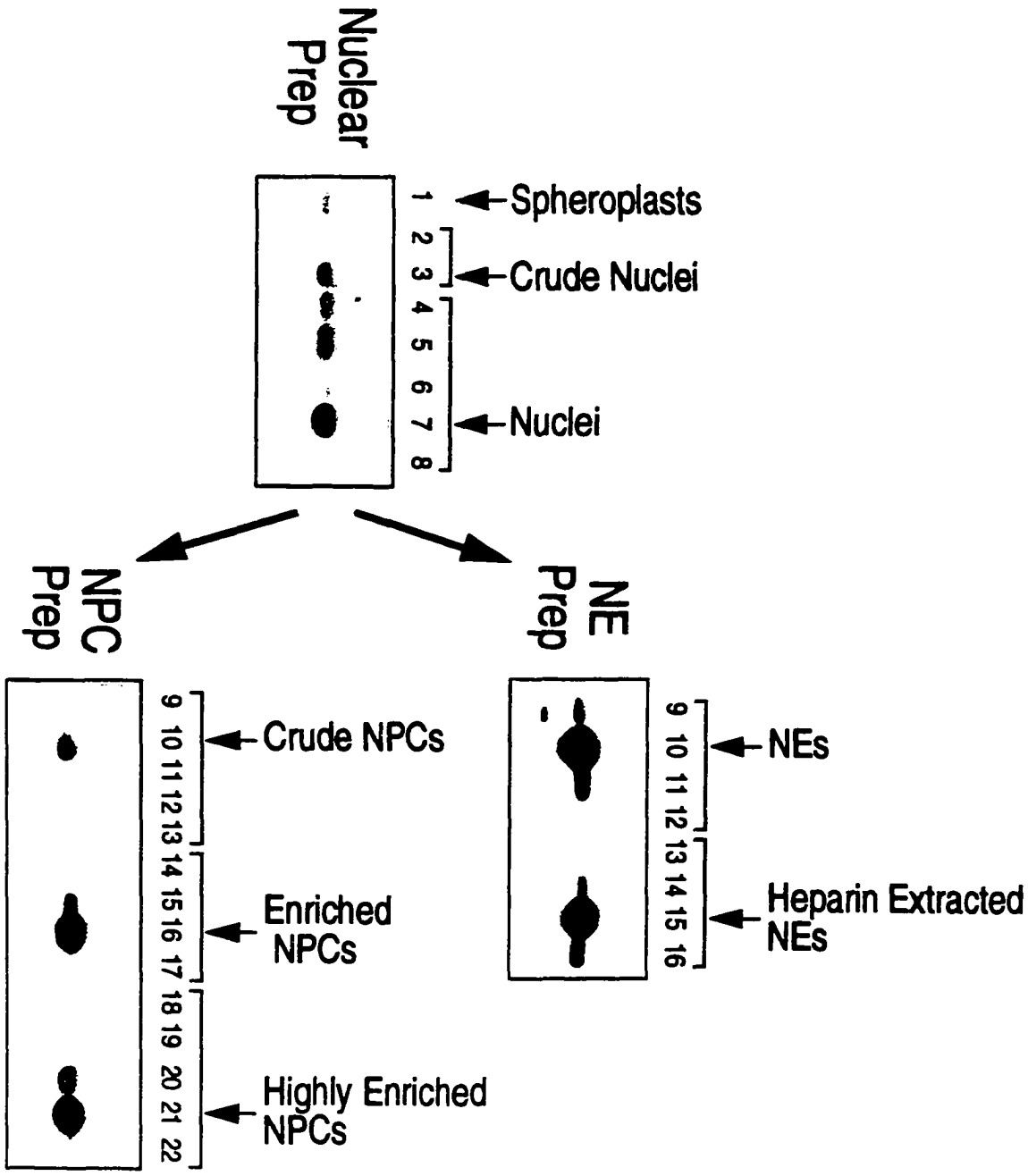

Figure 7. Double IF staining of wild type yeast cells showing *in vivo* Pom152p localization at the NE and at the ER.

Logarithmically growing wild type yeast cells were harvested, fixed and incubated with MAb118C3 (anti-Pom152p) followed by a rabbit anti-Sec61p antibody (A, B, C and D) or with the rabbit serum against Sec61p alone (E). All slides were incubated with a mixture of FITC-conjugated donkey anti-rabbit and Cy3-conjugated donkey anti-mouse IgGs and they were subsequently photographed on a fluorescent microscope. Cells at various stages of the cell-cycle starting from interphase (A) all the way to cytokinesis (D) can be observed. ER peripheral cisternae are indicated by *arrows*. The absence of any signal in Pom152p, panel E demonstrates that there was no bleed-through from the FITC-channel. Bar, 2 μm.

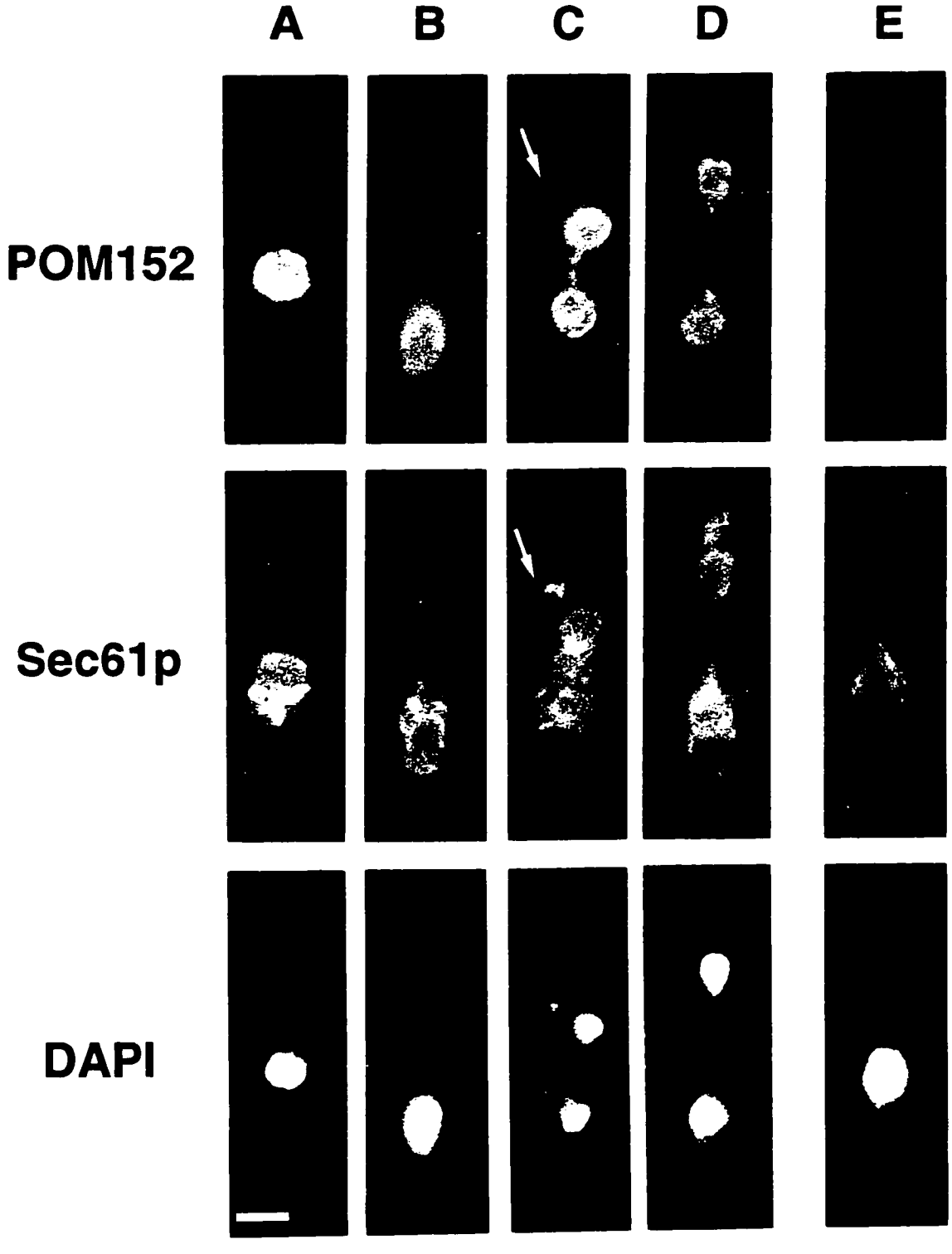

Figure 8. Quantitative analysis of the NE enrichment procedure.

(A, B, C, D and E) The immunoblots presented in Figs. 4 and 6 or similar ones were subjected to quantitative analysis. Fractions are numbered as in Fig. 1 and grouped with brackets as in Figs. 3 and 4. An estimate of the amount of a given marker present in each fraction is expressed here as a percentage of the total cellular amount calculated from the sum of the quantity found in fractions 2 (Crude Cytosol) and 3 (Crude Nuclei). The figures in parentheses represent the percentage yield of each of the markers relative to the NE containing fraction from the preceding fractionation step. The SPB proteins p90 and Spc110p/Nuf1p, and the NPC protein p65 were used to construct the histogram of panel A. Similarly, the data presented in panel C, reflect the results of the quantification of Cytochrome P450 reductase and Sec61p. (F) Total amount of protein present in each fraction. (G) The percentage yields of the peripheral NE markers (panel A, fractions 1-12) and of Pom152p (panel B, fractions 13-16) were used together with the numbers expressing the total amount of protein of each NE containing fraction to determine the fold-enrichment of nuclear membranes throughout the enrichment procedure.

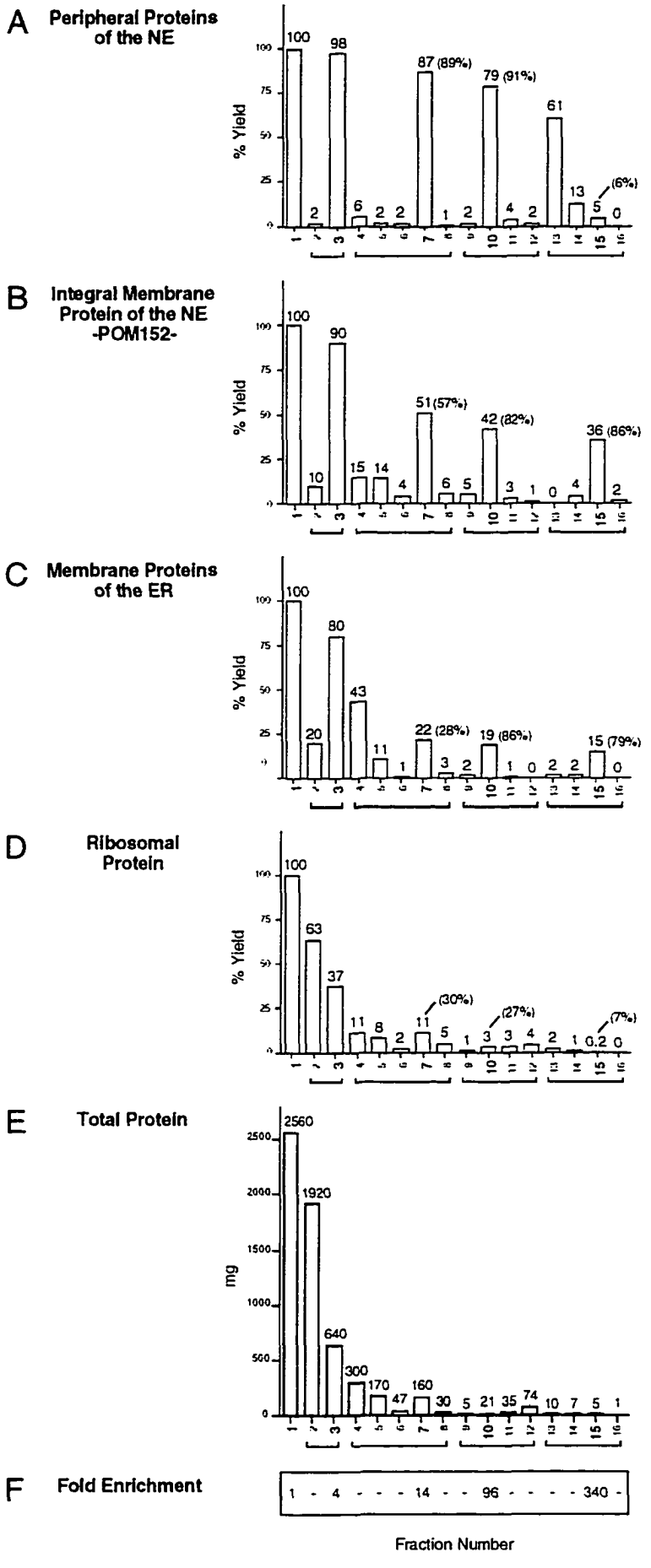

Protein Translocation Activity

Having determined the protein composition of the NE and the H-NE fractions it was necessary to evaluate their functional integrity. Cell-free systems have been developed to study various NE functions including nuclear transport, MTs nucleation, nuclear fusion, budding of ER to Golgi transport vesicles, and translocation of proteins across the rough ER membrane (i.e. outer nuclear membrane) The latter assay was chosen as it is comparatively straightforward, and since both the NE and the H-NE fractions would be expected to have ER protein translocation activity. "Active" NE and H-NEs fractions (see Materials and Methods for details) were mixed with radiolabeled, urea-denatured ppαF in the presence of yeast cytosol and an energy source (Chirico, et al., 1988). The presence of translocated pro-α-Factor was demonstrated using two standard criteria: 1) the acquisition of protease-resistance; and 2) the appearance of core-glycosylated forms of pro-α-Factor (glycosylated pro-α-Factor; gpαF). Moreover, both the absolute and the specific translocation activity were determined for each sample studied (Fig. 9).

When ppαF was incubated with either NEs or H-NEs (Fig. 9, *NEs* and *heparin-extracted NEs*, respectively a significant fraction of it was translocated into the ER lumen (*i.e.* perinuclear space) similar to that observed with for the CM fraction (Fig. 9, *crude microsomes*). Interestingly, the specific translocation activity of the NE and H-NE fractions appeared to be significantly higher (3- and 5-fold, respectively) as compared with the CM fraction (Fig. 9). All of the gpαF (Fig. 9) was protease resistant, unlike much of Kar2p/Bip (see previous section). Thus, either only sealed membranes are translocation-competent or translocated gpαF is associated with lumenal proteins such that is resistant to trypsin even in unsealed membranes. Detergent would disrupt this association

and make gpαF sensitive to proteolysis These results demonstrate that both the translocation apparatus and the glycosylating enzymes are active in our highly enriched NE and H-NE fractions. This provides evidence that the outer nuclear membrane and the perinuclear space not only share ER components but also its functions. That both of the NE fractions are functionally well-preserved suggests that they could be used to develop cell-free systems to investigate other NE and ER functions.

Figure 9. Both the isolated NEs and H-NE fraction are active in a cell-free protein translocation assay.

"Active" NEs and H-NEs and CMs were prepared as described in Materials and Methods. (Top panel) [^{35}S]-Methionine labeled, *in vitro* synthesized ppαF was denatured with urea immediately before adding it to a reaction mixture containing either buffer (*no additions*), NEs, H-NEs (*heparin-extracted NEs*) or CMs (*crude microsomes*) in the presence of ATP and crude cytosol. After 1 h at 20°C the reaction was stopped and each sample was divided in three equal aliquots. The first set of aliquots was incubated on ice without further treatments (lanes *a*). The second set was digested with trypsin (lanes *b*). The third set was treated with Triton X-100 before trypsin digestion (lanes *c*). All samples were analyzed by SDS-PAGE and fluorography. The position of ppαF and of the tri-glycosylated form of the protein (*gpαF*) is indicated. An α-Factor specific band migrating slower than the fully glycosylated product is indicated by an *asterisk*. This previously reported product presumably corresponds to gpαF prior to mannose and glucose trimming (Waters, et al., 1988). The position of the molecular weight standards is indicated at the right of the gel. (Middle panel) The intensity of the bands present in lanes *a* (no treatment), was measured with the PhosphorImager system and the translocation activity was determined in each case by calculating the percentage of the total radioactivity that corresponded to translocated material. (Bottom panel) The percentage translocation activity in successive 2-fold dilutions of each fraction was determined and a graph of activity *versus* volume of sample was constructed. The slope of the graph in the linear range (% activity/μl) was divided by the total amount of protein present in each fraction to yield the specific activity [*Specific activity (% activity/μg)*].

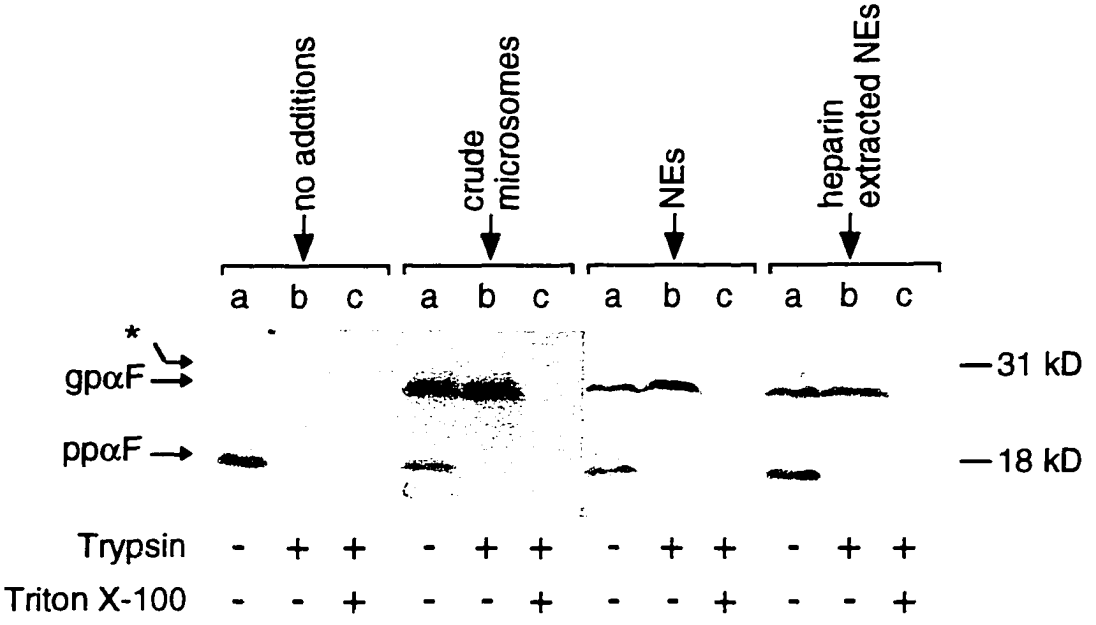

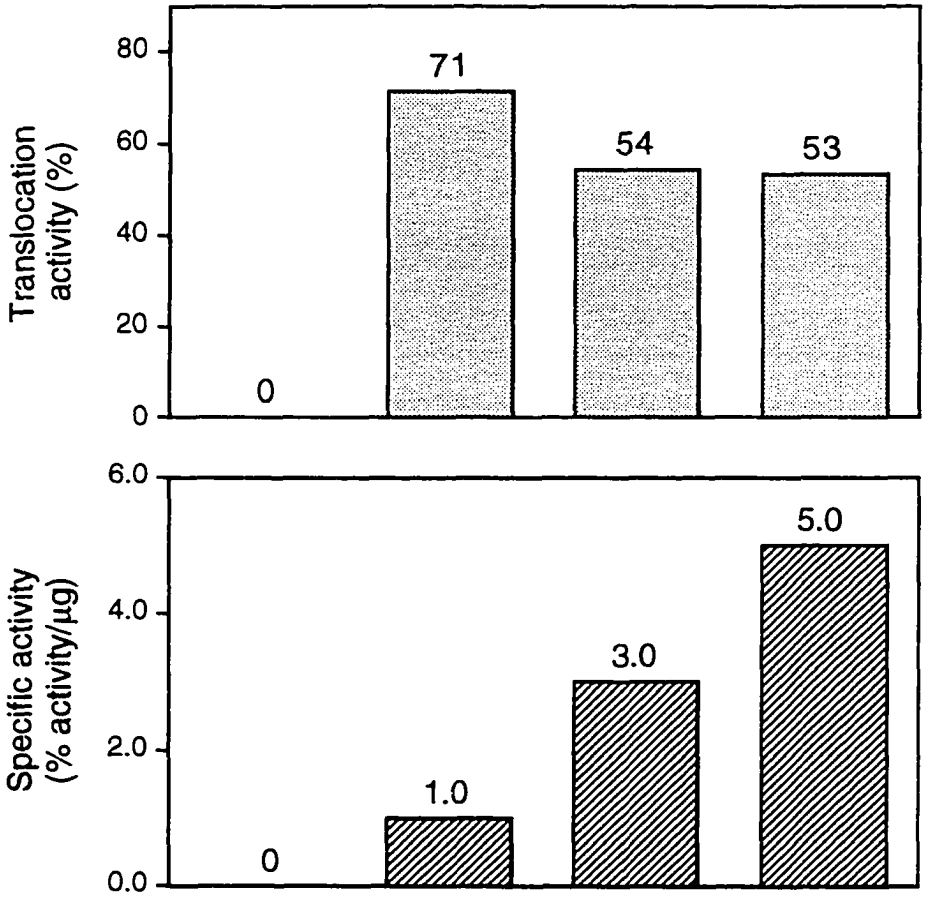

Detergent extraction of H-NEs

The retention of the NPC grommets after heparin extraction of the isolated NEs suggested that they were stabilized by a heparin-resistant NPC substructure associated with the membrane, most likely in the perinuclear space. H-NEs were therefore extracted with detergents after attachment to an EM grid in order to reveal any substructures underlying the grommets (Fig. 10). Negative staining of these samples revealed the presence of numerous rings of approximately the same internal diameter (~100 nm) and distribution as the grommets (Fig. *10A*, *arrows*), with an extensive filamentous network lying between them. To investigate this finding further, a highly enriched fraction of NPCs (Rout and Blobel, 1993) was treated with heparin under conditions similar to the ones used to extract isolated NEs. Heparin-resistant material was then sedimented onto an EM grid and negatively stained, as for the extracted H-NEs (above). This also produced ring-like structures, strongly resembling those seen in the extracted H-NEs but without any other associated material (Fig. *10B*). Preliminary experiments indicated that, when the highly enriched NPCs were similarly extracted in solution and sedimented over a velocity gradient, the rings thus isolated contained the pore membrane protein Pom152p as a major constituent; likewise, the detergent extracted H-NEs were also found to retain Pom152p (data not shown). The rings must therefore be derived from integral pore membrane proteins possibly associated with peripheral proteins present in the perinuclear space. Attempts to separate the rings directly from the H-NEs in solution have so far failed.

Figure 10. Detergent extraction of H-NEs suggests that ring structures associated with the NE may be involved in stabilizing the grommets of the NPCs.

(*A*) Isolated H-NEs were immobilized on EM grids, extracted with detergents and negatively stained as described in Materials and Methods. *Arrows* point to heparin-resistant ring structures that have the same internal diameter as the NPC grommets seen in Fig. 2*D*. (*B*) Highly enriched NPCs (Rout and Blobel, 1993) were extracted with heparin as described in Materials and Methods; following extraction, the heparin-resistant material was sedimented onto EM grids and negatively stained as above. Bar, 0.2 μm.

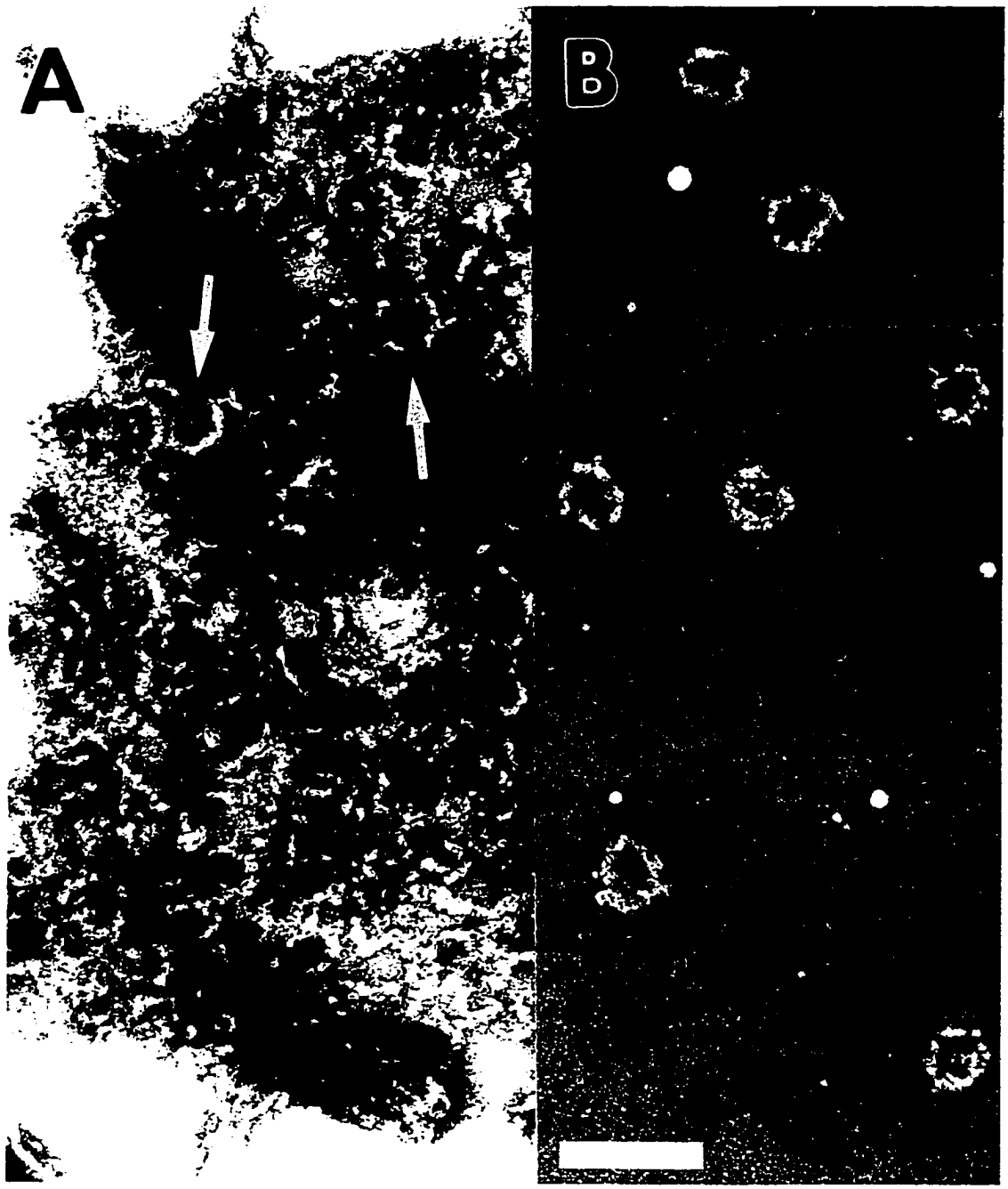

Chapter IV: Preparation Of Monoclonal Antibodies Against Yeast Enriched Nuclear Envelope Fractions

Outline of the Procedure

The generation of mAbs as a means to identify novel protein components of a complex sub-cellular fraction has been previously described and has proven successful in a variety of circumstances (Rout and Kilmartin, 1990; Rout and Kilmartin, 1991). In particular, yeast is a highly suitable source of antigens because of the relative ease with which large amounts of material can be prepared and because of the high level of AA sequence divergence between homologous proteins in yeast *versus* higher eukaryotes. The high degree of enrichment of the yeast NE fractions described in Chapter III makes them potentially excellent material for the production of mAbs against NE-associated antigens. Consequently, this strategy could prove invaluable for the identification of previously unidentified NE components that are not part of the core structure of the NPC.

The approach entailed the following steps: 1) large scale preparation of highly enriched NE fractions. 2) Immunization of mice with these fractions. 3) Generation of hybridoma cell lines from the spleen of the immunized mice. 4) Screening of the hybridomas by indirect IF microscopy to isolate the clones secreting antibodies that recognize components of the NE. 5) Secondary screening of the mAbs by immunoblot on enriched NEs. 6) Generation of stable lines of the hybridomas of interest by sub-cloning the initial positive clones.

Large Scale Preparation of Highly Enriched NE Fractions

Three different highly enriched NE fractions were used to immunize mice (Table II). In order to maximize the chances to obtain antibodies that recognized NE-associated integral membrane proteins, NEs were stripped of peripheral components using both heparin (H-NEs) and carbonate (C-NEs) as described in the Chapter III. In addition, proteins present in the highly-enriched NE fraction described in Chapter III were fractionated on a S-Sepharose column. The fractionation pattern of various known nucleoporins was followed by immunoblot using a mixture of MAb414 and MAb350 (see the legend to Fig. 4; Davis and Blobel, 1986). Using this method it was determined that the S-Sepharose unbound material was selectively depleted of numerous known highly antigenic nucleoporins (data not shown). This depleted, NE fraction was called the S-NE fraction and was used as the third antigen in the immunization procedure. Each of the three antigen preparations was produced in quantities sufficient for the entire immunization protocol following a large-scale version of the procedures described above and in Chapter III.

Table II. Antigens description

Group Number	Number of Mice	Antigen	Antigen Description	Total Antigen Amount (mg / mouse)	Total number of Injections
1	12	H-NE	Heparin-extracted NEs (see Chapter III)	3.70	5
2	6	H-NE	Heparin-extracted NEs (see Chapter III)	2.25	5
3	6	C-NE	Carbonate-extracted NEs (See Chapter II)	2.25	6
4	3	S-NE	S-Sepharose fractionated NEs (see this Chapter)	2.25	5

Mice Immunization

A total of 27 mice were divided into four test groups and each mouse of the group was immunized with either H-NE, C-NE or S-NE as detailed in Table II. Regardless of the antigen, each mouse received 1 initial sub-cutaneous immunization in the presence of complete Freund's adjuvant followed by either 4 or 5 sub-cutaneous booster injections with the same amount of antigen in the presence of incomplete Freund's adjuvant. The sera from mice were tested periodically by indirect IF microscopy and immunoblotting for reactivity against NE-associated proteins. Animals that appeared to be making antibodies against large numbers of NE specific antigens (judged by nuclear rim staining in IF microscopy and the presence of immunoreactive bands coenriching with NE fractions on immunoblots) were selected from each group for the production of hybridomas. 3-5 days before a fusion the selected mouse was given a full dose of antigen intra-peritoneally to obtain an optimal immune response.

Generation of Hybridoma Cell Lines and Primary IF microscopy Screens

The method for producing hybridomas was essentially as described (Galfre and Milstein, 1981; Rout and Kilmartin, 1990). Samples from the tissue culture supernatant of the hybridoma colonies were initially screened by indirect IF microscopy on whole fixed yeast cells (Kilmartin and Adams, 1984). This type of screening has the advantage of allowing the immediate classification of the individual mAbs on the basis of the intra-cellular localization of the antigen they recognize. Hybridoma colonies that secreted antibodies recognizing

antigens associated with the NE or at the ER were harvested for subsequent analysis. The small number of antibodies that were obtained that gave typical intranuclear, nucleolar, ribosomal or mitochondrial staining pattern were also harvested.

A total of 4 fusions were performed using 1 mouse from each test group. A total of 173 positive hybridoma lines were obtained. Of these, 48 gave a typical ER pattern which is distinguishable by the appearance of a continuous rim staining at the NE connected by long tubular structures within the cytoplasm to patchy staining beneath the plasma membrane; 114 gave a typical NE staining pattern recognizable by a punctate or patchy signal at the nuclear periphery; while the remaining 11 mAbs recognized either mitochondria, ribosomes, nucleoli or nuclei.

Secondary screening of the NE specific mAbs by immunoblot analysis

All of the mAbs obtained from the primary screening were then tested for their ability to recognize proteins on immunoblots of highly enriched yeast NE. Proteins from the highly enriched NE fraction described in Chapter III (fraction 10) were run on SDS-PAGE in a single large well spanning the whole gel and transferred to nitrocellulose. The nitrocellulose membrane was mounted on a multi-lane apparatus that allowed the screening of 26 individual mAbs per gel (see Chapter II). Fig. 11 shows the results obtained with a typical gel.

A summary of the results obtained from the primary and secondary screening is presented in Table III. Table IV presents the list of all mAbs that were obtained against NE localized antigens.

Four of the 114 anti-NE mAbs have been extensively characterized. The characterization of the anti-Pom152p MAb118C3 is described in details in Chapter III of this dissertation. MAb165C10 was found to recognize the previously uncharacterized Nup159p and was essential for its isolation and its ultrastructural localization (Kraemer, et al., 1995). Both MAb148G11 and MAb215B9 recognize a single band of ~200 kD on immunoblots of isolated NEs and they were used to localize this protein within the cell and to isolate the gene encoding for it as described in detail in Chapter IV of this dissertation.

Table III. *Summary of mAbs results*

	Total	Positive by immunoblot [b]
Hybridoma colonies screened	4900	n/a[c]
mAbs obtained	173	76
NE specific mAbs	114	44
ER specific mAbs	48	27
Other mAbs [a]	11	5

Footnotes:

[a] mAbs that were obtained against the following yeast structures and organelles: mitochondria (1); ribosomes (3); nucleolus (3); nucleus (4).

[b] A mAb was considered to be positive by immunoblot when it specifically stained one or more bands on an immunoblot of highly enriched NEs.

[c] not applicable.

Table IV. mAbs obtained against yeast NE components

Name	Group Nr	Antigen	IF Signal	Imm. Dot Signal	Number of Distinct Bands	Size of Major Band	Size of Additional Bands	Name of Antigen	Reference
119C9	1	H-NE	NE	yes	15	150		Rpm1p	Wozniak et al. (1994), Strambio-de-Castillia et al. (1995)
182G3	2	H-NE	NE	yes	5	116	100, 68, 58, 50		
183C3	2	H-NE	NE	yes	15	95			
185D3	2	H-NE	NE/ Nucleolus	yes	1	55			
187B5	2	H-NE	NE	yes	5	116	100, 68, 58, 50		
190F1	2	H-NE	NE	no					
191D2	2	H-NE	NE	yes	5	116	100, 68, 58, 50		
191H1	2	H-NE	NE	no					
194F6	2	H-NE	NE	yes	1-(2)	150	(100)		
195H8	2	H-NE	NE	yes	1-(2)	150	(100)		
201D11	2	H-NE	NE	no					
201E10	2	H-NE	NE	yes	5	116	100, 68, 58, 50		
203D5	2	H-NE	NE	yes	3-(4)	116	100, (68), 50		
204D10	2	H-NE	NE	yes	3-(4)	116	100, (68), 50		
206C2	2	H-NE	NE	yes	1-(2)	150	(100)		
208F2	2	H-NE	NE	no					
209B11	2	H-NE	NE	yes	5	116	100, 68, 58, 50		
212F3	2	H-NE	NE	yes	1-(2)	150	(100)		
216B12	2	H-NE	NE	yes	15	116	100, 68, 58, 50		
181E3	3	C-NE	NE	no					
182B3	3	C-NE	NE	no					
184F5	3	C-NE	NE (rim)	no					
184G10	3	C-NE	NE	yes	5-(11)	100	(130), 90, 85, (80), 75, (68), (64), (62), 60, (55)		
185B6	3	C-NE	NE	no					
185E1	3	C-NE	NE	no					
188G2	3	C-NE	NE (rim)	no					
188G3	3	C-NE	NE	yes	2-(10)	100	(85), (75), 72, (66), (62), (60), (58), (55), (50)		
189G5	3	C-NE	NE	no					
190A8	3	C-NE	NE	no					
191E8	3	C-NE	NE	no					
191G6	3	C-NE	NE	yes	7-(11)	100	(130), 85, 75, (72), 66, 62, 60, (58), 55, (50)		
192A6	3	C-NE	NE (patchy)	no					
192F7	3	C-NE	NE	yes	7-(10)	100	85, 75, (72), 66, 62, 60, (58), 55, (50)		
193F5	3	C-NE	NE	yes	7-(10)	100	85, 75, (72), 66, 62, 60, (58), 55, (50)		
194D10	3	C-NE	NE	no					
194F5	3	C-NE	NE	yes	5	116	100, 68, 58, 50		

Table IV. mAbs obtained against yeast NE components (continued)

Name	Group Nr.	Antigen	IF Signal	Imm. blot Signal	Number of Distinct Bands	Size of Major Band	Size of Additional Bands	Name of Antigen	Reference
195G2	3	C-NE	NE	no					
196F7	3	C-NE	NE	yes	2-(11)	100	(116), (85), (75), (72), 66, (62), (60), (58), (55), (50)		
197C2	3	C-NE	NE	no					
198B11	3	C-NE	NE (patchy)	yes	5-(10)	116	(150), 100, (85), (80), (75), (72), 66, 58, 49		
199D4	3	C-NE	NE	no					
199D8	3	C-NE	NE	yes	5-(9)	116	(130),100, (85), (80), (72), 66, 58, 49		
200C5	3	C-NE	NE	yes	5-(10)	100	85, 75, (72), 68, (62), (60), (58), 55, (49)		
202C9	3	C-NE	NE (rim)	no					
204A11	3	C-NE	NE	yes	5-(10)	100	85, 75, (72), 68, (62), (60), (58), 55, (49)		
204F11	3	C-NE	NE (rim)	no					
204F3	3	C-NE	NE (patchy)	no					
204G1	3	C-NE	NE	yes	6-(13)	100	(170), 150, 120, (116), 90, 75, (72), 68, (65), (62), (60), (55)		
205E4	3	C-NE	NE	no					
205G4	3	C-NE	NE	no					
205G9	3	C-NE	NE	no					
206B8	3	C-NE	NE	yes	2-(8)	100	(90), (80), 68, (65), (62), (60), (58)		
206C10	3	C-NE	NE	no					
206C8	3	C-NE	NE	no					
208C11	3	C-NE	NE (patchy)	no					
210D12	3	C-NE	NE	yes	7-(11)	100	(130), 85, 75, (72), 66, 62, 60, (58), 55, (50)		
210E5	3	C-NE	NE	no					
211B11	3	C-NE	NE	yes	1-(3)	100	(200), (130), (70)		
211D4	3	C-NE	NE	yes	5	116	100, 68, 58, 50		
211E1	3	C-NE	NE	no					
212E4	3	C-NE	NE (patchy)	no					
213F7	3	C-NE	NE	yes	1-(4)	170	(200), (116), (100), (66)		
214E10	3	C-NE	NE (patchy)	yes	1-(3)	60	(116), (52)		
214H3	3	C-NE	NE	yes	6-(10)	100	85, 75, (72), 66, (62), 60, (58), 55, (50)		
215B9	3	C-NE	NE (patchy)	yes	1	220		Mip1p	Kölling et al., 1993; this dissertation, Chapter V
215G4	3	C-NE	NE (patchy)	no					
216E5	3	C-NE	NE	yes	6-(10)	100	85, 75, (72), 66, (62), 60, (58), 55, (50)		
216H6	3	C-NE	NE	no					
217C6	3	C-NE	NE	no					
218F9	3	C-NE	NE (rim)	no					
219E11	3	C-NE	NE	yes	6-(10)	100	85, 75, (72), 68, (62), 60, (58), 55, (50)		
141E11	4	S-NE	NE	no					

Table IV. mAbs obtained against yeast NE components (continued)

Name	Group Nr.	Antigen	IF Signal	Imm. blot Signal	Number of Distinct Bands	Size of Major Band	Size of Additional Bands	Name of Antigen	Reference
142B2	4	S-NE	NE	no					
143F3	4	S-NE	NE	no					
144C1	4	S-NE	NE	no					
144C2	4	S-NE	NE	yes	1	100			
144H10	4	S-NE	NE	no					
147B10	4	S-NE	NE	no					
147B2	4	S-NE	NE	no					
148G11	4	S-NE	NE (patchy)	yes	1	220		Mlp1p	Kolling et al., 1993; this dissertation, Chapter V
149B6	4	S-NE	NE	no					
149D5	4	S-NE	NE	no					
149D9	4	S-NE	NE	no					
151E3	4	S-NE	NE	no					
151G4	4	S-NE	NE	no					
153B10	4	S-NE	NE	no					
153C5	4	S-NE	NE	no					
153F1	4	S-NE	NE	no					
153F6	4	S-NE	NE	no					
154E2	4	S-NE	NE	no					
154G1	4	S-NE	NE	no					
154G10	4	S-NE	NE	no					
155C8	4	S-NE	NE	no					
156C9	4	S-NE	NE	no					
156D12	4	S-NE	NE	no					
156E5	4	S-NE	NE	no					
156H5	4	S-NE	NE	no					
158B12	4	S-NE	NE	no					
158B5	4	S-NE	NE	no					
158C2	4	S-NE	NE	yes	1	100			
160B7	4	S-NE	NE	no					
160G10	4	S-NE	NE	no					
161G3	4	S-NE	NE	yes	2-(11)	100	116, (90), (80), (75), (72), (62), (60), (55), (52), (49)		
162D11	4	S-NE	NE	no					
163A5	4	S-NE	NE	no					
164A4	4	S-NE	NE	yes	1 (2)	100	(95)		
164A9	4	S-NE	NE	no					
164C4	4	S-NE	NE	yes	2-(5)	116	(100), (68), (58), 50		

Table IV. mAbs obtained against yeast NE components (continued)

Name	Group Nr.	Antigen	IF Signal	Imm blot Signal	Number of Distinct Bands	Size of Major Band	Size of Additional Bands	Name of Antigen	Reference
166C10	4	S-NE	NE	yes	6/7	180	150, 120, 115, 100	Nup159p	Kraemer et al., 1995; Gorsch et al., 1995; Del Priore et al., 1996
168C8	4	S-NE	NE	no					
171D10	4	S-NE	NE	no					
171E3	4	S-NE	NE	no					
174H4	4	S-NE	NE	no					
179F3	4	S-NE	NE	no					

Footnotes:
-Name: All the mAbs that gave a NE specific staining by IF are listed in this table.
Listed in bold are the mAbs for which the antigen has been identified.
-Group Nr.: Antibodies are listed according to the test group number of the mice from which they were derived (refer to Table III for details).
-Antigen: The names of the antigen refers to the nomenclature used in Table III.
-IF Signal: The following categories are used: NE indicates punctate staining of the nuclear periphery; rim indicates a possible continuous rim staining at the nuclear periphery; patchy indicates the presence of larger patches of signal at the nuclear periphery that are distinguishable from the finer punctate staining typical of nucleoporins; NE/Nucleolus indicates the presence of a nucleolar staining pattern in association with a typical rim staining.
-WB signal: yes indicates the ability of the mAb to specifically recognize one or more bands on an immunoblot of NE specific proteins. no indicates the absence of bands or the presence of bands that were considered to be too faint to be specific.
-Number of Distinct Bands: The number of individual bands of equal intensity recognized by the antibody on immunoblot is listed. The numbers in brackets indicate the number of bands whose intensity was less intense than the major bands but that were considered to be above background.
-Size of Major Band: The apparent Mw (kD) of the major bands is listed. In the case of multiple bands of equal intensity the size of the band with highest apparent MW is listed.
-Size of Additional Bands: The apparent MW of additional bands is listed. The number in brackets indicate the size of the less intense bands.
-Name of Antigen: The standard yeast protein nomenclature is followed.

Figure 11. Secondary screening of mAbs obtained against yeast NE fractions.

Proteins present in the highly enriched NE fraction, prepared as described in the text, were subjected to SDS-PAGE and immobilized on nitrocellulose. The nitrocellulose filter was inserted in a multi-lane apparatus and incubated with aliquots from 26 different hybridoma supernatants. The mAbs were detected using a secondary rabbit anti-mouse antibody conjugated with HRP. The bound HRP was revealed by the ECL reaction (see Chapter II for details on the procedure). The numbers at the top of the gel represent the position of the individual lanes of the multi-screen apparatus. The names of each mAb that gave a significant positive signal are indicated on top of the gel in bold character together with the subcellular localization of the antigen as determined by the primary screen (indirect IF microscopy). The names of mAbs that were considered negative by immunoblot are indicated in a smaller font and are not bold. The group number to which each mAb isolate belongs is indicated at the bottom of the gel (see Table II and IV). Numbers at the side of the gel reflect the position of the MW standards.

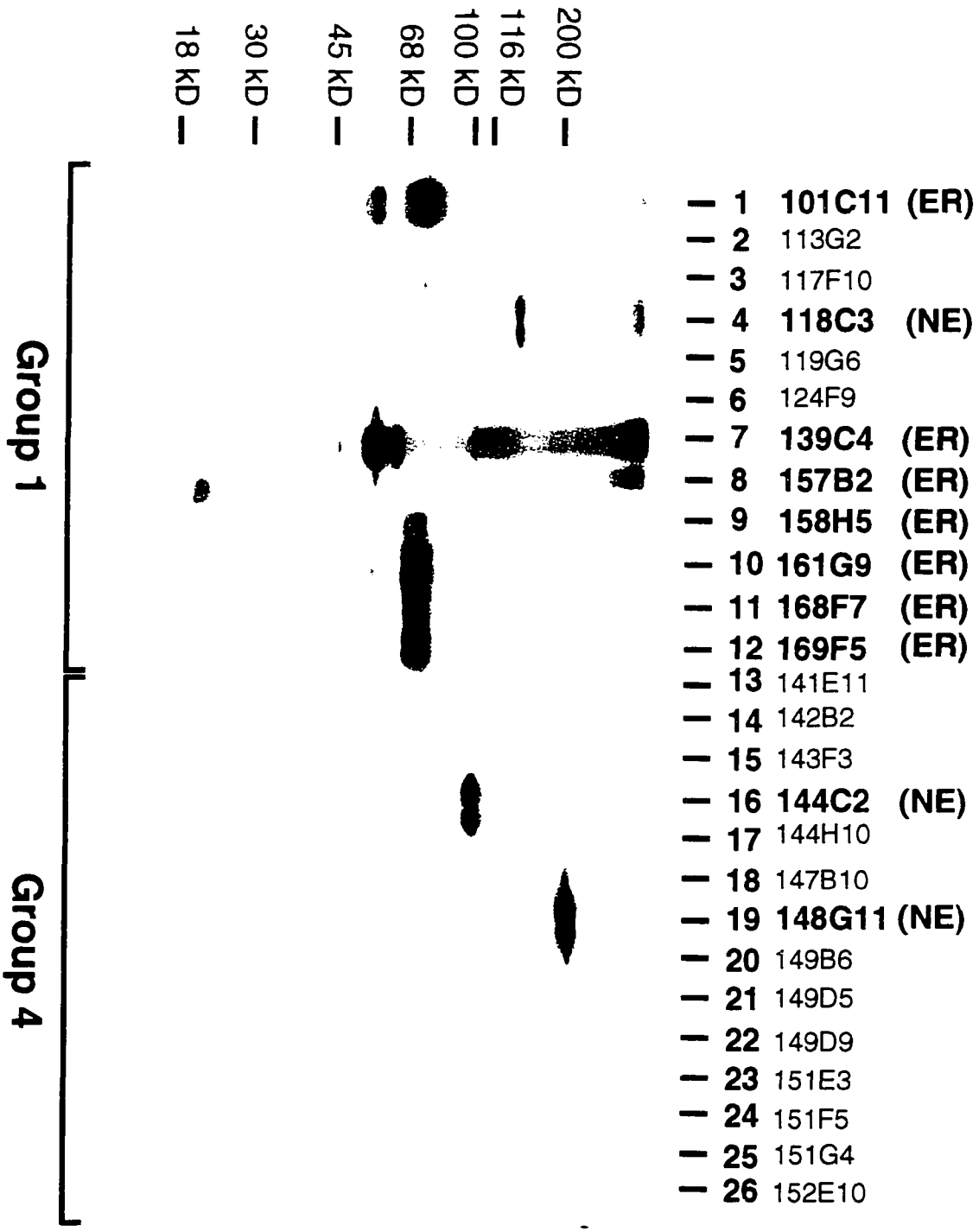

Chapter V: The Identification And Characterization Of Components Of Nuclear Filaments That Connect The Nuclear Pore Complex To The Nuclear Matrix

A Screen for non-NPC Proteins Associated with the NE

Mutations or deletions of the genes that encode for various nucleoporin (for example, Nup133p, Nup120p, Nup145p and Nup159p) cause the NPC to accumulate at one side of the NE, giving rise to tight clusters that can be easily identified as spots or patches when cells from such strains are stained with a nucleoporin specific antibody (Doye, et al., 1994; Fabre, et al., 1994; Wente and Blobel, 1994; Aitchison, et al., 1995; Heath, et al., 1995; Kraemer, et al., 1995; Li, et al., 1995; Pemberton, et al., 1995). It was reasoned that proteins only partially associated with the NPC or localized to areas of the NE that are not in close contact with the NPC, would either fail to cluster or would only partially cluster with the NPCs in these strains. In order to identify such NE components, the 114 mAbs produced against the yeast NE as described in the previous Chapter were screened by a NPC clustering assay. The indirect IF pattern generated by each of the individual mAbs on fixed whole wild type yeast cells was compared to the staining pattern obtained on a yeast strain carrying a gene disruption in the *NUP133* gene (Pemberton, et al., 1995). MAb215B9 and MAb148G11, were identified by this screen as recognizing antigens that appeared to only partially cluster in the *NUP133* disrupted strain. Both of these mAbs gave similar pattern by indirect IF microscopy on wild type yeast cells; furthermore they both recognized a single band of ~220 kD (apparent MW) on immunoblots of enriched NEs (see below and Table IV). The subcellular

fractionation behavior of the antigens recognized by these two mAbs during the NE and H-NE fractionation procedure (see Chapter III), was also found to be similar (data not shown). Based on these results it was tentatively concluded that MAb148G11 and MAb215B9 recognized the same protein, that was thus termed p220. This result was indeed confirmed when the gene encoding p220 was isolated and genetically disrupted (see below).

In order to better understand the relationship of p220 with the NPC, both wild type yeast cells and *NUP133* deleted cells were double stained with MAb215B9 and a rabbit polyclonal antibody against the nucleoporin Nsp1p. The results of this experiment are presented in Fig. 12. It is evident from this figure that Nsp1p and p220 only partially colocalize in wild type cells. The difference in the localization of these two proteins is even more striking in the clustering strain (Fig. 12, *ΔNUP133*). In these cells, while the Nsp1p signal clearly forms tight clusters localized at the NE consistent with its localization at the NPC, p220 appears to be localized in large patches or even in continuous rims at the nuclear periphery that only partially overlap with the NPC clusters (see discussion in Chapter VI). The localization of Nsp1p and p220 was also analyzed at various stages of the yeast cell cycle (Fig 12, panel *B*: *I-IV*). Although areas of coincident staining (*yellow*) are present, regions apparently devoid of one or the other protein are also evident. This is true regardless of the division cycle stage. Another conclusion that can be drawn from the results presented in Fig. 12*B* is that there does not appear to be any association between p220 and the yeast spindle at any stage throughout the cell division cycle (see also below). Identical results were obtained with MAb148G11 (data not shown).

For technical reasons, the cell line producing MAb215B9 proved difficult to culture and large amounts of this mAb could not be generated. Therefore, the

rest of the experiments presented in this study were conducted using MAb148G11 that could be produced in sufficient quantities.

Figure 12. Double IF staining of wild type and ΔNUP133 yeast cells showing the *in vivo* localization of p220 at NE-associated patches that colocalizes only partially with NPCs.

(*A*) Logarithmically growing wild type (diploid strain) and ΔNUP133 (haploid strain), yeast cells were harvested, fixed and incubated with MAb215B9 (anti-p220), followed by a rabbit anti-Nsp1p polyclonal antibody. The bound immunoglobulin was revealed as described in Chapter II. Slides were photographed on a fluorescent microscope. (*B*) The images presented here are computer generated composites of individual cells double-labeled as in panel *A* . Cells at various stages of the cell-cycle starting at interphase (*I*) all the way to cytokinesis (*IV*) can be observed. Bar, 2 μm.

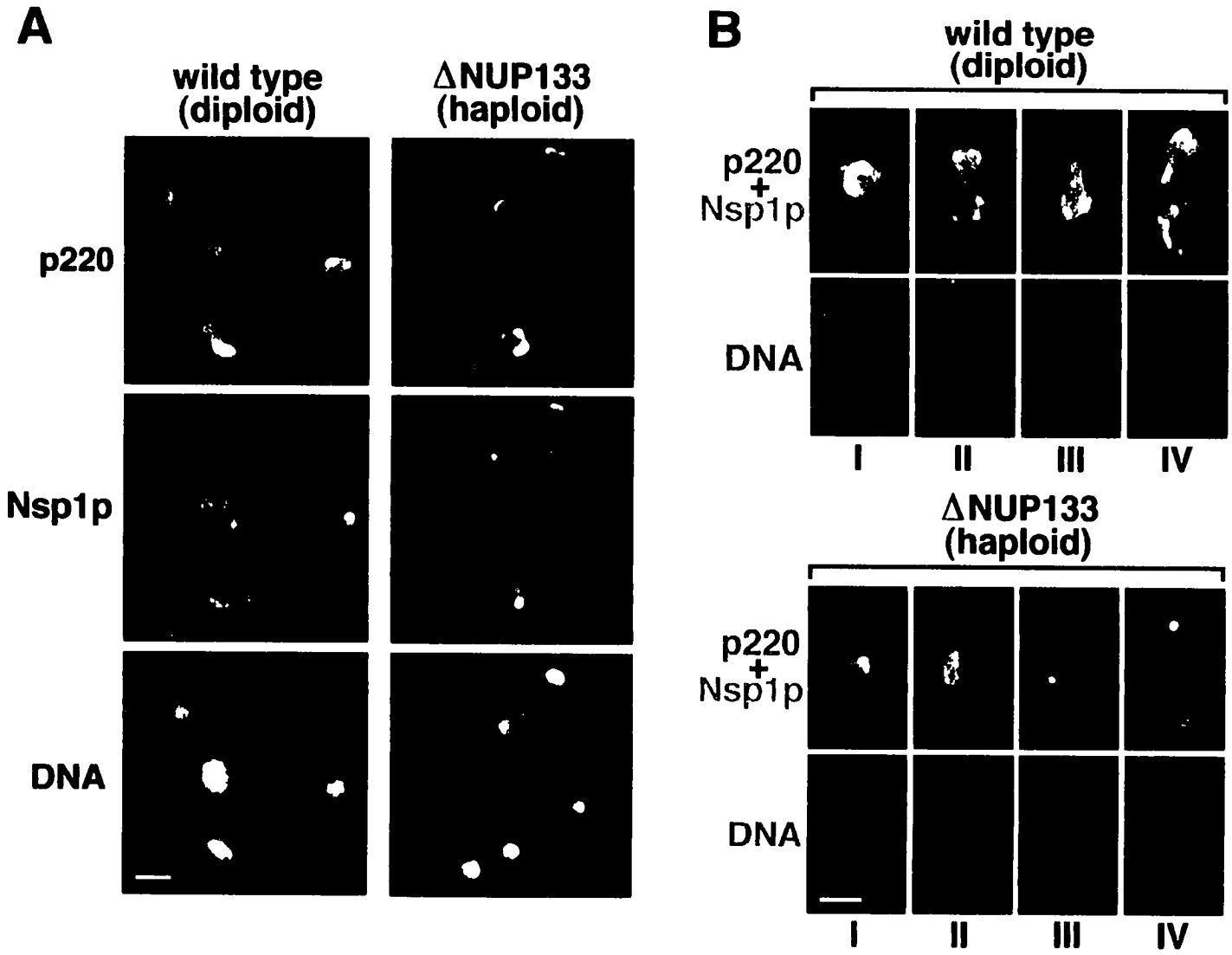

Isolation of the Gene Encoding p220

In order to investigate the structure and functions of p220, MAb148G11 was used to screen a yeast expression library. Three λ clones that expressed antigens recognized by MAb148G11 were isolated and purified by 4 subsequent screening rounds. These three clones contained an insert of 1.8 kb that appeared to be identical by restriction enzymes analysis. The insert of one of these identical clones was sequenced by standard methods and its DNA sequence was compared to DNA sequences present in the whole yeast genome database. A sequence present in the λ insert was identical to AA 1105-1700 of the coding region of *MLP1* (Myosin Like Protein 1; Kolling, et al., 1993). This demonstrates that the epitope of MAb148G11 lies within this region of Mlp1p. *MLP1* encodes for a protein of 1875 AA with a predicted MW of 218 kD that was originally cloned on the basis of its cross-reactivity with a mAb directed against human platelet myosin (Kolling, et al., 1993). This protein was found to be non essential and was hypothesized to have a nuclear function on the basis of its subcellular localization (see discussion in Chapter VI). The major structural features of Mlp1p together with the position of the cloned fragment of the gene and of the epitope of MAb148G11 are shown in Fig. 13. The predicted secondary structure of Mlp1p presents a very clear bipartite organization. The first ~80% of the protein has an extremely high α-helical content and contains the heptad-repeats pattern predictive of coiled-coil proteins. The final ~400 AA of the protein are predicted to form a globular tail that is rich in phenylalanine and proline residues (8% frequency over residues 1468-1832; 20% frequency over residues 1678-1765; 3% overall frequency; see discussion in Chapter VI). Interestingly, using a FASTA sequence analysis, two sequences were found that had a very high degree of sequence similarity to

the *MLP1* sequence (Fig. 14). The sequence with the highest degree of similarity (probability score 2.0 x 10^{-22}; 28% identical and 66% similar) was found to be the uncharacterized yeast ORF, YIL149C. YIL149C is expected to encode for a protein of 1680 AA with a predicted MW of 195 kD. Interestingly, both *MLP1* and YIL149C belong to the same duplicated chromosome region of the yeast genome (Block 38; Wolfe and Shields, 1997) present both on Chromosome XI and on Chromosome IX. The sequence similarity between Mlp1p and the deduced AA sequence of YIL149C (referred to as *MLP2* in Fig. 14, see below) extends over the whole AA sequence and is underscored by the similarity of the overall predicted secondary structure of the proteins. Based on the degree of primary and secondary structure similarity to Mlp1p and the fact that *MLP1* and YIL149C appear to have arisen from a genome duplication event, we propose the name *MLP2* (Myosin Like Protein 2) for YIL149C (see discussion in Chapter VI). Interestingly, the complete yeast genomic database (Clayton, et al., 1997) contains no other putative homologues of *MLP1*. The disruption of the genes encoding for Mlp1p and Mlp2p would therefore present a good opportunity to investigate the functions of these proteins in the living cell because no other protein is expected to be able to complement their functions (see next section).

The second most similar sequence in the database was that of the human gene *Tpr* (probability score 3.8 x 10^{-16}; 22% identical and 58% similar; Mitchell and Cooper, 1992; Byrd, et al., 1994). This gene encodes a protein of 2348 AA and 265 kD that has recently been localized to nuclear filaments that appear to connect the NPC with the nucleolus (Cordes, et al., 1997). Also in the case of Tpr, the similarity to Mlp1p spans the whole length of the protein and is associated to an overall similarity in the predicted secondary structure. The main difference between Tpr and Mlp1p is that the non coiled-coil tail of Tpr is

relatively much longer, spanning the final 30% of the protein, and has a much more marked acidic character (Byrd, et al., 1994). Interestingly, a *Drosophila* protein called Bx34 was recently identified that presents moderate levels of primary and secondary structure similarity to Tpr (Frasch, et al., 1988; Zimowska, et al., 1997). As with Tpr, this protein is found both in the vicinity of the NPCs and at extrachromosomal channels in the nuclear interior. As expected, Mlp1p is also similar to Bx34 (probability score 5.2 x 10^{-7}; 20% identical; 56% similar).

Figure 13. Schematic diagram representing some of the primary and secondary structural features of Mlp1p.

Shown as a function of the position in the sequence are the probability of forming coiled-coil displayed as the probability value; the position of the region of the protein that is encoded by the λ clone isolated from the expression library using MAb148G11 and therefore contains the epitope of this mAb; and the position of the proline/phenylalanine rich blocks together with the frequency of these residues within each block (the overall frequency of these two residues along the entire AA sequence is 3%). Coiled-coil predictions were performed as described in Chapter II of this dissertation.

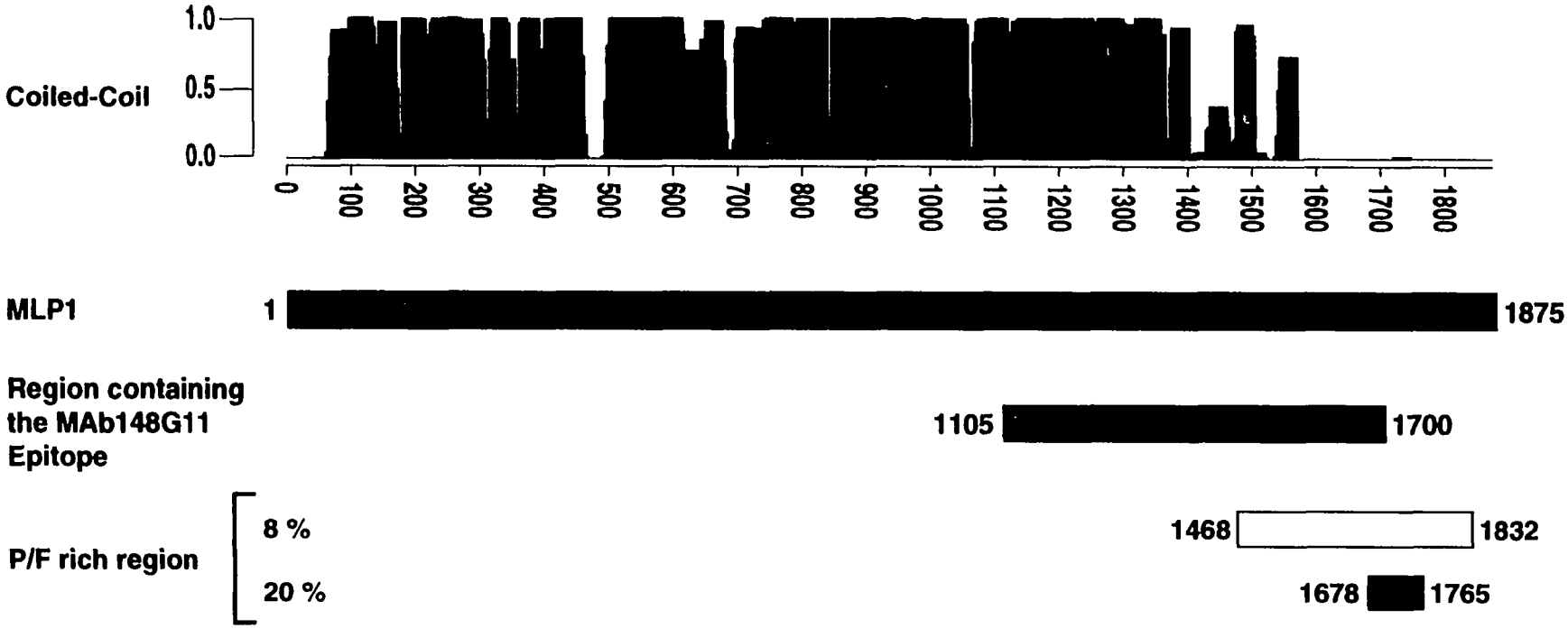

Figure 14. Mlp1p shares similarities with Mlp2p and Tpr.

Comparison of AA sequences of Mlp1p, Mlp2p (the yeast ORF YIL149C) and the human protein Tpr. The proteins were aligned using CLUSTALW. Identical AA are shaded in white on black; similar AA are shaded in gray.

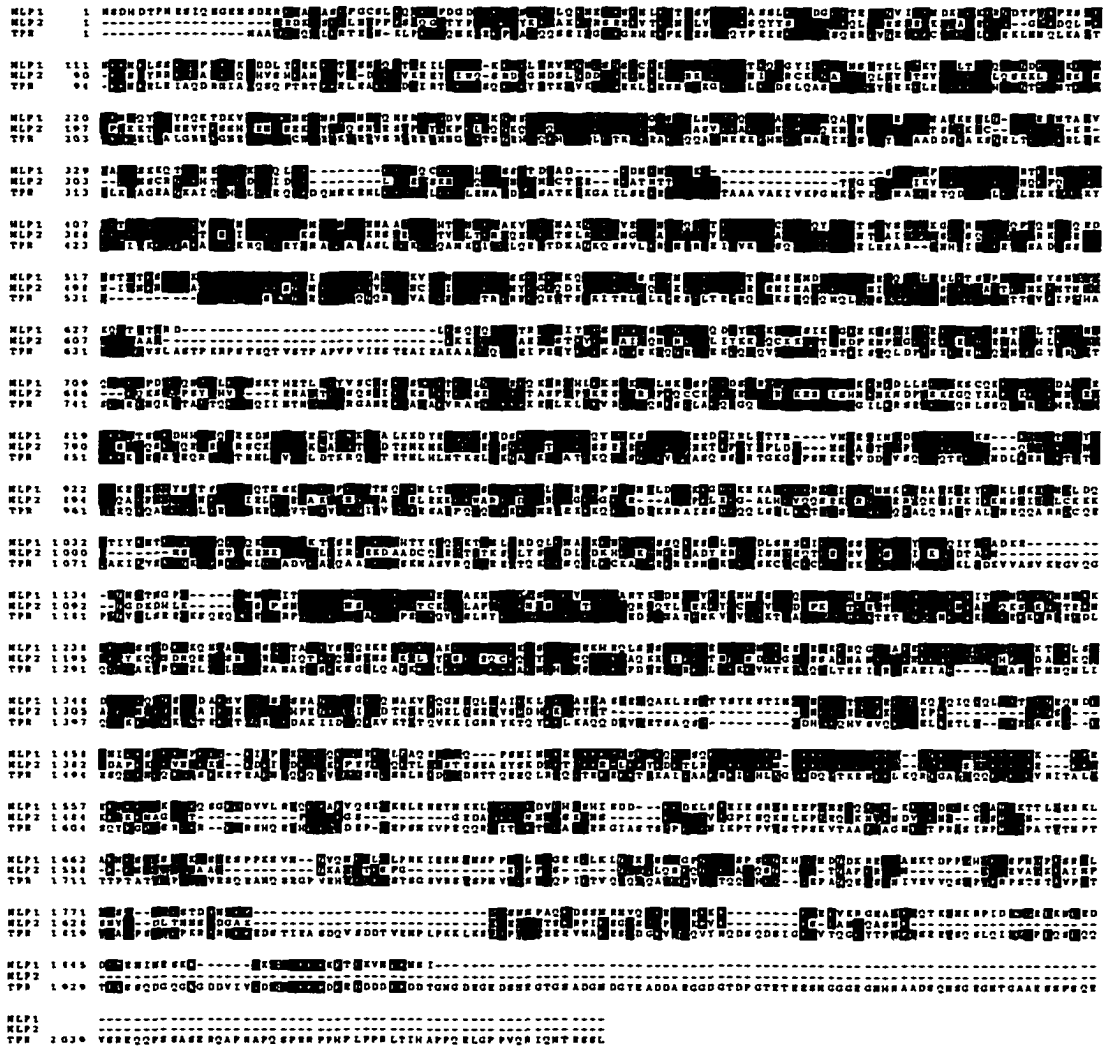

Double Deletions of *MLP1* and *MLP2* Cause a Marked Decrease in the Yeast Comparative Fitness

The entire coding regions of both *MLP1* and *MLP2* were individually disrupted in the diploid yeast strain W303 by integrative transformation of the *URA3* and *HIS3* genes respectively. Each heterozygous diploid strain (*mlp1::URA3/+* and *mlp2::HIS3/+*) was sporulated and tetrads were dissected. In both cases four viable spores from most tetrads were observed, demonstrating that neither of these genes is essential and confirming and extending published results (data not shown; Kolling, et al., 1993). Immunoblots with MAb148G11 and MAb215B9 revealed that the band recognized by both antibodies was absent in *mlp1::URA3* cells but was present in *mlp2::HIS3* cells (data not shown; see below). This confirmed that both MAb148G11 and MAb215B9 bind specifically to Mlp1p (see above). This result also demonstrated that neither MAb148G11 nor MAb215B9 crossreacts with Mlp2p.

Segregants of opposite mating types carrying the individual disruptions as confirmed by both phenotypic and genotypic analyses (see below; *MATa, mlp1::URA3* and *MATα, mlp2::HIS3*) were mated. After sporulation and tetrad dissection, again four viable spores were visible in most cases (Fig. 15). Individual spores from 10 tetrads showing 4:0 segregation were subjected to standard phenotypic analysis to confirm the viability of the segregants carrying the double disruption and to ascertain the proper segregation of mating type genes. Based on this phenotypic analysis, two tetrads were selected that presented a 1:1:1:1 segregation pattern (HIS^+/URA^+: HIS^-/URA^+: HIS^+/URA^-: HIS^-/URA^-). The genomic DNA of each individual segregant from these two tetrads was analyzed by PCR to reveal the presence of copies of the *MLP1*, *MLP2*,

HIS3 and *URA3* genes; furthermore, total cell lysates isolated from each individual haploid strain were analyzed by immunoblotting to follow the expression of Mlp1p using MAb148G11. The results obtained with one of these tetrads are shown in Fig. 15 *A* . In all cases the ability of each individual segregant to grow on the His^- or Ura^- selective plates cosegregated with the presence of a copy of the *HIS3* or *URA3* genes respectively, while it segregated away from the presence of a copy of *MLP1* and *MLP2* . As expected the presence of a MAb148G11 reactive band correlated with the presence of a copy of *MLP1* but not of *MLP2* (see above). This result was also confirmed by Indirect IF analysis of each of the four segregants from the same 1:1:1:1 tetrad using MAb148G11 (data not shown). As expected, this antibody detected no signal in either of the haploid strains that carried the deletion of *MLP1* (*mlp1Δ*, *mlp1Δ*, *mlp2Δ*) while it specifically stained the NE in the other two segregants.

To assess the degree of selective disadvantage conferred by individual and double disruptions in the *MLP1* and *MLP2* genes, haploid strains 1) *mlp1Δ* , 2) *mlp2Δ* and 3) *mlp1Δ*, *mlp2Δ* and their wild type counterpart were grown together competitively in rich medium (Smith, et al., 1996; Rout, et al., 1997; Thatcher, et al., 1998). While *mlp1Δ* and *mlp2Δ* competed nicely with wild type, the strain harboring the double deletion lost ground rapidly even though it was initially added in two-fold excess (Fig. 15 *B*), and appeared to be eliminated from the population after 30 generations (data not shown). These results demonstrated that *mlp1Δ*, *mlp2Δ* had a fitness defect relative to the parental stock equal to 24% (selection coefficient 0.235 ± 0.021; Thatcher, et al., 1998) and was effectively "non-viable" outside the "protected" laboratory environment. These results also showed that *MLP1* and *MLP2* exhibited a synthetically

"lethal" phenotype and strongly suggested that they are functionally related and are indeed homologues.

Figure 15. Yeast cells carrying a double disruption of *MLP1* and *MLP2* exhibit a marked fitness deficit with respect with their wild type counterpart.

(*A*) Haploid yeast cells carrying individual deletions in *MLP1* (*mlp1::URA3*) or *MLP2* (*mlp2:HIS3*) were mated, sporulated and tetrads were dissected. The results of the phenotypic and genotypic analysis of one typical tetrad are presented. *Phenotype*: Cells derived from individual spores were restreaked on Ura$^-$ and His$^-$ plates to determine their growth requirements and were mated to tester strains to determine their mating type. *Genotype*: Genomic DNA was purified from each individual haploid strain and the presence of copies of the *MLP1* , *MLP2* , *URA3* and *HIS3* genes were assessed by PCR analysis using appropriate oligonucleotides pairs. *MAb148G11.* Proteins isolated from each individual haploid strain were tested by immunoblot using MAb148G11 to reveal the expression of Mlp1p. (*B*) Top: Cultures in which the parental strain (*wt*) was grown with cells harboring either a single deletion of MLP1 (*mlp1Δ*) or MLP2 (*mlp2Δ*) or a double disruption of the two genes (*mlp1Δ, mlp2Δ*), were sampled at the indicated time points (*0, 6, 12 and 24 hr*). Aliquots containing ~100 logarithmically growing cells were plated on either YPD (representing the total number of cells present in the aliquot) or on the appropriate selective medium (Ura$^-$ plates for *mlp1Δ*; His$^-$ plates for *mlp2Δ*; and Ura$^-$/His$^-$ plates for *mlp1Δ, mlp2Δ*; representing the number of cells harboring the mutation in the aliquot). The initial ratio of wild type to mutant cells in each culture was 1:2 and the initial total cell concentration was 3 x 10^5/ml. Cells were diluted at each time point back to the original concentration to ensure constant logarithmic growth. Bottom: Graphical representation of the percentage of the mutant cells in the culture at each individual time point.

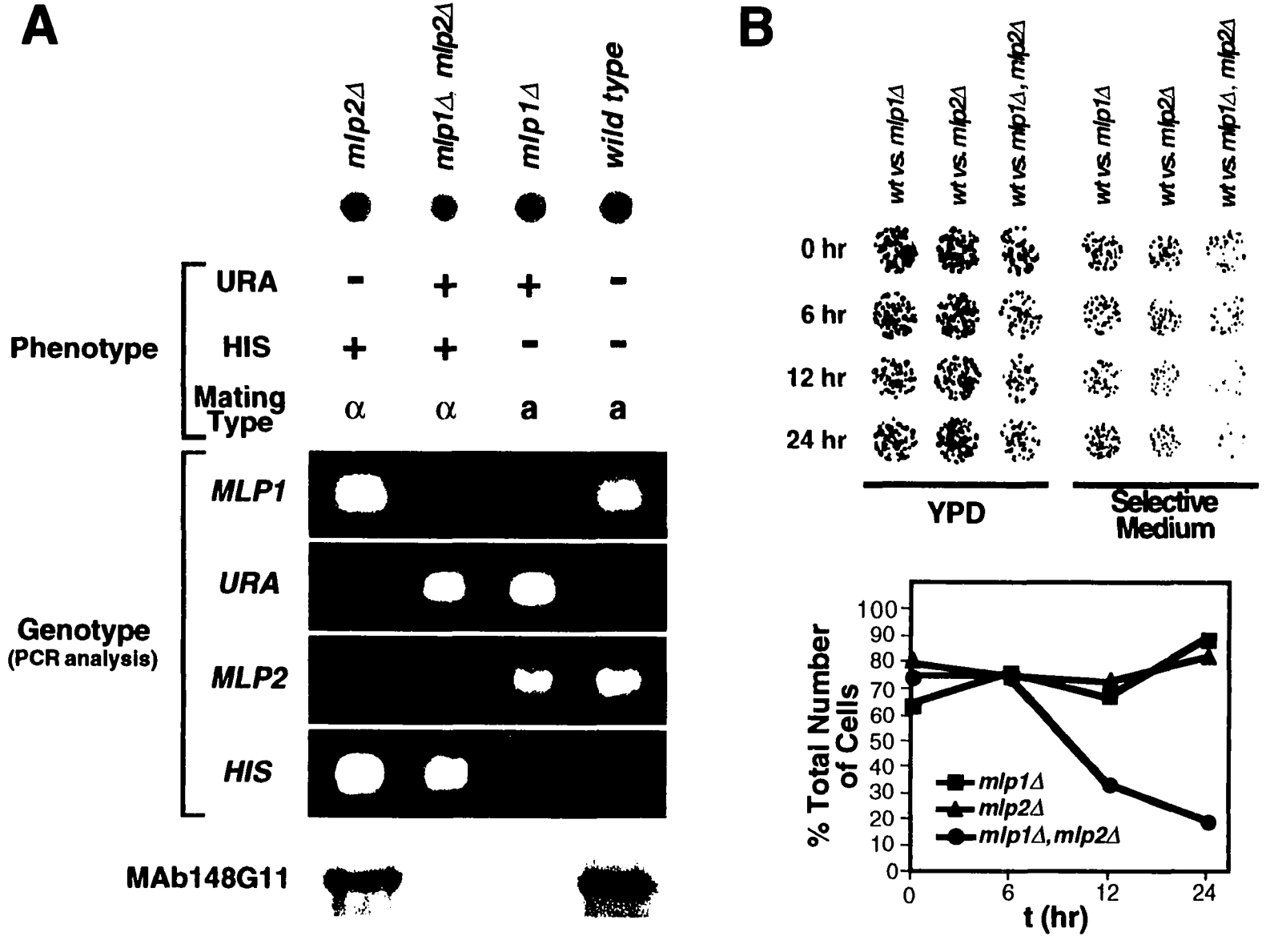

Mlp1p is Associated with Intranuclear Filaments that Connect the NPC with the Nuclear Interior

Results from the indirect IF analysis shown in Fig. 12 demonstrated that Mlp1p is localized at the NE in areas that are only partly occupied by NPCs. To better understand its association with the NE and the NPC, the fractionation pattern of Mlp1p on NE and NPC preparations (Chapter III; Rout and Blobel, 1993; Strambio-de-Castillia, et al., 1995), was followed using MAb148G11 (Fig. 16). As expected the great majority of the Mlp1p specific signal fractionated with the nuclei (88% of the total cellular amount). 86% of the nuclear pool of Mlp1p (76% of the total) fractionated with the highly enriched NE fraction thus confirming the indirect IF data (Fig. 12). After heparin-extraction of NEs, 89% of the NE-associated pool of Mlp1p (68% of the total) was found in the heparin supernatant (Fig. 16, *NE Prep, Fractions 13-14*), demonstrating it is not strongly associated with the membrane and in accordance with the secondary structure of the protein. While 83% of the total cellular amount of Mlp1p (94% of the nuclear pool) appeared to co-fractionate with the crude NPC fraction (Fig. 16, *C-NPCs*), only 22% (18% of the total) of this was found in enriched NPCs (Fig. 16, *E-NPCs*), suggesting only a partial or weak association of Mlp1p with this cellular structure, and again confirming the indirect IF results (Fig. 12). It is important to note at this point that Mlp1p represents the first NE-associated protein to display such a subcellular fractionation pattern (see discussion in Chapter VI).

The ultrastructural localization of Mlp1p was investigated by pre-embedding labeling IEM using MAb148G11 (Figs. 17 and 18). Both isolated NEs (Fig. 17 *A* , *B* and *B'*) and isolated whole nuclei that had been subjected to mild osmotic shock to expose the nuclear interior (Fig. 17 *C* and *D*), were

labeled with this antibody. Fourteen images of individual NPCs that were sectioned perpendicular to their mid-plane were collected from isolated NEs immunolabeled either with MAb165C10 to reveal the localization of Nup159p (Fig. 18*A* ; see Table IV; Kraemer, et al., 1995) or with MAb148G11 to localize Mlp1p (Fig. 18*B*). A radius of ~150 nm around the center of each NPC was used as the cut-off point for each individual image, and the images were computationally superimposed to show the distribution of the gold particles relative to the NPC. Fig. 18*C* shows a plot of the distribution for 50 gold particles from each of the immunolabeled samples, relative to the mid-plane of the NE (*y*) and to the cylindrical axis of the NPC (*x*).

On isolated NEs labeled with MAb148G11, 86% of the gold particles (n=251) were found within a 150 nm distance from the mid-plane of the NE. In the best examples these gold particles where found in association with fibrils that appeared to stretch from the nuclear side of the NE towards the nucleoplasm (Fig 17 *B'* , *arrow*). Interestingly however, while the majority of the NE-associated gold particles (70%) were observed within a 150 nm radius from the center of at least one recognizable NPC, the remaining 30% was outside this radius. The average of the distance between gold particles and the NPC on the y axis was 66 ± 19 nm; while the average distance on the x axis was found to be 41 ± 34 nm (n=50; Fig. 18*C*). This was in marked contrast to the labeling of Nup159p, a nucleoporin known to be associated with the cytoplasmic fibrils attached to the outer ring of the NPC. In this case, and consistent with published results (Kraemer, et al., 1995), the gold particles were found significantly closer to the NPC (y= 33 ± 13; x= 8 ± 8; n=50; Fig. 18C; see discussion in Chapter VI).

On whole nuclei immunolabeled to reveal the localization of Mlp1p, 85.9% of all gold particles (n=291) were found in the nucleoplasm. While the majority

of these gold particles (62%) were observed in immediate vicinity of the NE, a considerable fraction of them (38%) were found more than 110 nm from the mid-plane of the NE. No obvious structure was observed in association with gold localized in the interior of the nucleus, although filaments could again be seen associated with gold particles found near the NE. The results of the IEM localization studies are consistent with the indirect IF and immunoblot results presented above (Figs. 12 and 16); and suggest that Mlp1p is localized on filaments localized at an interface between the nuclear interior and the NPC.

Figure 16. Mlp1p is peripherally associated with the NE and with NPCs.

Yeast nuclei were used as the starting point for the preparation of either highly enriched NEs fractions (*NE Prep* ; Chapter III; Strambio-de-Castillia, et al., 1995) or enriched NPCs (*NPC Prep* ; Rout and Blobel, 1993). Blots similar to the ones used in Figs. 4 and 6 were probed with MAb148G11 that reacts against Mlp1p and subjected to quantitative analysis similar to the one described in Fig. 8. The figures on top of the gels refers to the fraction numbers exactly as described in Fig. 1 and by Rout and Blobel (Rout and Blobel, 1993). Fractions that belong to each individual enrichment steps of the NE and NPC enrichment procedures are grouped as indicated by brackets on top of the gel. The total spheroplasts lysate (*Cells*) and subsequent NE and NPC containing fractions are indicated. In all cases *C-* stands for Crude and *E-* stands for Enriched. *H-NEs* denotes heparin-extracted NEs. A *small arrow* points to a band that disappears together with Mlp1p in strains harboring a deletion of the gene (data not shown) and therefore it is believed to be a major Mlp1p breakdown product. Numbers at the bottom of the gels (*% Total Cellular Amount*) represent an estimate of the amount of Mlp1p specific signal present in each fraction based on quantitative immunoblotting, expressed as a percentage of the total cellular amount. The figures below the bottom brackets (*Loading Equivalents*) indicate the number of cell equivalents (*n*) that were used as the starting material to prepare each fraction.

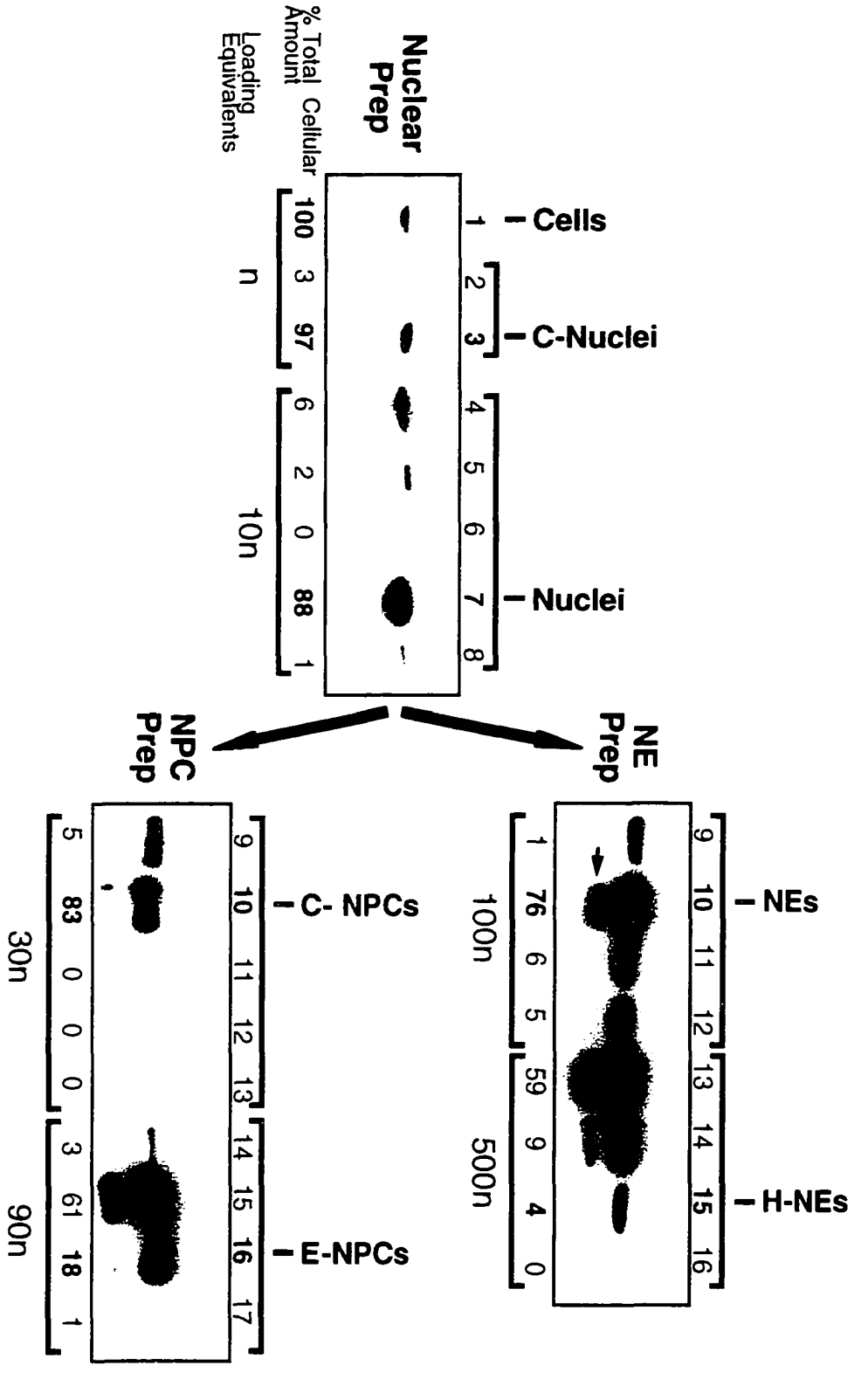

Figure 17. Mlp1p is predominantly associated with nuclear filaments that appear to connect the NPCs with the nuclear interior.

Isolated NEs (*A*, *B* and *B'*) and osmotically shocked isolated nuclei (*C* and *D*) were incubated with MAb148G11 and the labeling was visualized with either 10 nm (*A*, *B* and *B*) or 5 nm (*C* and *D*) gold conjugated secondary antibodies. Labeled NEs were subsequently prepared for transmission EM analysis. The inset presented in panel *B'* represent a 3-fold magnification of an area presented in panel *B*. The *arrow* points to nucleoplasmic fibrils immunostained with MAb148G11. *c*, cytoplasm; *n*, nucleoplasm. Bars, 500 nm (*A*, *B*, *C* and *D*, 50 nm (*B'*).

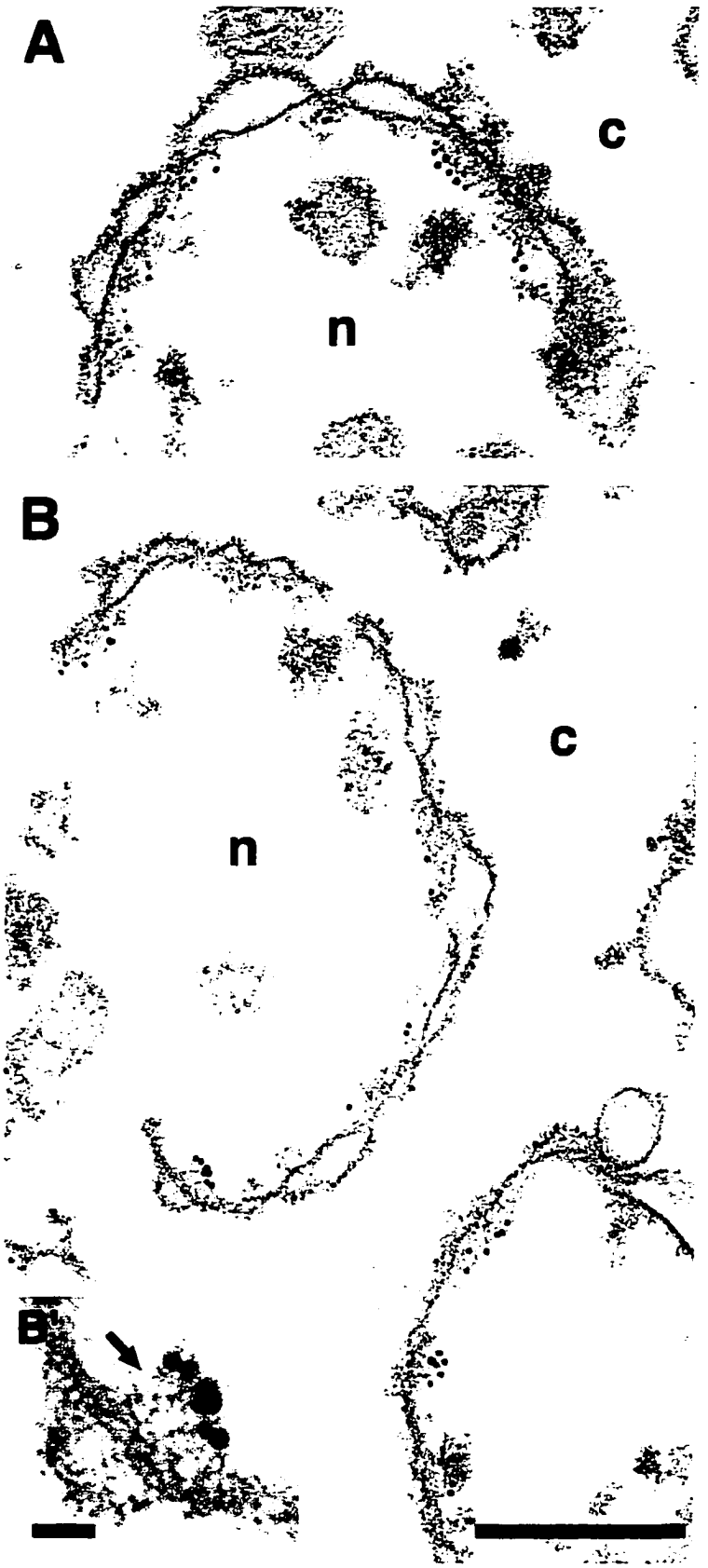

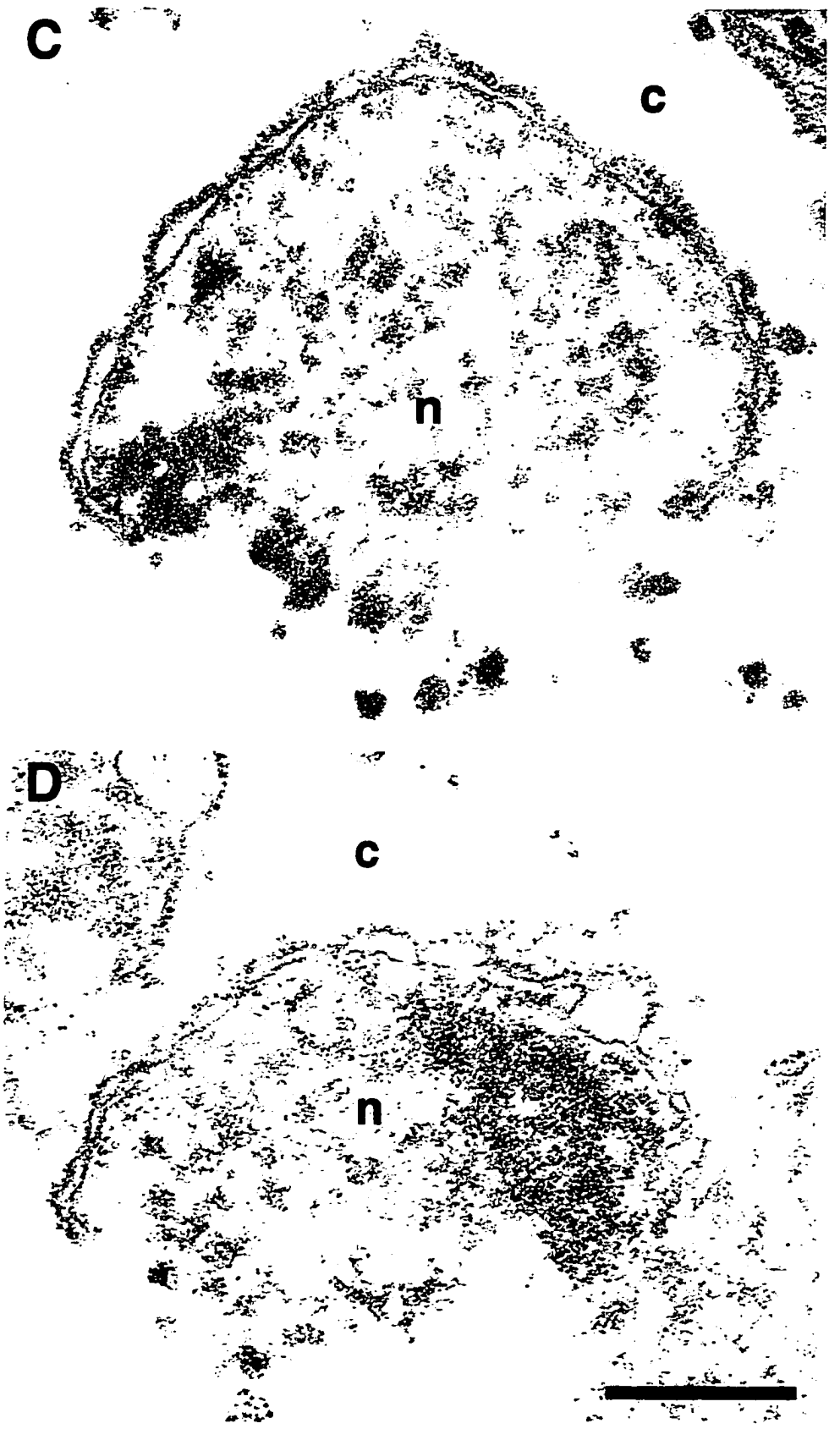

Figure 18. Mlp1p is peripherally localized relatively to the NPC.

(A and *B*) Isolated NEs were incubated either with MAb165C10 that binds specifically to Nup159p (*A*) or with the anti-Mlp1p antibody, MAb148G11 (*B*) as in Fig. 17. Fourteen images of individual NPCs that had been clearly sectioned orthogonally to the mid-plane of the NE were selected from each sample. A radius of ~150 nm around the center of each NPC was selected as the cut-off point for each image. The 14 images derived from each sample were superimposed using Adobe Photoshop v 3.05 (Adobe Systems, Inc., Mountain View, CA) to produce the composites presented here. (*C*) The distances to the mid-plane of the NE (*y*) and to the cylindrical axis of the NPC (*x*) were measured for each of 50 gold particles for isolated NEs labeled either with MAb165C10 (*Nup159p*) or MAb148G11 (*Mlp1p*). These distances were found to have the following averages: *y* , Nup159p 33 ± 13; Mlp1p 66 ± 19. *x* , Nup159p 8 ± 8; Mlp1p 41 ± 34.

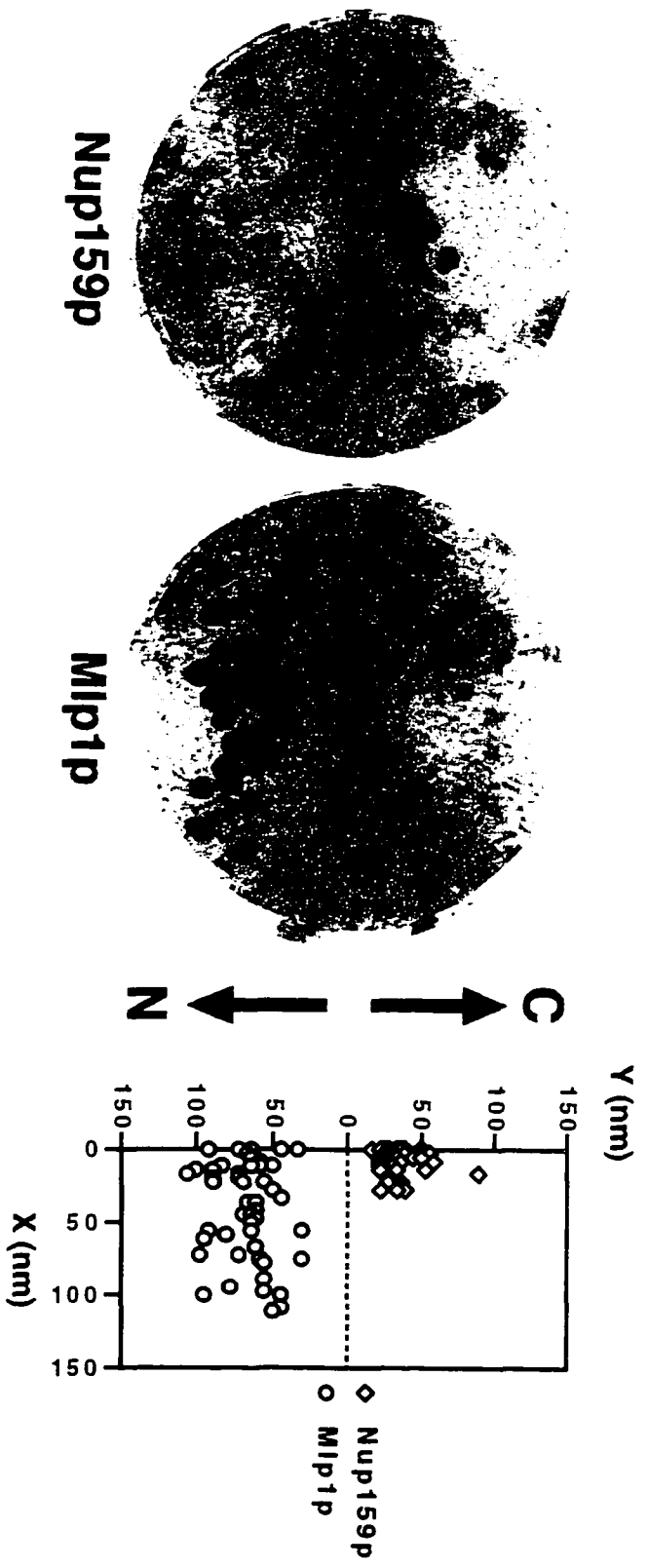

Mlp2p Resembles Mlp1p in its Fractionation Behavior and Ultralocalization

To determine the subcellular localization of Mlp2p, the gene was genomically tagged with an in-frame carboxy-terminal fusion of the IgG binding domains of protein A (pA) (Aitchison, et al., 1995). As a control, *MLP1* was also similarly tagged in parallel. Highly enriched NEs fractions were prepared from the Mlp1p and Mlp2p tagged strains (Strambio-de-Castillia, et al., 1995) and the fractionation pattern of the proteins was assessed on immunoblots (Fig. 19*A* and data not shown). As expected, the fractionation pattern of Mlp1p-pA was indistinguishable from the one observed in Fig. 16 (data not shown). Similarly, Mlp2p-pA co-fractionated with the highly enriched NE fraction (Fig. 19*A* , fraction *10*) but was almost entirely stripped off by the heparin treatment. The tagged strains were used to determine the subcellular localization of the proteins by indirect IF microscopy (Fig. 19*B*). Both proteins were found localized predominantly at patches found at the nuclear periphery when compared with DAPI-stained DNA, consistent with what was previously observed for Mlp1p (Fig. 12). The localization of Mlp1p and Mlp2p in tagged strains was also determined by pre-embedding IEM on isolated NEs (data not shown). Again these two proteins displayed a very similar localization pattern to that observed for Mlp1p (Figs. 17 and 18). These observations are consistent with the hypothesis that Mlp1p and Mlp2p are functional homologues in accordance with their structural similarities and their synthetic "lethality" (Figs. 14 and 15).

Figure 19. Mlp2p is a Mlp1p homologue.

(*A*) Highly enriched NE fractions (Fig. 1; Strambio-de-Castillia, et al., 1995; Rout and Strambio-de-Castillia, 1998) were prepared from a yeast haploid strain expressing a pA tagged version of Mlp2p. A blot similar to the ones described in Figs. 4, 6 and 16 was incubated with rabbit anti-mouse IgG that specifically binds to the pA tag. Bound IgG was visualized using a HRP conjugated anti-rabbit secondary antibody and the presence of bound HRP was revealed by ECL. Fraction numbers and names are as in Figs. 1 and 16. (*B*) The localization of Mlp1p-pA or Mlp2p-pA (as indicated on the top of the images) was examined by indirect IF detection of the pA tag. The staining of DNA with DAPI is also shown. The left most panels (*no TAG*) show a negative control in which a wild type haploid strain was similarly stained. Bar, 2 μm.

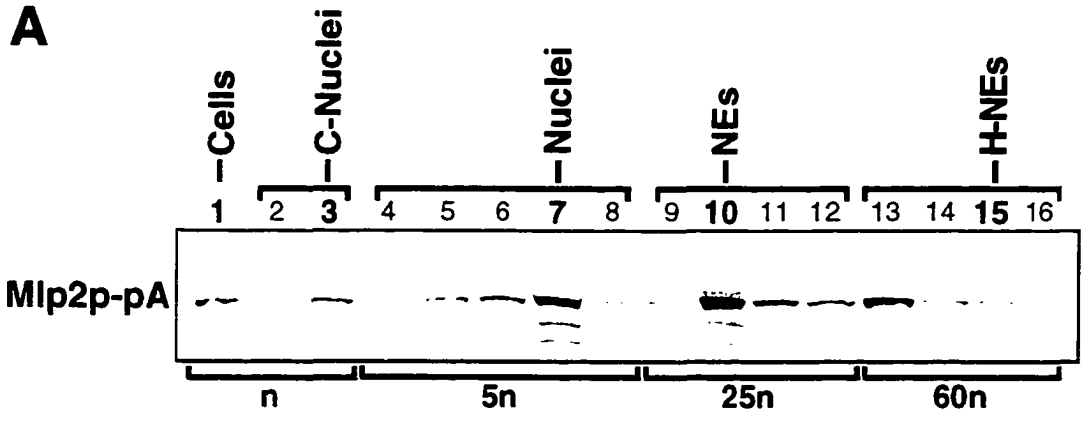

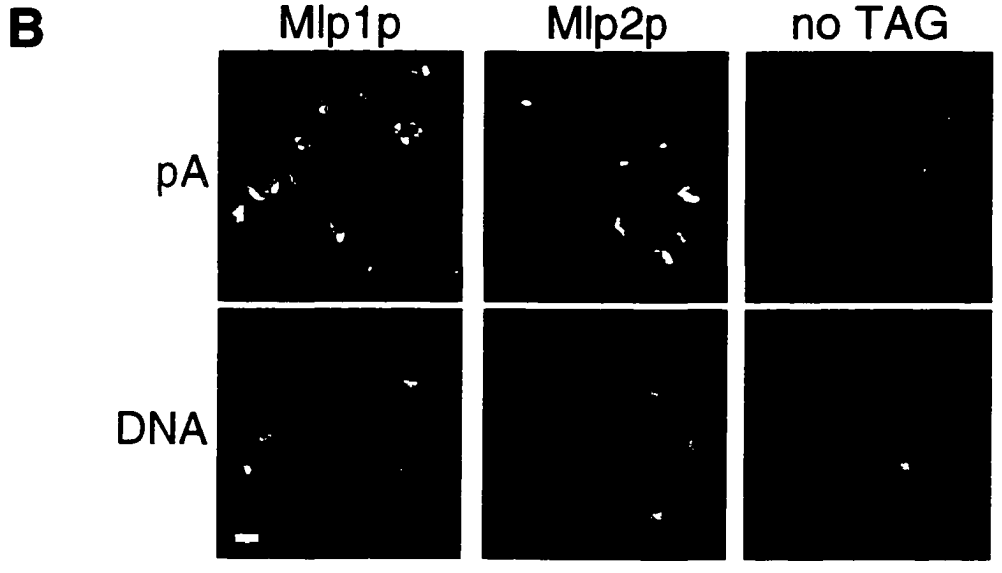

Effects of *MLP1* and *MLP2* Deletion on Cellular and Colony Morphology and on the Distribution of Nuclear Markers

To further investigate the function of Mlp1p and Mlp2p, a strain harboring a deletion of both genes (*mlp1Δ, mlp2Δ*) was subjected to a thorough phenotypic analysis (Figs. 20, 21, 22, 23 and 24). *mlp1Δ, mlp2Δ* cells displayed an aberrant morphology by both light microscopy (data not shown) and by transmission EM (Fig. 20*A*, left). Mutant cells appeared larger in size than their wild type counterpart. This phenotype was further analyzed by measuring the cell volume of the mutant and wild type cells using a Coulter counter (Fig. 20*A*, right). This instrument confirmed that the *mlp1Δ, mlp2Δ* population had a significantly higher proportion of cells with a larger than average fluid volume relative to the control. Exponentially growing cultures of *mlp1Δ, mlp2Δ* mutants presented a marked alteration in the distribution of cell-cycle morphological classes relative to the wild type control (Fig. 21). The most striking observation was the reduction in the frequency of unbudded cells (*NB*) representing cells in the G1 phase of the cell cycle and the concurrent elevation in the frequency of large-budded (*LB*) cells representing cells in the late stages of M in the mutant population. In addition, a significant proportion of the mutant cells were double-budded (*DB*), an occurrence found only very rarely in the control. *mlp1Δ, mlp2Δ* grew as indented or "nibbled" colonies that appeared markedly different from the smooth colonies produced by wild type cells (Fig. 20*B*, left). This phenotype has been observed in association with clonal lethality (Holm, 1982) and may be due to chromosome segregation defects. To investigate the possibility that Mlp1p and Mlp2p could be required for accurate mitotic chromosome segregation, a homozygous diploid *mlp1::URA3, mlp2:HIS3/ mlp1::URA3, mlp2:HIS3* (*mlp1Δ, mlp2Δ hd*) was constructed by mating two

double mutant haploid strains of opposite mating types. The ability of *mlp1Δ, mlp2Δ hd* to correctly segregate chromosomes during mitosis was investigated using the chromosome III segregation assay described by Shore and coworkers (Chi and Shore, 1996; Wotton and Shore, 1997; Fig. 20*B* , right). In this assay, wild type and mutant diploid cells of interest are mated with cells from haploid tester strains of both mating types and the frequency of mating events is measured. An increase of the mating rate of the mutant over the wild type background reflects the frequency of events in the original population in which individual mutant cells had failed to inherit chromosome III (see Chapter II for details). The rate of chromosome loss observed with *mlp1Δ, mlp2Δ hd* (homozygous diploid) cells was 15.05 ± 6.71 x 10^{-6} events/cell/generation with the *MATa* tester strain and 2.08 ± 0.48 x 10^{-6} events/cell/generation with the *MATα* tester strain. This represented a 22 and 34 fold increase respectively relative to wild type (*MATa*, 0.70 ± 0.32 x 10^{-6} events/cell/generation; *MATα*, 0.06 ± 0.02 x 10^{-6} events/cell/generation). This result shows that *mlp1Δ, mlp2Δ hd* cells cannot accurately segregate chromosomes in mitosis. Taken together with the other results presented in this section, the chromosome segregation defect suggests that Mlp1p and Mlp2p are together required for efficient cell division. To investigate this further, the DNA content of wild type and *mlp1Δ, mlp2Δ* cells was analyzed by flow cytometry (Fig. 20*C*). No significant alteration in the ploidy of the double mutant cells with respect to wild type was observed using this assay. This observation indicated that Mlp1p and Mlp2p are probably not involved in the direct regulation of the yeast cell cycle.

To show that the defects described above were linked to the *MLP1* and *MLP2* disruptions, two 1:1:1:1 tetrads (see above) derived from diploid strains heterozygous for the double disruption were examined in some detail (data not shown). This analysis demonstrated that both the cellular morphology defects

and the "nibbled" colony phenotype segregated 1:3 with the double disruption. These results indicate that the phenotypes displayed by *mlp1Δ, mlp2Δ* cells are indeed caused by the deletion of both *MLP1* and *MLP2*.

In order to determine whether the deletion of *MLP1* and *MLP2* affected nuclear structure, we compared the localization of different nuclear markers by indirect IF microscopy in *mlp1Δ, mlp2Δ* and wild type cells (Fig. 22). The shape of the nucleus and structure of the NE were studied by staining wild type and mutant cells with the mAb MAb165C10, that specifically recognizes the nucleoporin Nup159p (Table IV; Kraemer, et al., 1995). The characteristic punctate pattern of NPCs throughout the NE was observed in both wild type and mutant cells, indicating that deletion of *MLP1* and *MLP2* had no direct effect on NPC structure. Nevertheless, in mutant cells, staining with MAb165C10 revealed an alteration of the overall nuclear morphology. Nuclei appeared larger and irregularly shaped and again multinucleated cells were often observed.

The most striking observation was that of an altered nucleolar morphology in *mlp1Δ, mlp2Δ* cells as visualized using a mAb against the nucleolar protein Nop1p (Aris and Blobel, 1988; Henriquez, et al., 1990). In wild type cells, nucleoli stained with this mAb appeared as typical crescent-shaped structures closely juxtaposed to the NE. In mutant cells, the nucleoli often appeared as larger irregularly shaped structures that showed signs of fragmentation. The morphology of the nucleolus was further studied by transmission EM of thin-sectioned mutant and wild type cells (Fig. 23). In wild type cells the nucleolus appeared a single denser region of chromatin closely associated to the NE. In *mlp1Δ, mlp2Δ* , it was possible to observe multiple small dense patches of chromatin in a single nucleus; these fragmented structures were often not in

direct contact with the NE but they appeared to be connected to one another to form a continuous network.

The structure of the mitotic spindle in *mlp1Δ, mlp2Δ* was investigated using a rabbit polyclonal antibody against yeast tubulin (Fig. 24). Measurements of the spindle lengths in normal haploid yeast cells revealed that while a large proportion of the spindles ranged between 0.5 and 1.5 μm long (37%) representing cells in G1, S or G2 phases of the cell cycle, a minority (27%) were longer than 3 μm displaying cells between G2 and the end of M (Byers and Goetsch, 1975; Winey, et al., 1995). In contrast, *mlp1 Δ, mlp2Δ* cells appeared to be partially impaired in their ability to form extended spindles with only 14% of the spindles exceeding 3 μm.

The involvement of Mlp1p and Mlp2p in DNA repair was investigated using a UV-sensitivity assay (data not shown). Mutant strains did not show any increase in their sensitivity to UV irradiation with respect to wild type, contradicting the results published by Botstein and coworkers (Kolling, et al., 1993; see discussion in Chapter VI).

Alterations in various components of the nuclear transport pathways have been associated with phenotypes similar to the ones described above, such as: mitotic defects [Srp1p/Kap60p (Loeb, et al., 1995; Cse1p, Xiao, et al., 1993; Brinkmann, et al., 1995; Irniger, et al., 1995)]; aberrant nuclear structure [Nup170p (Aitchison, et al., 1995; Kenna, et al., 1996); Crm1p (Adachi and Yanagida, 1989)]; defective nucleolar morphology [Nup120p (Aitchison, et al., 1995; Heath, et al., 1995); Srp1p/Kap60p (Yano, et al., 1994); Nup145p (Fabre, et al., 1994)]; and altered spindle morphology [Nup120p, (Aitchison, et al., 1995); Srp1p/Kap60p, (Yano, et al., 1994)]. This suggested that Mlp1p and Mlp2p may similarly have a role in nucleocytoplasmic transport. Furthermore, the localization of Mlp1p and Mlp2p on intra-nuclear filaments connecting the

NPC with the nuclear interior (Figs. 17 and 18), and their homology with the human protein Tpr, also pointed to a possible role in facilitating nuclear movement of molecules.

Figure 20. Yeast strains carrying a double disruption of *MLP1* and *MLP2*, display significant cellular and colony morphology alterations associated with defects in chromosome segregation.

(*A*) Left: Low-magnification electron micrographs of thin-sectioned fixed whole yeast cells showing the marked difference in size of the mutant cells with respect to wild type. Bar, 2 μm. Right: Logarithmically growing wild type and *mlp1Δ, mlp2Δ* cells were sonicated and were subjected to cell volume analysis using a Coulter counter. (*B*) Left: Photographs of single colonies of wild type and *mlp1Δ, mlp2Δ* cells revealing the "nibbled" morphology of the mutant colonies. Right: Graphical representation of the results of a chromosome III stability assay performed on wild type and *mlp1Δ, mlp2Δ hd* (homozygous diploid) cells, showing a significant increase in chromosome loss rate in mutant cells relative to wild type. The results presented represent the averages of at least three independent experiments. The experiments were performed as described in Chapter II. (*C*) Logarithmically growing wild type and *mlp1Δ, mlp2Δ* cells were harvested and prepared for flow cytometry as detailed in Chapter II. No significant change was observed in the DNA content distribution of the *mlp1Δ, mlp2Δ* population relative to wild type.

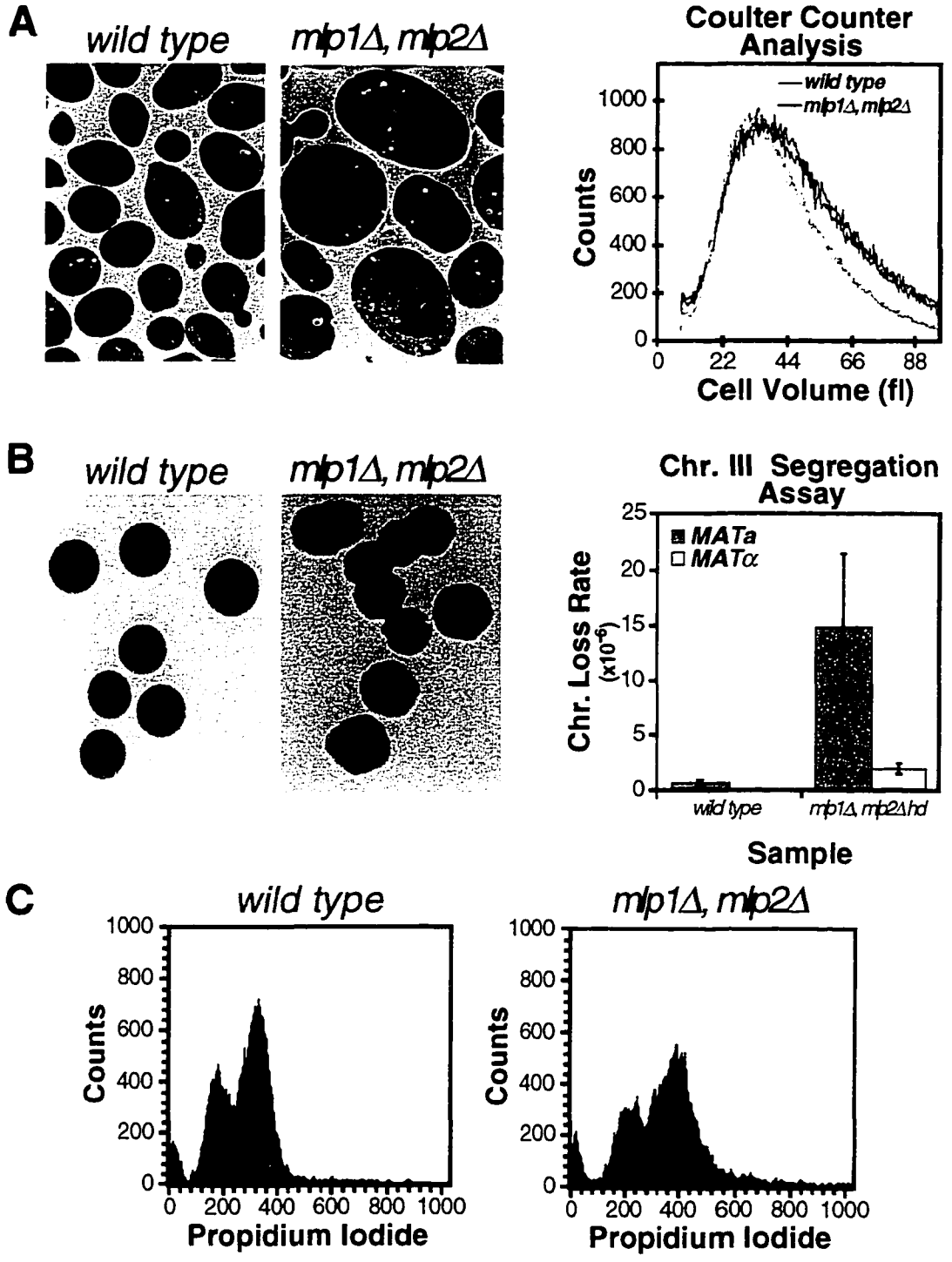

Figure 21. Distribution of morphological classes in wild type and *mlp1Δ, mlp2Δ* mutant cells.

Exponentially growing wild type and mutant cells were harvested by centrifugation, fixed and observed by light microscopy. Cells belonging to four different morphological subtypes (*NB*, unbounded cells; *SB*, small-budded cells; *LB*, large budded cells; *DB*, double-budded cells) were counted and the percentage of each group is presented.

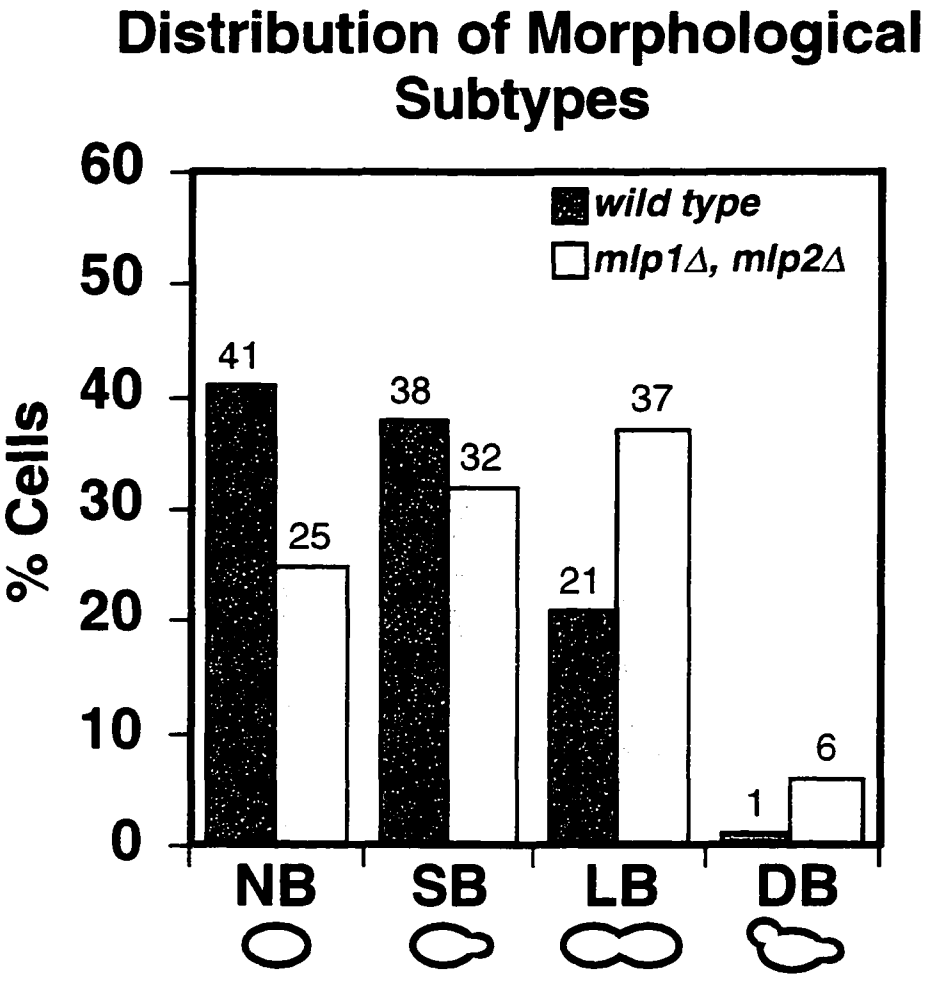

Figure 22. Distribution of nuclear markers in *mlp1Δ, mlp2Δ* cells.

Examination of wild type and *mlp1Δ, mlp2Δ* cells by IF directed against the nucleoporin Nup159p and the nucleolar marker Nop1p, showing altered nuclear and nucleolar morphology. NPCs were visualized using MAb165C10 that recognizes Nup159p (Table IV; Kraemer, et al., 1995) and nucleoli were visualized using the mAb to Nop1p D77 (Aris and Blobel, 1988; Henriquez, et al., 1990). In both cases bound immunoglobulin was revealed using a Cy3 conjugated donkey anti-mouse antibody. The nuclear DNA was coincidentally stained with DAPI. Bar, 3 μm.

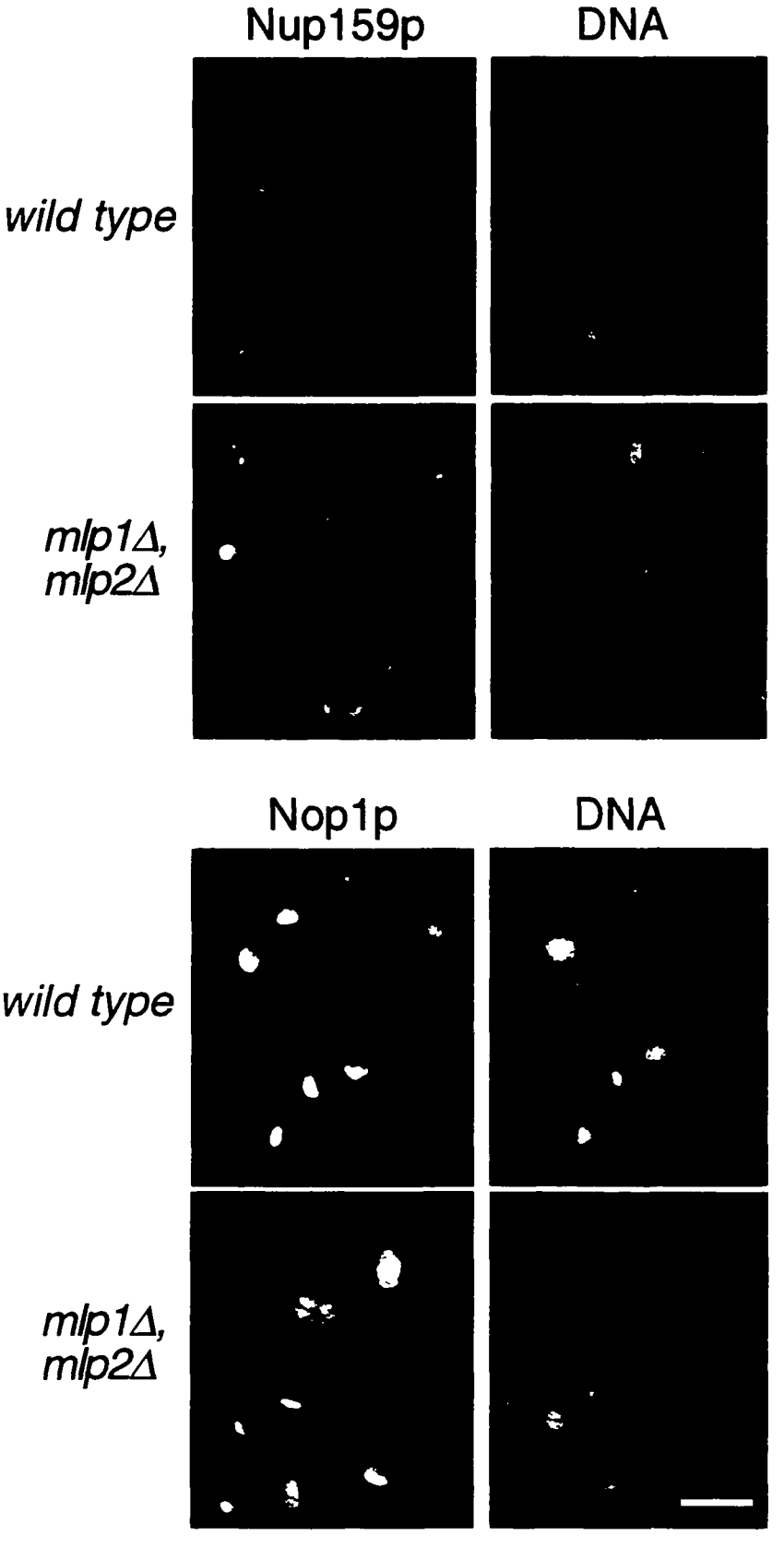

Figure 23. Nucleoli fragment in *mlp1Δ, mlp2Δ* cells.

Thin sectioned, fixed wild type (*A*) and *mlp1Δ, mlp2Δ* (*B*) cells were examined by transmission EM. Mutant cells show signs of nucleolar fragmentation. The position of dense chromatin regions corresponding to the nucleolus are indicated (*arrows*). Bar, 0.25 μm.

B

Figure 24. Altered spindle morphology in *mlp1Δ, mlp2Δ* cells.

Logarithmically growing wild type and mutant haploid cells were harvested, fixed and immunolabeled with a rabbit polyclonal antibody to reveal the position of tubulin. The length of mitotic spindles was measured for both wild type (n=136) and mutant cells (=186) and the results of the analysis are presented as percentages of the total number of spindles.

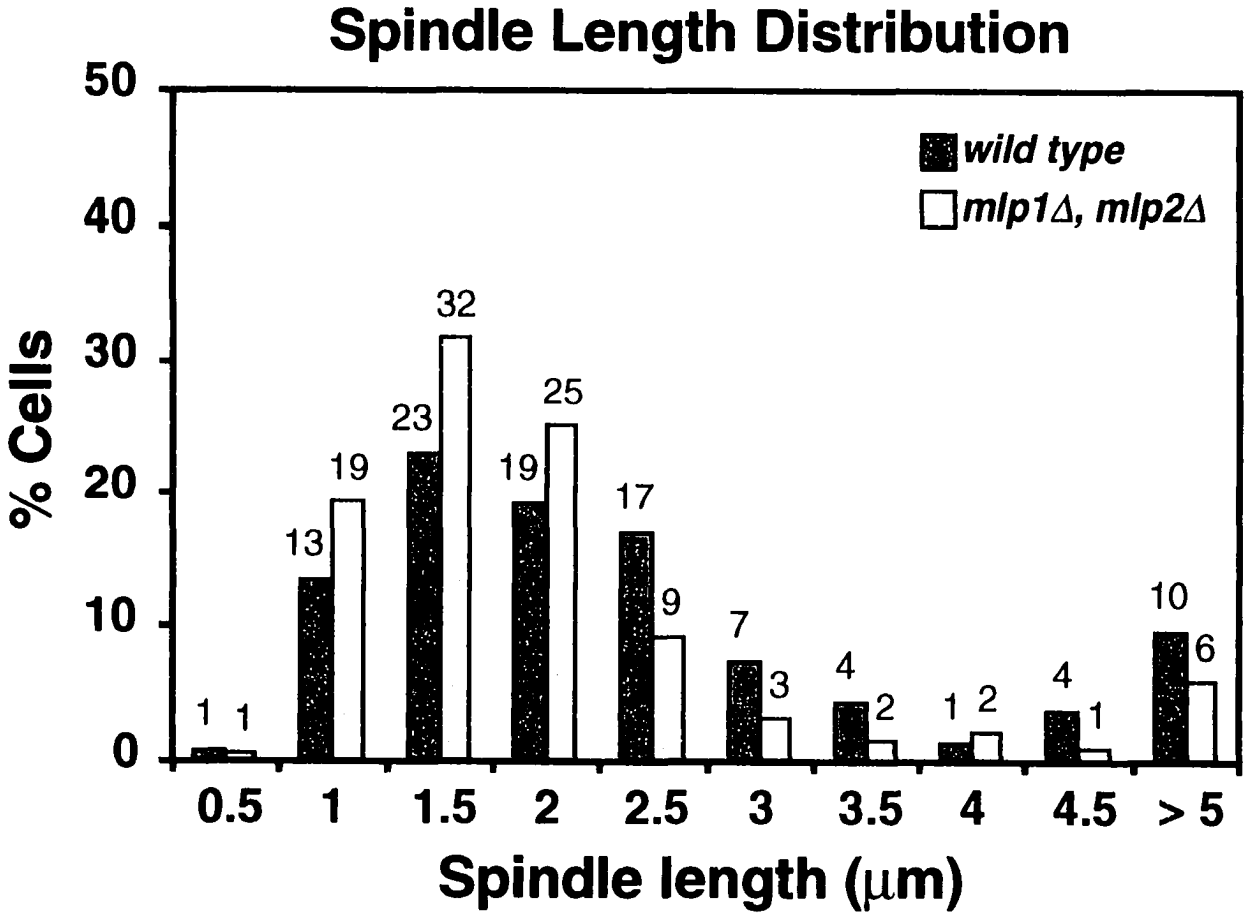

Deletion of *MLP1* and *MLP2* Affects the Efficiency of Nuclear Import

To investigate the possibility that Mlp1p and Mlp2p may be involved in transport of molecules in and out of the nucleus, an *in vivo* import assay was performed as described by Goldfarb and coworkers (Shulga, et al., 1996). This assay allows the detection of kinetic defects in the import rates of a NLS-GFP reporter (Fig. 24). In this assay logarithmically growing yeast cells constitutively expressing NLS-GFP are harvested and poisoned with deoxyglucose and sodium azide in order to block the production of energy. Under these conditions the active import of the NLS-GFP reporter into the nucleus is blocked resulting in the equilibration of the GFP signal between the nucleus and the cytoplasm, most likely by passive diffusion across the NPC. When the metabolic inhibitors are removed and the cells are allowed to recover in medium containing dextrose, NLS-GFP is once again actively imported in the nucleus. The relative rates of accumulation of the mutant strain are compared with the ones found with wild type, revealing any defect in the mutant's efficiency of nuclear import. The steady state distribution of NLS-GFP was indistinguishable in homozygous diploid cells carrying a double deletion of *MLP1* and *MLP2* as compared to wild type (data not shown). Nevertheless, *mlp1Δ, mlp2Δhd* (homozygous diploid) cells displayed a markedly slower relative accumulation rate of NLS-GFP into the nucleus with respect to their wild type counterpart, 13.5 ± 0.2% / min (wild type) *versus* 8.9 ± 0.1% / min (*mlp1Δ, mlp2Δhd*). Significantly, when double mutant cells were allowed to recover for extended periods of time (up to double the time required for wild type), the initial equilibrium distribution of reporter protein was regained, again indicating that the efficiency of import and not its steady state balance was affected by the

absence of Mlp1p and Mlp2p. The rates of passive equilibration of the NLS-GFP reporter during the incubation with deoxyglucose and sodium azide were also measured in both wild type and mutant cells (Fig 24; see Chapter II for details on the method). In this case, *mlp1Δ, mlp2Δhd* displayed a significant increase in the relative passive nuclear egress rates of the NLS-GFP reporter as compared to wild type, -8.75 ± 1.0% / min (wild type) *versus* -13.1 ± 0.6% / min (*mlp1Δ, mlp2Δhd*). This result is entirely consistent with a reduced efficiency of nuclear import in mutant cells (see discussion in Chapter VI).

The involvement of Mlp1p and Mlp2p in active nuclear export was investigated using two steady state assays (data not shown). In the first assay, the subcellular distribution of poly(A)$^+$ RNA was analyzed by *in situ* hybridization using digoxigenin-labeled oligo(dT)$_{30}$ as a probe (Wente and Blobel, 1993). In this assay, a block in mRNA nuclear export is reflected in the accumulation of the poly(A)$^+$ RNA-specific signal in the nucleus at steady state. In the second assay, the steady state distribution of a GFP reporter carrying both an NLS and an NES was studied by direct fluorescent microscopy as described by Weis and coworkers (Stade, et al., 1997). In this scenario, the NES usually wins out over the NLS resulting in a cytoplasmic distribution of the reporter at equilibrium. Therefore, a defect in the NES-dependent nuclear export pathway is revealed by the appearance of GFP-specific nuclear signal. In both cases no effect on export was detected at steady state and the double mutant cells appeared indistinguishable from wild type (see discussion in Chapter VI).

Figure 25. Mlp1p and Mlp2p are involved in facilitating nuclear import of a NLS-GFP reporter.

Top: Graphical representation of the results of an *in vivo* nuclear import assay performed as described in Chapter II. During recovery from an incubation in the presence of the metabolic inhibitors deoxyglucose and sodium azide, wild type cells reimported a NLS-GFP reporter very rapidly and the reaction was complete in 15 min. The mutant (*mlp1Δ, mlp2Δhd*) on the other hand, displayed a much slower rate of reimport and took up to twice as much as the wild type to reach steady state levels of nuclear signal. At least 40 cells were scored per time point. The results presented reflect the averages of at least 4 independent measurement per time point. Bottom: Graphical representation of the results of an *in vivo* nuclear diffusion assay analogous to the import assay described above (see Chapter II for details). During incubation in the presence of the metabolic inhibitors deoxyglucose and sodium azide, aliquots were collected from both wild type and *mlp1Δ, mlp2Δhd* and the percentage of normal cells displaying clear nuclear localization of the reporter protein NLS-GFP was scored as a function of time. The kinetic of passive diffusion is significantly faster in mutant cells relative to wild type, consistent with the reduced import rate of the mutant observed in the top panel. At least 40 cells were scored per time point. The results presented in the graph reflect the averages of at least 3 independent measurement per time point.

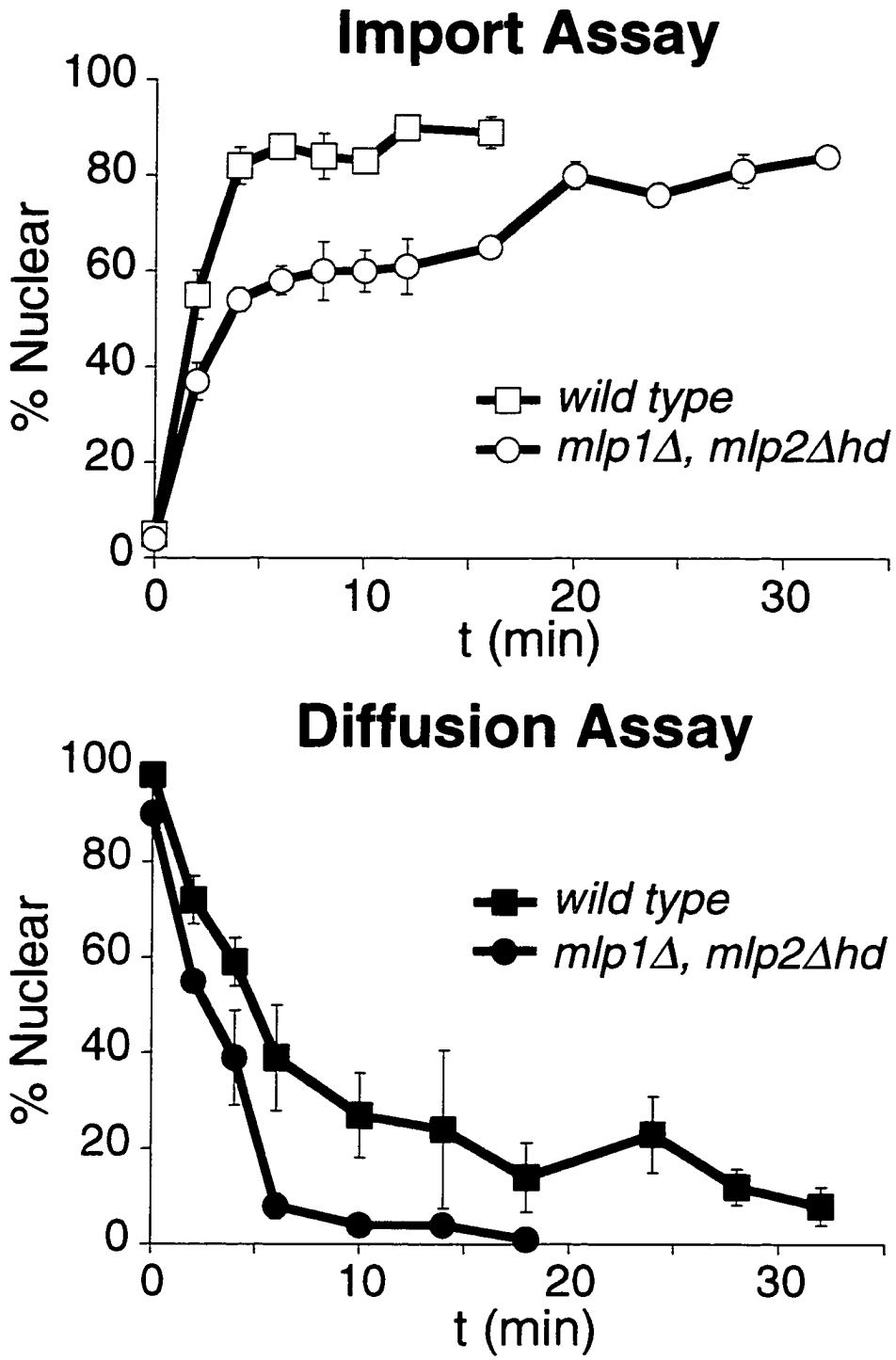

Overexpression of MLP1 in *Saccharomyces*

The potential coiled-coil region of Mlp1p suggest that this protein may be capable of self-assembly. Mlp1p was overexpressed in yeast cells to determine whether extended polymers could be formed that could clarify the role of this protein in providing a connection between the NPCs and the nuclear interior. The entire coding region of *MLP1* was subcloned in a 2 μm-based yeast expression vector under the control of the *GAL* inducible promoter (see Chapter II for details). Using this plasmid (pGALMLP1), it was possible to overexpress Mlp1p at least ~100-fold over wild type levels as demonstrated by quantitative immunoblotting performed with MAb148G11 (Fig. 26). Strikingly, overexpression of Mlp1p at these levels was not toxic as demonstrated by the ability of cells carrying pGALMLP1 to grow on galactose plates (data not shown). Cells containing this construct were induced with galactose for various periods of time and analyzed by Indirect IF microscopy using MAb148G11 to reveal the localization of Mlp1p (Fig. 27). As expected, uninduced cells (0 hr time point) showed a staining pattern very similar to the one observed in wild type cells. In contrast, induced cells showed an increase of the Mlp1p-specific signal as a function of the induction time. Initially, small dots (1-4 per cell) could be seen at the nuclear periphery at or adjacent to the NE. Subsequently, these dots appeared to coalesce and generally gave rise to one prominent circular patch per cell. Finally, this large patch grew to occupy most of the nuclear interior. The morphology of the NE, the NPCs, the nucleolus and of the spindle were studied in cells overexpressing Mlp1p by double-staining indirect IF microscopy (data not shown). The morphology of all of these nuclear structures appeared normal after extended induction periods and none appeared to be in association with the large Mlp1p dots or patches. Nuclei isolated from cell

overexpressing Mlp1p were observed by EM to reveal whether any novel structure could be detected (Fig. 28*B*). As a comparison, isolated nuclei from cells that had been grown in dextrose to repress the expression of the non-chromosomal copy Mlp1p were also analyzed using the same technique (Fig. 28*A*). Extensive electron-dense patches that extended from different areas of the NE towards the nuclear interior were observed in cells grown in galactose but were absent in cells grown in dextrose. These electron-dense patches did not appear to have any obvious ordered structure but appeared to be fibrillogranular in nature. In addition they appeared to be distinct from the nucleoli both in number and in morphological appearance. No other structure or filaments were observed in induced cells that were not present in repressed cells. To determine if these structures were indeed formed of large accumulations of Mlp1p, isolated nuclei from cells grown in both galactose (Fig. 28*C*, *D*) and dextrose (data not shown) were immunostained with MAb148G11 and prepared for IEM . As expected, the dense fibrillogranular patches present in induced cells specifically stained with MAb148G11 demonstrating that they contain large quantities of Mlp1p (see discussion in Chapter VI). In cells grown in dextrose, Mlp1p appeared to have a localization that was indistinguishable from wild type (see Fig. 17*C*, *D*).

Figure 26. Mlp1p can be overexpressed at least 100-fold in yeast.

Wild type W303 cells were transformed with pGALMLP1, expressing the entire *MLP1* gene under the control of the inducible *GAL* promoter (see Chapter II for details of the cloning procedure). Transformants were exponentially grown in selective medium containing raffinose before induction with galactose. Samples of the culture were taken at the indicated time points (*0, 0.5, 1, 2, 4 hr*) and total cell lysates were prepared as described in Chapter II. Lysates were loaded on SDS-PAGE and transferred to nitrocellulose before immunoblotting with the anti-Mlp1p MAb148G11. Numbers below the gel indicated the relative expression level of Mlp1p at each time point. Quantitation of the Mlp1p-specific signal was performed as described in Chapter II.

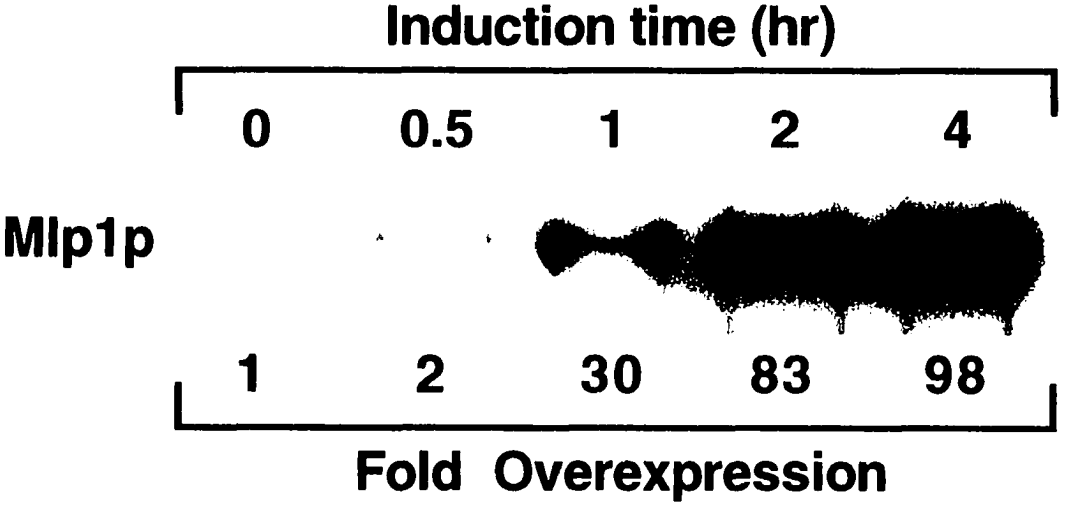

Figure 27. Upon overexpression, Mlp1p forms multiple peripheral nuclear dots that subsequently coalesce and take over the majority of the nuclear volume.

W303 cells containing pGALMLP1 were grown to mid-logarithmic phase in selective medium containing raffinose before induction with galactose. Cells were sampled at the indicated time points after induction (*0, 0.5, 1, 2, 4 hr*), fixed and immunostained with MAb148G11 to reveal the position of Mlp1p. As a comparison, the position of the DNA was revealed using DAPI. Bar, 2 μm

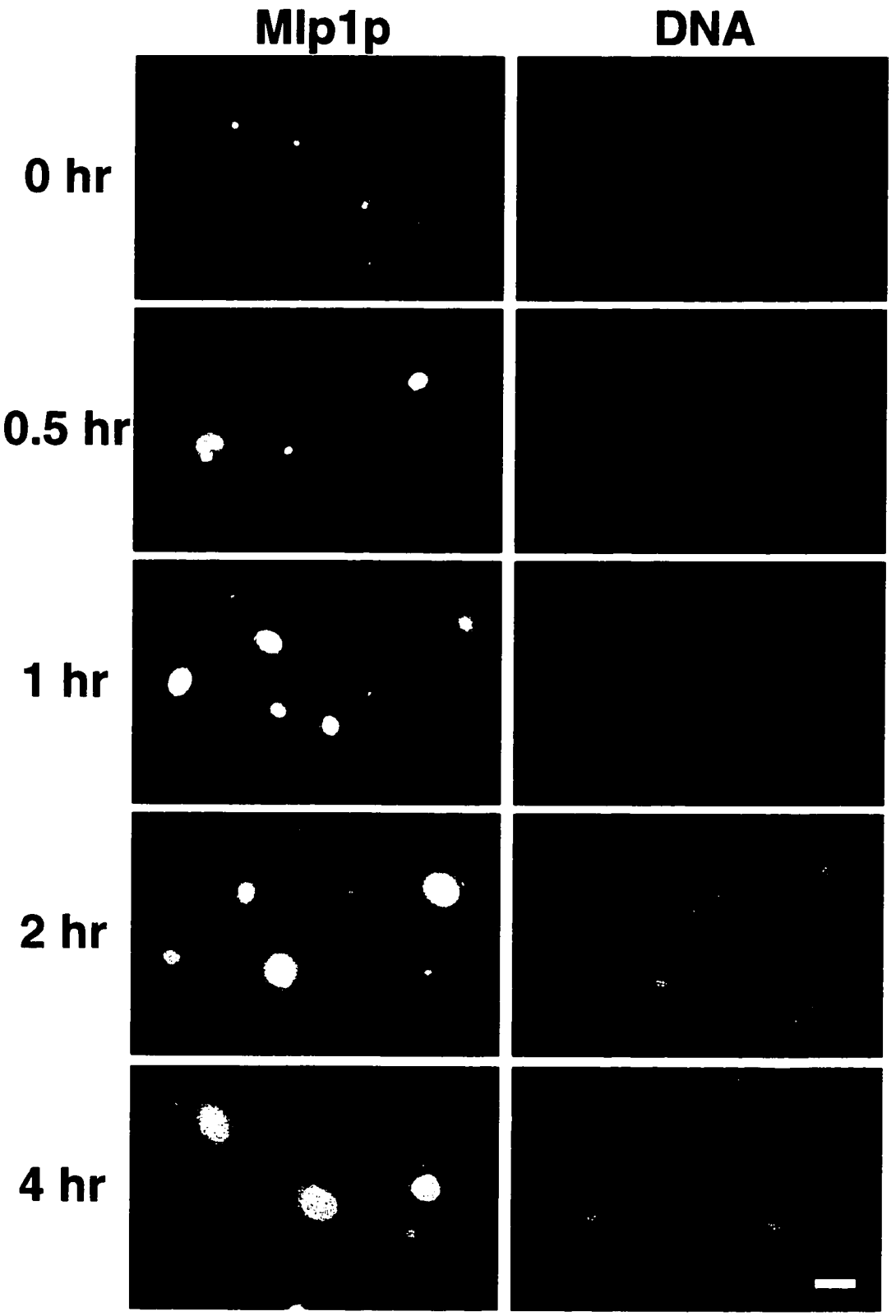

Figure 28. When overexpressed in yeast, Mlp1p forms dense fibrillogranular patches underneath the NE that are easily distinguishable from the nucleolus.

Exponentially growing cells containing pGALMLP1 were transferred to selective medium containing either dextrose (*A*) or galactose (*B-D*) and the incubation was continued for 4 hr. At the end of the induction/repression period, cells were harvested and nuclei were isolated using the method described in Chapter II. Isolated nuclei were either subjected to thin-section EM analysis (*A-B*) or to IEM analysis using MAb148G11(*C*, *D*) as described in Chapter II. *Arrows* point to large fibrillogranular electron-dense patches that were observed in induced cells and contained Mlp1p. Bar, 250 nm.

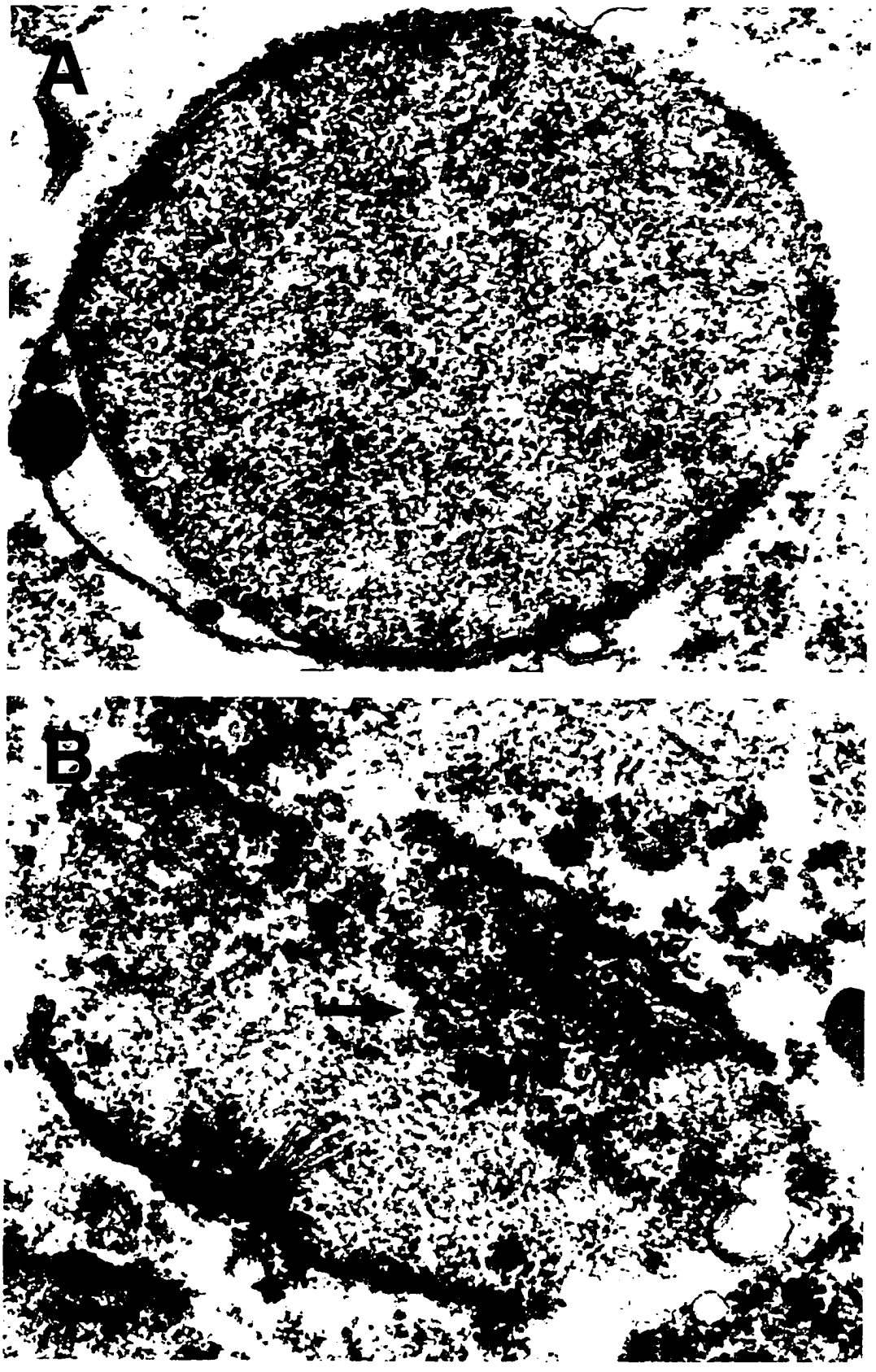

Chapter VI: Discussion

A Method for the Preparation of Highly Enriched NE Fractions from the Yeast *Saccharomyces*

Presented in the first part of this thesis dissertation is a method for the large scale isolation of yeast NEs and the for the extraction of isolated NEs with heparin. EM analysis showed that both of these preparations are virtually devoid of gross contaminants and are morphologically well-preserved. Moreover, negative staining of H-NEs showed that heparin extraction removes the main structure of the NPCs leaving open pores in the membrane. Using biochemical criteria it was demonstrated that key cytoplasmic and nucleoplasmic contaminants are absent from both NE fractions and that NE-associated proteins were recovered with yields ranging between 80 and 90%. The NE and H-NE fractions are respectively 100- and 340-fold enriched based on the yields of NE specific markers. Both the NEs and H-NEs were shown to be active in a cell-free ER translocation assay, each having a higher specific activity than that of previously published crude microsomes (Hansen, et al., 1986; Rothblatt and Meyer, 1986; Waters and Blobel, 1986). Finally, extraction of H-NEs with detergents showed that the grommets left in the NE after heparin treatment are apparently stabilized by previously uncharacterized ring structures of approximately the same internal diameter as the grommets themselves. It is hoped that the compositional analysis of these rings may shed light on the mechanism by which the NPCs are retained in the NE (see below).

The high yields of the NE fractions allowed the construction of a balance-sheet that tallies the distribution of representative markers in various nuclear

and non-nuclear compartments. For example, this strategy was used to determine the quantitative localization of ribosomal proteins within the cell. It was also possible to show that the NE represents approximately 20% of the ER, similar to what was previously reported (Preuss, et al., 1991). Using the same approach it was established that while the majority of the Golgi integral membrane protein Sed5p (98% of the total cellular amount) is indeed found in low-density membranes that characterize this organelle, a small pool of this protein is associated with the ER, consistent with its role in ER to Golgi transport and with previous observations (C. Hopkins, personal communication). A possible caveat of the results presented here is that cells are subjected to exhaustive cell-wall digestion (3 h at 30°C) before lysis. This treatment stops cell division and could alter the amount and composition of various organelles. However, the qualitative subcellular localization of each of the markers used here has been previously ascertained. In all cases (with the possible exception of Nup2p, see below), this localization corresponds with the quantitative distribution of the marker, and the organelle(s) with which it is associated, in the enrichment procedure presented here. This indicates that the quantitative data obtained from the subcellular fractionation of a given marker accurately reflect the subcellular distribution of that marker *in vivo*. Hence, quantitative analysis of the fractionation behavior predicted that a proportion of Pom152p would be associated with the ER, which was confirmed by IF staining of cells. This suggests that the balance-sheet approach could be used to predict the subcellular localization and proportional distribution of other cellular components.

As mentioned above, NEs and H-NEs are competent in the translocation of ppαF to the perinuclear space. These fractions therefore provide a viable source of yeast rough ER membranes that could be used to develop cell-free

systems for the study of various rough ER functions and to further purify the molecular components involved in these functions. For example, systems for the reconstitution of protein translocation into proteoliposomes have been developed and used successfully in yeast (Brodsky, et al., 1993; Brodsky and Schekman, 1993). The utilization of the highly-enriched NE fractions described here instead of crude microsomal membrane fractions may enhance the potentiality of these systems. In addition, the NE and H-NE fractions could be used to develop cell-free systems that will allow the molecular dissection of other important NE related functions. These include: nuclear transport, at least in the aspect of specific docking and undocking of the substrate to the NPC (Kraemer, et al., 1995; Aitchison, et al., 1996; Rout, et al., 1997); chromatin-NE interactions, such as the binding of telomeric structures to the inner nuclear membrane (Dresser and Giroux, 1988; Klein, et al., 1992; Palladino, et al., 1993); assembly of the mitotic spindle (Kilmartin and Fogg, 1982; Rout and Kilmartin, 1990; Masuda, et al., 1992); regulation of events involving the nucleus such as karyokinesis and karyogamy (Latterich and Schekman, 1994); and regulation of gene expression (Cox, et al., 1993; Mori, et al., 1993).

The ring structures underlying the grommets in H-NEs, as revealed by detergent extraction, appear to be the same as those produced by heparin treatment of highly enriched NPCs (which were extracted with detergents in the course of their isolation). These rings are derived from the periphery of the NPC disks, contain the pore membrane protein Pom152p as a major component, and apparently serve to support the membrane grommets in the H-NEs. These rings may correspond to the rings of central/2 radial spoke domains found in isolated yeast NPCs that are thought to be the functional and structural analogue of the CSR of vertebrate NPCs (Akey and Radermacher, 1993; Yang, et al., 1998). In addition, recent findings obtained using an *in vitro* nuclear reconstitution

system from *Xenopus* oocytes are consistent with "empty" pores being one of the steps of NPC reassembly after mitosis (Goldberg, et al., 1997). These findings support the hypothesis that the rings observed after heparin-extraction of isolated NEs could both anchor the NPC within the nuclear membrane and stabilize the reflexed membrane of the pore grommet; they may also resemble an intermediate of *de novo* NPCs biogenesis.

The only data suggesting that some NE-associated structures have not been preserved during the enrichment procedure is the loss of Nup2p. This protein may be part of a fragile, peripheral structure that is sheared off during NPC and NE preparations (Rout and Blobel, 1993). On the other hand it should be remembered that the status of Nup2p as a *bona fide* nucleoporin has been recently brought into question by the discovery that its closest homologue Yrb2p/Nup36p, might not be a component of the core structure of the NPC (Noguchi, et al., 1997; Taura, et al., 1997). If this were to be the case the loss of Nup2p form the NE and from the NPCs may be entirely expected.

No structures resembling the NL or major components that could be lamins were found in the NE preparations. Consistent with this observation, database searches have failed to reveal any yeast proteins with significant sequence similarities to vertebrate lamins. In addition, antibodies that were previously reported to cross-react with lamins A and B analogues in yeast (Georgatos, et al., 1989), did not detect any co-enriching bands of the expected molecular weight either in the NE or in the H-NE fractions (data not shown). The most natural conclusion from these findings is that budding yeast do not contain a NL.

In conclusion, the isolated NE fractions described here can provide the source material to generate the reagents necessary to study the activities

associated with the NE (see below), and at the same time be the substrates with which these activities can be studied.

A Successful Strategy to Generate mAbs Against NE-Associated Antigens

The high degree of enrichment of the NE fractions described in this dissertation makes them excellent material for raising mAbs against NE and ER specific components. Three different NE-derived fractions (NEs, H-NEs and S-NEs; Chapter IV, Table II) were used to immunize mice and a panel of 173 mAbs were obtained. Of these mAbs 114 recognized NE-associated antigens as judged by indirect IF microscopy. The remaining 59 were either against ER components (48) or against other cellular structures and organelles (Chapter IV, Table III). Four of the NE-specific mAbs have been extensively characterized. Of these, the anti-Pom152p MAb118C3 has been used to gain new insights into the *in vivo* behavior of Pom152p (Strambio-de-Castillia, et al., 1995). Pom152p is a type II integral membrane protein found at the pore membrane (Wozniak, et al., 1994). This protein is one of the most abundant NPC-associated proteins found in isolated NPCs and it is thought to help anchor the structural core of the yeast NPC to the NE (Aitchison, et al., 1995; Nehrbass, et al., 1996). The unexpected partial localization of Pom152p to the ER could have important implications for the understanding of the mechanisms that lead to the assembly of new NPCs in actively growing yeast cultures. This result could only have been obtained by use of a mAb that allows the detection of the unaltered protein at normal levels of expression. The second of the mAbs to be characterized was MAb165C10. This mAb specifically recognizes the previously unidentified essential nucleoporin Nup159p and was crucial in the study of this protein

(Kraemer, et al., 1995). Nup159p was the first yeast nucleoporin to be localized at the ultrastructural level and this was achieved because of the availability of MAb165C10. The sublocalization of Nup159p together with its homology with Nup214/CAN makes it a strong candidate for one of the components of the short cytoplasmic fibers that project from the NPC. Nup159p contains a region with repeated motifs including FXFG repeats shared by several other nucleoporins as well as other related repeat motifs. This repeat-containing domain of the protein interacts directly with Kap95p in an overlay assay pointing to a possible role of Nup159p in docking transport substrates on their way across the NPC. Accordingly, Nup159p is one of the class of nucleoporins whose mutants exhibit the double mRNA export / NPC-clustering phenotype and is thought to be directly involved in the export of RNA from the nucleus (Gorsch, et al., 1995). Interestingly, the epitope of MAb165C10 has been mapped to a region of Nup159p that contains none of the repeats and is not recognized by the poly-specific anti-nucleoporin MAb414 (Davis and Blobel, 1986; Aris and Blobel, 1989). This finding is consistent with the high degree of specificity of MAb165C10 and underscores the importance of such a reagent in the characterization of individual NPC components. The other two mAbs that have been characterized (MAb215B9 and MAb148G11) were essential in the identification of Mlp1p as a component of nuclear filaments linking the NPCs to the nuclear interior and will be discussed in length in the next section

The remaining 110 as yet uncharacterized anti-NE mAbs gave at least 10 distinct staining patterns on immunoblots of highly enriched NEs (Chapter IV, Table V). Of these, at least 6 recognize what appear to be unique bands and will represent an invaluable and largely untapped resource in the functional analysis of both known and unknown NE-specific proteins. In addition, the 48

anti-ER mAbs generated during the course of this study may be equally important in the study of ER-related functions.

The Identification of Novel Components of Nuclear Filaments Connecting the NPC with the Nuclear Interior

The final part of this dissertation describes the identification of two yeast proteins, Mlp1p and Mlp2p, as strong candidates for components of nuclear filaments connecting the NPC to the nuclear interior. Mlp1p was identified using a novel NPC-clustering assay devised to isolate mAbs recognizing non-nucleoporin, NE-associated proteins (Chapter V, Fig. 12). Using this indirect IF microscopy screen, it was observed that the antigen of the anti-NE MAb215B9 and MAb148G11 only partially colocalizes with the NPCs in a NPC-clustering strain. This antigen was isolated from a yeast expression library using MAb148G11 and was found to be the previously identified nuclear protein of unknown function, Mlp1p (Kolling, et al., 1993; see below). Interestingly, while the IF-staining pattern of Mlp1p in wild type cells was reminiscent of the punctate rim pattern typical of nucleporins, this protein failed to completely colocalizes with NPCs in these cells. The localization pattern of Mlp1p both in wild type and in NPC-clustering cells strongly suggest that Mlp1p is not a constituent component of the NPC and cannot be considered a nucleoporin based on current criteria (reviewed in, Rout and Wente, 1994). Furthermore, these observations have a second important implication. In NPC-clustering cells, Mlp1p is often found around the rim of the NE even when the majority of the NPCs are clearly assembled in a tight cluster to one side of the NE (Chapter V, Fig. 12). This strongly suggests that Mlp1p differ from nucleoporins in

another crucial way in that it does not exclusively require NPCs to be anchored to the nuclear periphery. This observation is consistent with the results of the ultrastructural localization studies that showed a significant although limited proportion of the Mlp1p-specific signal near the NE but at a distance from recognizable NPCs (see below). It is possible that a proportion of the Mlp1p molecules are anchored to the NE via as yet uncharacterized factors. Such putative anchoring-factors will be the subject of intense future investigations.

The second protein of this novel family, Mlp2p (the uncharacterized yeast ORF, YIL149C), was found in searches of the complete yeast genomic database as the only putative homologue of Mlp1p (Chapter V, Fig. 14). Importantly, both *MLP1* and *MLP2* belong to genomic Block 38 present on both chromosome IX and XI, suggesting that these two genes arose from a genome duplication event (Wolfe and Shields, 1997). Both of these proteins have a large predicted MW (Mlp1p, 218 kD; Mlp2p, 195 kD) and are expected to have two major structural domains: a coiled-coil amino terminus occupying ~80% of the primary sequence and a carboxy-terminus of unknown structure (Chapter IV, Fig. 13). An obvious speculation based on this predicted structure is that the large coiled-coil domain forms a filamentous structure that may in turn be involved in organizing higher order polymers (for example, filaments). In contrast, the carboxy-terminus might participates in interactions with heterologous factors and in anchoring these polymeric structures to the NPCs or to the nuclear interior (see also below). It should be noted that while other structural proteins localized in the nucleus have large coiled-coil domains, the domain organization of these proteins is different from the one found in Mlp1p and Mlp2p. NuMA, the nuclear lamins and Spc110p/Nuf1p all have central coiled-coil regions flanked by globular "heads" and "tails" (McKeon, 1991; Mirzayan, et al., 1992; Cleveland, 1995; Kilmartin and Goh, 1996). Myosins on the other

hand, have a globular "head" followed by a large coiled-coil domain at the carboxy-terminus (for examples of "nuclear" myosins see, (Berrios and Fisher, 1986; Berrios, et al., 1991). This indicates that Mlp1p and Mlp2p may belong to a novel and as yet uncharacterized type of structural proteins of the nucleus. Insight into the possible roles of Mlp1p and Mlp2p came form the observation that their closest relatives in the database are Tpr and the *Drosophila* Tpr-homologue, Bx34 (Frasch, et al., 1988; Byrd, et al., 1994). These proteins share a double localization at the nuclear periphery in the vicinity of the NPCs and at the nuclear interior in regions of the nucleoplasm that are excluded from the chromatin and the nucleoli (Cordes, et al., 1997; Zimowska, et al., 1997). In addition, new evidence indicates that Tpr is localized at nuclear filaments connecting the NPCs to the nucleolus.

The genes encoding Mlp1p and Mlp2p were disrupted by integrative transformation revealing that neither of the gene products is essential (Chapter V, Fig. 15). A strain harboring the double deletion of *MLP1* and *MLP2* was obtained by crossing the individual haploid knockout strains and was found to have a significant fitness deficit when grown in competition with its wild type counterpart (Chapter V, Fig. 15). This demonstrated that Mlp1p and Mlp2p are essential for the ability of yeast to survive under conditions that mimic the wild type environment and that Mlp1p and Mlp2p have a synthetic growth defect and therefore most likely functionally interact with each other.

The localization of Mlp1p within the cell was studied both by immunoblotting and by IEM using MAb148G11 (Chapter V, Figs. 16,17 and 18). While Mlp1p was found to cofractionate almost exclusively with isolated NEs it was lost when NEs were extracted with heparin. These results are in accord with indirect IF results. In addition, secondary structure predictions together with the fractionation behavior of Mlp1p demonstrate that this protein is peripherally

associated with the NE. Interestingly, Mlp1p was found to fractionate away from an enriched NPC fraction prepared as described by Rout and Blobel (Rout and Blobel, 1993). The fractionation pattern of Mlp1p is consistent with the non-clustering behavior of Mlp1p in the *nup133Δ* strain and reinforces the notion that this protein is only partially associated with the NPCs and is not a *bona fide* nucleoporin. Interestingly, Mlp1p and Mlp2p represent the only known examples of proteins that display a similar fractionation pattern.

Ultrastructural localization studies also point in the same direction. Mlp1p specific staining on both isolated NEs and isolated "broken" nuclei was found exclusively in the nucleoplasm and in the majority of the cases within a 150 nm distance from the mid-plane of the NE. In the best preserved cases, such signal was found in association with nucleoplasmic fibers that for the most part (though not exclusively) emanated from the vicinity of visible NPCs. Some internal nuclear signal was also observed on immunostained whole-nuclei although this signal was not seen in association with obvious structures. Strikingly, the average distances of gold particles both from the mid-plane of the NPC and from the cylindrical axis of the NPC in isolated NEs immunostained for Mlp1p was significantly increased with respect to the same distances measured for the peripheral nucleoporin Nup159p. It should be remembered that only the position of the epitope of the antibody is being localized rather then the position of the protein as a whole. On the scale of the immunostained structures here this may not actually reflect the extent of the localization of the entire protein. A second important caveat of many immunolocalization techniques is that the dimensions of the antibody-gold conjugate have to be taken into account in determining the precise localization of the epitope. Nevertheless, knowing the approximate position of the epitope along the primary structure of the protein and knowing the predicted filamentous nature of the protein estimates of the

position of Mlp1p relative to the NE and NPCs can be made. Based on these estimates, Mlp1p could extend towards the nucleoplasm as much as ~210 nm from the mid-plane of the NE on the x axis and as much as ~180 nm from the cylindrical axis of the NPC on the y axis. This is in sharp contrast with similar estimates concerning Nup159p whose epitope is found ~30 nm from the middle of the NPC on the y axis and ~ 10 nm on the x axis (Chapter V, Fig. 18; Kraemer, et al., 1995). In this case an estimate of the position of the whole protein with respect to the NPC is more difficult because the secondary structure of the protein is less predictable. Under the assumption that this protein has an extended filamentous structure (see also predictions of the structure of the Nup159p vertebrate homologue Nup214/CAN; Wootton, 1994), estimates similar to the ones employed for Mlp1p would predict that Nup159p could extend a maximum of ~60 nm from the center of the NPC on the y axis and a maximum of ~ 40 nm on the x axis. Incidentally, such predictions are consistent with the localization of Nup159p on the short cytoplasmic filaments of 30-50 nm that project from the cytoplasmic side of the NPCs. It is worth stressing again that the localization of Mlp1p at such a significant distance from NPCs is not consistent with the expected behavior of a nucleoporin, especially when compared with the localization of the peripheral nucleoporin Nup159p. Indeed, such a localization underscores once more that Mlp1p belongs to a novel type of nuclear proteins that molecularly define a novel structural domain of the nucleus that provides a link between NPCs and the nuclear interior.

The fractionation behavior and ultrastructural localization of Mlp2p was studied utilizing a yeast strain expressing an epitope-tagged version of the protein. The results obtained in this case were very similar to the ones obtained with Mlp1p, again supporting the view that Mlp2p and Mlp1p are structurally and functionally closely related.

A thorough phenotypic analysis of a yeast mutant strains carrying deletions of both *MLP1* and *MLP2* was performed to investigate the *in vivo* functional roles of these proteins (Chapter V, Figs. 20-24). Double knockout cells (*mlp1Δ, mlp2Δ*) were considerably larger than their wild type counterpart. Furthermore, mutant populations presented a significant increase in the percentages of large-budded cells consistent with a general inhibition of the cell-cycle. In addition double mutant cells grew as "nibbled" colonies typical of strains undergoing clonal lethality. Consistent with these results, *mlp1Δ, mlp2Δ* cells correctly segregated chromosomes at mitosis with a markedly reduced efficiency. On the other hand, *mlp1Δ, mlp2Δ* cells did not show a clear cell-cycle arrest phenotype as judged by the analysis of the DNA-content distribution in the population. The morphological distribution of various nuclear marker in mutant cells as compared to wild type was studied to reveal possible alterations. This study revealed alterations in the overall shape of the nucleus although the distribution of NPCs around the NE appeared unaffected. In addition, the nucleoli appeared larger and less compact than normal. They had lost their crescent shape and instead appeared fragmented. Finally, marked spindle aberrations were observed with mutants appearing to be unable to build the extended spindles necessary for the final stages of karyokinesis and cytokinesis.

This phenotypic picture is consistent with a general inefficiency in the ability of cells to undergo the cell division cycle but are not consistent with a direct role of Mlp1p and Mlp2p in the regulation of this process. In addition, there appear to be a general malfunction in the ability of cells to maintain the proper internal nuclear architecture. These phenotypes could be expected for proteins whose primary role is to maintain the structural organization of the nucleus. However, similar phenotypes to the ones described here have been

repeatedly observed in association with mutations of proteins that are directly involved in nucleocytoplasmic transport, such as several nucleoporins and transport factors (Adachi and Yanagida, 1989; Xiao, et al., 1993; Fabre, et al., 1994; Yano, et al., 1994; Aitchison, et al., 1995; Brinkmann, et al., 1995; Heath, et al., 1995; Imiger, et al., 1995; Loeb, et al., 1995; Kenna, et al., 1996). This led to the hypothesis that Mlp1p and Mlp2p could also be involved in nuclear transport. Of course, the predicted ability of both of these proteins to form extended coiled-coil filaments, and their ultrastructural localization at an interface between the NPCs and the nuclear interior, strongly encouraged such an hypothesis. To investigate this further, the ability of *mlp1Δ, mlp2Δ* cells to import a NLS-reporter protein was compared to wild type by way of an *in vivo* nuclear import assay (Shulga, et al., 1996). The results of this assay suggest that Mlp1p and Mlp2p may be involved in facilitating import of transport substrates to the nucleus. Interestingly, the results of a similar nuclear passive export assay appear to mirror the results of the import assay in that the kinetics of egress of the reporter out of the nucleus during conditions of metabolic inhibition are faster in the mutant than in the wild type. This could be explained by assuming that the rates of egress that are observed in this assay are in fact the results of the combined rates of active import and the rates of passive diffusion from the nucleus. In this case, if one assumes that the rates of diffusion are constant even in the presence of the metabolic inhibitors that block the production of energy (i.e. they do not require energy), then a reduced efficiency of import (i.e. as it is known to occur in double mutant cells) will be reflected in a faster net egress rate of the reporter towards the cytoplasm. The involvement of Mlp1p and Mlp2p in active nuclear export of mRNA was investigated using a poly(A)$^+$ RNA nuclear accumulation assay (Wente and Blobel, 1993). Similarly, the steady state subcellular distribution of a GFP reporter carrying both an NES

and NLS was studied to assess the ability of the double mutant to actively export NES-containing proteins (Stade, et al., 1997). Both of these assays showed no change in the steady state distributions of the reporters in the mutant as compared to wild type. However, this cannot be taken as a prove that Mlp1p and Mlp2p are not involved in nuclear export especially because the subcellular distribution of the import substrate (i.e. NLS-GFP) at equilibrium was also unaffected in the double knockout and only the kinetics of import were altered. The export assays available to date do not allow the assessment of possible changes in rates of export. Therefore, further studies and the development of new kinetic assays will be required to establish the role of Mlp1p and Mlp2p in export.

To investigate the ability of Mlp1p to self-assemble and give rise to large polymeric structures within the nucleus, this protein was overexpressed in yeast. Overexpression lead to the formation of large nuclear dots that appear to nucleate at the or near the NE and progressively invade the nucleoplasm. The ultrastructural analysis of these dots revealed a fibrillogranular structure with no obvious high order regularity. In addition, IEM proved that this fibrillogranular network contained large amounts of Mlp1p and suggested that Mlp1p is its major constituent. Strikingly, cells expressing vast excesses of Mlp1p were viable and did not show any obvious growth defect. Taken together these data suggests that Mlp1p may be capable of forming an extensive fibrillar network that emanates from the NE and penetrates the nucleoplasm interweaving between the chromatin without disrupting the architecture or the functions of the nucleus. The ability to form such network is consistent with a structural function of Mlp1p in aiding the connection of the NPC with the nuclear interior. On the other hand, the ability of Mlp1p to self-assemble and form regular polymers that

could account for such structural functions remains to be demonstrated and will be the subject of future studies.

The results obtained with Mlp1p are in large part consistent with the data published by Kolling et al. (Kolling, et al., 1993) but they extend their observations. These authors isolated Mlp1p (Myosin like protein 1) in screening for myosin cross-reacting clones in a yeast expression library. Indeed, Mlp1p was found to contain a large coiled-coil domain at the amino-terminus that most likely accounts for this cross-reactivity. However, Kolling and coworkers agreed that Mlp1p does not belong to the myosin family due to the different organization of the structural domains along the primary sequence of the protein (see above). The gene encoding Mlp1p was disrupted and found to be non-essential consistent with results presented here. In an attempt to investigate possible functions of Mlp1p, Botstein and coworkers localized it by indirect IF microscopy using an affinity-purified rabbit polyclonal antibody raised against the recombinant protein. It should be noted though that their anti-Mlp1p antibody did not give any signal in wild type cells containing only normal levels of Mlp1p. For this reason a strain was constructed that contained *MLP1* on a 2 μm plasmid. In this strain, the anti-Mlp1p antibody recognized "intensely staining dots and sometimes rings" that appeared to be localized "adjacent to the nucleus". Although this staining pattern does not correspond with the native localization of Mlp1p described in this dissertation (determined by both indirect IF microscopy and by IEM), it does correlate with the results obtained here upon Mlp1p overexpression (Chapter V, Fig. 26) fully accounting for the discrepancy. When the anti-Mlp1p antibody was used to immunolabel mouse epithelial cells, Kolling et al. observed an intense internal nuclear staining that appeared to be excluded from nucleolar and chromosomal areas. Although, this pattern could be at first glance considered similar to the pattern observed with Tpr and Bx34,

it differs from it in a crucial way — namely the lack of a clear peripheral rim staining. This, and the appearance of numerous cross-reacting bands on immunoblot of mouse cells extracts, argues against the specificity of this result. When, Kolling et al. examined the phenotype of *MLP1* knockout cells, no defects in chromosome stability were observed. This is not surprising due to the existence of the Mlp1p yeast homologue, Mlp2p. This protein complements the growth defect associated with loss of Mlp1p and is expected to similarly suppress chromosome segregation defects. Indeed, these defects were observed only in *mlp1Δ, mlp2Δ* cells and not in either *mlp1Δ* or *mlp2Δ* cells (Chapter V, Fig. 20; data not shown). The only real discrepancy between Kolling et al. and data presented in this dissertation is the failure to detect an increased UV-sensitivity in either *mlp1Δ, mlp2Δ* , *mlp1Δ* or *mlp2Δ* cells (data not shown). Although the defect observed in Kolling et al. is admittedly "slight", it cannot be dismissed particularly because it cosegregated with the absence of *MLP1*. However, the significance of this phenotype remains unclear especially due to its apparent strain- or experimental condition-dependency.

It has been long observed that the NPCs are in fact structurally continuous with the nuclear interior (Monneron and Bernhard, 1969; Franke and Falk, 1971). These observations have led to the speculations that efficient exchange of material between the nuclear periphery and the nuclear interior could occur along "tracks" connecting the two (Blobel, 1985; Meier and Blobel, 1992; Meier and Blobel, 1994). Unfortunately, the molecular definition of these long hypothesized and controversial "tracks" has proven hard to achieve. Several criteria could be thought of that could help define constituents of this domain. In one model, such components could be expected to be filamentous in nature and to give rise to extended polymers of variable sizes that emanate from peripheral structures of the NPCs and possibly from other sites on the NE and

extend into the nucleoplasm. This model has a number of natural consequences. The first corollary would be that components of such structures would be localized further away from the center of the NPCs than the most peripheral structures of the NPCs (for example a reasonable cut-off distance could be a distance equal to 1 NPC radius). Second, they would be easily extracted from NPCs and therefore they would fractionate only partially with isolated NPCs fractions. Furthermore, such components would be present in isolated NPCs fractions only in non-stoichiometric amounts. Another important consequence of the model would be that components of these extended polymeric structures would be expected to trail behind the NPCs in NPC-clustering strains and therefore only partially cluster with them. Needless to say, Mlp1p and Mlp2p satisfy all of the criteria mentioned above. As a consequence it is natural to suggest that Mlp1p and Mlp2p, together with their vertebrate counterparts Tpr and Bx34, represent the strongest candidates to date for the molecular components of the long hypothesized nuclear "tracks" connecting the NPCs with the nuclear interior. This idea receives further strength from the functional data available exclusively for Mlp1p and Mlp2p and pointing to a possible involvement in nuclear transport.

Various model of how such "tracks" could function in facilitating transport can be proposed based on the available data for the potential components. In one model Mlp1p/Mlp2p (and Tpr) could form extended and hollow cables similar to the ones visualized by Ris and others (Franke, 1970; Franke and Scheer, 1970; Franke and Scheer, 1970; Kartenbeck, et al., 1971; Richardson, et al., 1988; Ris and Malecki, 1993; Ris, 1997), that could help clear the substrate away from the immediate vicinity of the pore and move it towards the interior. In a similar way, these cables could facilitate export of RNA and proteins by facilitating their movement towards the nuclear periphery. This

could be achieved either by facilitated diffusion of substrates inside an open tunnel or by active transport of substrate between binding sites positioned opportunely along the filaments. In this light, one can speculate that the FP-rich region present at the carboxy-terminus of Mlp1p and Mlp2p could represent a highly degenerated FG repeats region. If one imagines that Mlp1p and Mlp2p form long filaments and that the globular tails of each monomer are exposed at the surface of such filaments, the degenerated repeats domains present on each of the globular tails could function as low affinity docking sites for the active transport substrates along the filaments. Indeed, a recent study has pointed to the possibility that the NES may be required not only for translocation across the NPC but also for accumulation of substrates to the nucleoplasmic face of the NPC (Feldherr and Akin, 1997). In this study, PEG-coated gold particles of two different sizes were injected either in the nucleoplasm or in the cytoplasm of amphibian oocytes and their movements towards the NPCs were followed at the ultrastructural level. Gold particles injected in the cytoplasm were able to freely diffuse and were seen to accumulate at the cytoplasmic side of the NPCs regardless of their size. In contrast, while small (4-7 nm) particles injected in the nucleoplasm were also able to diffuse towards the NPCs, large particles (11-27 nm) did not appear to move from their site of injection unless they contained an NES.

While Mlp1p and Mlp2p appear to have a role in nucleocytoplasmic transport, a concomitant structural role in helping maintaining the architectural organization and integrity of the nucleus cannot be excluded. Indeed, mutants lacking Mlp1p and Mlp2p show alterations in various nuclear structures and these effects may equally be due to a direct structural role as well as be a pleiotropic consequence of inefficient nucleocytoplasmic transport. Further

studies will have to be performed to distinguish between these two equally intriguing possibilities.

An important drawback of this dissertation is the lack of any data regarding the interaction of Mlp1p and Mlp2p with other molecules. Preliminary experiments aimed to this goal have not so far yield the desired results. Two main strategies were employed (data not shown). In the first, nuclei were prepared from cells expressing Mlp1p-pA and they were lysed under mild conditions before immunoaffinity purification of the tagged protein on an IgG-column. Although Mlp1p was reliably isolated in this way no specifically interacting band was purified under the conditions used. The isolation of Mlp1p interacting components was also attempted by employing overlay assays. Also in this case no specific interactions were detected. Needless to say, the efforts to isolate Mlp1p and Mlp2p interacting components will be redoubled in the future. A number of different strategies in addition to the ones that have been started can be envisioned to this aim. These include genetic methods such as synthetic lethal and two-hybrid screens and biochemical methods such as the use of cross-linking agents that could help stabilize labile interactions.

In conclusion, the proteins described in this dissertation molecularly define a novel structural and functional domain of the nucleus and open with their characterization a new and unprecedented area of studies that will considerably extend our current understanding of nuclear and cellular physiology.

References

Adachi Y, Yanagida M (1989). Higher order chromosome structure is affected by cold-sensitive mutations in a *Schizosaccharomyces pombe* gene crm1+ which encodes a 115- kD protein preferentially localized in the nucleus and its periphery. J Cell Biol 108:1195-207.

Adam EJ, Adam SA (1994). Identification of cytosolic factors required for nuclear location sequence-mediated binding to the nuclear envelope. J Cell Biol 125:547-555.

Adam SA, Marr RS, Gerace L (1990). Nuclear protein import in permeabilized mammalian cells requires soluble cytoplasmic factors. J Cell Biol 111:807-16.

Aitchison JD, Blobel G, Rout MP (1995). Nup120p: a yeast nucleoporin required for NPC distribution and mRNA transport. J Cell Biol 131:1659-75.

Aitchison JD, Blobel G, Rout MP (1996). Kap104p: a karyopherin involved in the nuclear transport of messenger RNA binding proteins. Science 274:624-7.

Aitchison JD, Rout MP, Marelli M, Blobel G, Wozniak RW (1995). Two novel related yeast nucleoporins Nup170p and Nup157p: complementation with the vertebrate homologue Nup155p and functional interactions with the yeast nuclear pore-membrane protein Pom152p. J Cell Biol 131:1133-48.

Akey CW (1990). Visualization of transport-related configurations of the nuclear pore transporter. Biophys J 58:341-55.

Akey CW, Goldfarb DS (1989). Protein import through the nuclear pore complex is a multistep process. J Cell Biol 109:971-82.

Akey CW, Radermacher M (1993). Architecture of the *Xenopus* nuclear pore complex revealed by three-dimensional cryo-electron microscopy. J Cell Biol 122:1-19.

Allen JL, Douglas MG (1989). Organization of the nuclear pore complex in *Saccharomyces cerevisiae*. J Ultrastruct Mol Struct Res 102:95-108.

Altschul SF, Gish W, Miller W, Myers EW, Lipman DJ (1990). Basic Local Alignment Searc Tool. J Mol Biol 215:403-410.

Amberg DC, Goldstein AL, Cole CN (1992). Isolation and characterization of RAT1: an essential gene of *Saccharomyces cerevisiae* required for the efficient nucleocytoplasmic trafficking of mRNA. Genes Dev 6:1173-89.

Anderson JT, Wilson SM, Datar KV, Swanson MS (1993). NAB2: a yeast nuclear polyadenylated RNA-binding protein essential for cell viability. Mol Cell Biol 13:2730-41.

Aris JP, Blobel G (1988). Identification and characterization of a yeast nucleolar protein that is similar to a rat liver nucleolar protein. J Cell Biol 107:2059-2067.

Aris JP, Blobel G (1989). Yeast nuclear envelope proteins cross react with an antibody against mammalian pore complex proteins. J Cell Biol 108:2059-67.

Baba M, Osumi M (1987). Transmission and scanning electron microscope examination of intracellular organelles in freeze-substituted *Kloeckera* and *Saccharomyces cerevisiae* yeast cells. J Elec Microsc Tech 5:249-261.

Bangs PL, Sparks CA, Odgren PR, Fey EG (1996). Product of the oncogene-activating gene Tpr is a phosphorylated protein of the nuclear pore complex. J Cell Biochem 61:48-60.

Bastos R, Pante N, Burke B (1995). Nuclear pore complex proteins. Int Rev Cytol 162B:257-302.

Bataille N, Helser T, Fried HM (1990). Cytoplasmic transport of ribosomal subunits microinjected into the *Xenopus laevis* oocyte nucleus: a generalized, facilitated process. J Cell Biol 111:1571-82.

Beck LA, Hosick TJ, Sinensky M (1988). Incorporation of a product of mevalonic acid metabolism into proteins of Chinese hamster ovary cell nuclei. J Cell Biol 107:1307-16.

Becker J, Melchior F, Gerke V, Bischoff FR, Ponstingl H, Wittinghofer A (1995). *RNA1* encodes a GTPase-activating protein specific for Gsp1p, the Ran/TC4 homologue of *Saccharomyces cerevisiae*. J Biol Chem 270:11860-5.

Belanger KD, Kenna MA, Wei S, Davis LI (1994). Genetic and physical interactions between Srp1p and nuclear pore complex proteins Nup1p and Nup2p. J Cell Biol 126:619-30.

Belgareh N, Doye V (1997). Dynamics of Nuclear Pore Distribution in nucleoporin Mutant Yeast Cells. J Cell Biol 136:747-749.

Belhumeur P, Lee A, Tam R, DiPaolo T, Fortin N, Clark MW (1993). *GSP1* and *GSP2*, genetic suppressors of the *prp20-1* mutant in *Saccharomyces cerevisiae*: GTP-binding proteins involved in the maintenance of nuclear organization. Mol Cell Biol 13:2152-61.

Berezney R, Coffey DS (1974). Identification of a nuclear protein matrix. Biochem Biophys Res Commun 60:1410-7.

Berezney R, Coffey DS (1977). Nuclear matrix. Isolation and characterization of a framework structure from rat liver nuclei. J Cell Biol 73:616-37.

Berezney R, Mortillaro MJ, Ma H, Wei X, Samarabandu J (1995). The nuclear matrix: a structural milieu for genomic function. Int Rev Cytol 162A:1-65.

Bernhard W (1969). A new staining procedure for electron microscopical cytology. J Ultrastruct Res 27:250-65.

Berrios M, Fisher PA (1986). A myosin heavy-chain-like polypeptide is associated with the nuclear envelope in higher eukaryotic cells. J Cell Biol 103:711-24.

Berrios M, Fisher PA, Matz EC (1991). Localization of a myosin heavy chain-like polypeptide to Drosophila nuclear pore complexes. Proc Natl Acad Sci U S A 88:219-23.

Bischoff FR, Klebe C, Kretschmer J, Wittinghofer A, Ponstingl H (1994). RanGAP1 induces GTPase activity of nuclear Ras-related Ran. Proc Natl Acad Sci U S A 91:2587-91.

Bischoff FR, Krebber H, Kempf T, Hermes I, Ponstingl H (1995). Human RanGTPase-activating protein RanGAP1 is a homologue of yeast Rna1p involved in mRNA processing and transport. Proc Natl Acad Sci U S A 92:1749-53.

Bischoff FR, Ponstingl H (1991). Catalysis of guanine nucleotide exchange on Ran by the mitotic regulator RCC1. Nature 354:80-2.

Bischoff FR, Ponstingl H (1991). Mitotic regulator protein RCC1 is complexed with a nuclear Ras-related polypeptide. Proc Natl Acad Sci U S A 88:10830-4.

Black SD, Coon MJ (1982). Structural features of liver microsomal NADPH-cytochrome P-450 reductase. J Biol Chem 257:5929-5938.

Blobel G (1985). Gene gating: a hypothesis. Proc Natl Acad Sci U S A 82:8527-9.

Bogerd HP, Fridell RA, Madore S, Cullen BR (1995). Identification of a novel cellular cofactor for the Rev/Rex class of retroviral regulatory proteins. Cell 82:485-94.

Bonifaci N, Moroianu J, Radu A, Blobel G (1997). Karyopherin β2 mediates nuclear import of a mRNA binding protein. Proc Natl Acad Sci U S A 94:5055-60.

Borer RA, Lehner CF, Eppenberger HM, Nigg EA (1989). Major nucleolar proteins shuttle between nucleus and cytoplasm. Cell 56:379-90.

Brinkmann U, Brinkmann E, Gallo M, Pastan I (1995). Cloning and characterization of a cellular apoptosis susceptibility gene, the human homologue to the yeast chromosome segregation gene CSE1. Proc Natl Acad Sci U S A 92:10427-31.

Brodsky JL, Hamamoto S, Feldheim D, Schekman R (1993). Reconstitution of protein translocation from solubilized yeast membranes reveals topologically distinct roles for BiP and cytosolic Hsc70. J Cell Biol 120:95-102.

Brodsky JL, Schekman R (1993). A Sec63p-BiP complex from yeast is required for protein translocation in a reconstituted proteoliposome. J Cell Biol

Bucci M, Wente SR (1997). In vivo dynamics of nuclear pore complexes in yeast. J Cell Biol 136:1185-99.

Buss F, Stewart M (1995). Macromolecular interactions in the nucleoporin p62 complex of rat nuclear pores: binding of nucleoporin p54 to the rod domain of p62. J Cell Biol 128:251-61.

Byers B, Goetsch L (1975). Behavior of Spindles and Spindle Plaques in the cell cycle and conjugation of *Saccharomyces cerevisiae*. J Bacteriol 124:511-523.

Byrd DA, Sweet DJ, Pante N, Konstantinov KN, Guan T, Saphire AC, Mitchell PJ, Cooper CS, Aebi U, Gerace L (1994). Tpr, a large coiled coil protein whose amino terminus is involved in activation of oncogenic kinases, is localized to the cytoplasmic surface of the nuclear pore complex. J Cell Biol

Chi M-H, Shore D (1996). *SUM1-1*, a Dominant Suppressor of *SIR* Mutations in *Saccharomyces cerevisiae*, Increases Transcriptional Silencing at Telomeres and HM Mating-Type Loci and Decreases Chromosome Stability. Mol Cell Biol 16:4281-4294.

Chi NC, Adam EJ, Visser GD, Adam SA (1996). RanBP1 stabilizes the interaction of Ran with p97 nuclear protein import. J Cell Biol 135:559-69.

Chirico WJ, Waters MG, Blobel G (1988). 70K heath shock related proteins stimulate protein translocation into microsomes. Nature 332:805-810.

Clayton RA, White O, Ketchum KA, Venter JC (1997). The First Genome From the Third Domain of Life. Nature 387:459-462.

Cleveland DW (1995). NuMA: a Protein Involved in Nuclear Structure, Spindle Assembly and Nuclear Reformation. Trends Cell Biol 5:60-64.

Cody CW, Prasher DC, Wester WM, Prendergast FG, Ward WW (1993). Chemical Structure of the Hexapeptide Chromophore of the *Aequorea* Green Fluorescent Protein. Biochem 32:1212-1218.

Corbett AH, Koepp DM, Schlenstedt G, Lee MS, Hopper AK, Silver PA (1995). Rna1p, a Ran/TC4 GTPase activating protein, is required for nuclear import. J Cell Biol 130:1017-26.

Cordes VC, Reidenbach S, Rackwitz HR, Franke WW (1997). Identification of protein p270/Tpr as a constitutive component of the nuclear pore complex-attached intranuclear filaments. J Cell Biol 136:515-29.

Courvalin JC, Dumontier M, Bornens M (1982). Solubilization of nuclear structures by the polyanion heparin. J Biol Chem 257:456-463.

Coutavas E, Ren M, Oppenheim JD, D'Eustachio P, Rush MG (1993). Characterization of proteins that interact with the cell-cycle regulatory protein Ran/TC4. Nature 366:585-7.

Cox JS, Shamu CE, Walter P (1993). Transcriptional induction of genes encoding endoplasmic reticulum resident proteins requires a transmembrane protein kinase. Cell 73:1197-1206.

Daneholt B (1997). A look at messenger RNP moving through the nuclear pore. Cell 88:585-8.

Davis LI, Blobel G (1986). Identification and characterization of a nuclear pore complex protein. Cell 45:699-709.

Davis LI, Fink GR (1990). The NUP1 gene encodes an essential component of the yeast nuclear pore complex. Cell 61:965-978.

Del Priore V, Snay CA, Bahr A, Cole CN (1996). The product of the *Saccharomyces cerevisiae RSS1* gene, identified as a high-copy suppressor of the *rat7-1* temperature-sensitive allele of the *RAT7/NUP159* nucleoporin, is required for efficient mRNA export. Mol Biol Cell 7:1601-21.

Dingwall C, Kandels-Lewis S, Seraphin B (1995). A family of Ran binding proteins that includes nucleoporins. Proc Natl Acad Sci U S A 92:7525-9.

Dingwall C, Laskey RA (1991). Nuclear targeting sequences--a consensus? Trends Biochem Sci 16:478-81.

Doye V, Hurt E (1997). From nucleoporins to nuclear pore complexes. Curr Opin Cell Biol 9:401-11.

Doye V, Hurt EC (1995). Genetic approaches to nuclear pore structure and function. Trends Genet 11:235-41.

Doye V, Wepf R, Hurt EC (1994). A novel nuclear pore protein Nup133p with distinct roles in poly(A)+ RNA transport and nuclear pore distribution. Embo J 13:6062-75.

Drake JW (1970). The Molecular Basis of Mutation. San Francisco, CA: Holden-Day.

Dresser ME, Giroux CN (1988). Meiotic chromosome behavior in spread preparations of yeast. J Cell Biol 106:567-573.

Dworetzky SI, Feldherr CM (1988). Translocation of RNA-coated gold particles through the nuclear pores of oocytes. J Cell Biol 106:575-84.

Enenkel C, Blobel G, Rexach M (1995). Identification of a yeast karyopherin heterodimer that targets import substrate to mammalian nuclear pore complexes. J Biol Chem 270:16499-16502.

Fabre E, Boelens WC, Wimmer C, Mattaj IW, Hurt EC (1994). Nup145p is required for nuclear export of mRNA and binds homopolymeric RNA in vitro via a novel conserved motif. Cell 78:275-89.

Fabre E, Hurt E (1997). Yeast genetics to dissect the nuclear pore complex and nucleocytoplasmic trafficking. Ann Rev Genet 31:277-313.

Fakan S, Bernhard W (1971). Localization of rapidly and slowly labeled nuclear RNA as visualized by high resolution autoradiography. Exp Cell Res 67:129-41.

Fakan S, Bernhard W (1973). Nuclear labeling after prolonged 3H-uridine incorporation as visualized by high resolution autoradiography. Exp Cell Res 79:431-44.

Fakan S, Puvion E, Sphor G (1976). Localization and characterization of newly synthesized nuclear RNA in isolate rat hepatocytes. Exp Cell Res 99:155-64.

Favreau C, Worman HJ, Wozniak RW, Frappier T, Courvalin JC (1996). Cell cycle-dependent phosphorylation of nucleoporins and nuclear pore membrane protein Gp210. Biochem 35:8035-44.

Fawcett DW (1966). An Atlas of Fine Structure. In: The Cell. Its Organelles and Inclusions, p. 448. Philadelphia, PA: W. B. Saunders Co.

Feldherr CM, Akin D (1997). The location of the transport gate in the nuclear pore complex. J Cell Sci 110:3065-70.

Feldherr CM, Kallenbach E, Schultz N (1984). Movement of a karyophilic protein through the nuclear pores of oocytes. J Cell Biol 99:2216-22.

Fey EG, Krochmalnic G, Penman S (1986). The nonchromatin substructures of the nucleus: the ribonucleoprotein (RNP)-containing and RNP-depleted matrices analyzed by sequential fractionation and resinless section electron microscopy. J Cell Biol 102:1654-65.

Finlay DR, Forbes DJ (1990). Reconstitution of biochemically altered nuclear pores: transport can be eliminated and restored. Cell 60:17-29.

Finlay DR, Meier E, Bradley P, Horecka J, Forbes DJ (1991). A complex of nuclear pore proteins required for pore function. J Cell Biol 114:169-83.

Fischer U, Huber J, Boelens WC, Mattaj IW, Luhrmann R (1995). The HIV-1 Rev activation domain is a nuclear export signal that accesses an export pathway used by specific cellular RNAs. Cell 82:475-83.

Fischer U, Meyer S, Teufel M, Heckel C, Luhrmann R, Rautmann G (1994). Evidence that HIV-1 Rev directly promotes the nuclear export of unspliced RNA. Embo J 13:4105-12.

Floer M, Blobel G (1996). The nuclear transport factor karyopherin beta binds stoichiometrically to Ran-GTP and inhibits the Ran GTPase activating protein. J Biol Chem 271:5313-6.

Foisner R, Gerace L (1993). Integral membrane proteins of the nuclear envelope interact with lamins and chromosomes, and binding is modulated by mitotic phosphorylation. Cell 73:1267-1279.

Fornerod M, Ohno M, Yoshida M, Mattaj IW (1997). CRM1 is an export receptor for leucine-rich nuclear export signals [see comments]. Cell 90:1051-60.

Fornerod M, van Deursen J, van Baal S, Reynolds A, Davis D, Murti KG, Fransen J, Grosveld G (1997). The human homologue of yeast CRM1 is in a dynamic subcomplex with CAN/Nup214 and a novel nuclear pore component Nup88. Embo J 16:807-16.

Franke WW (1970). On the universality of nuclear pore complex structure. Z Zellforsch Mikrosk Anat 105:405-29.

Franke WW, Falk H (1971). Appearance of nuclear pore complexes after Bernhard's staining procedure. Histochemie 24:266-78.

Franke WW, Scheer U (1970). The ultrastructure of the nuclear envelope of amphibian oocytes: a reinvestigation. I. The mature oocyte. J Ultrastruct Res 30:288-316.

Franke WW, Scheer U (1970). The ultrastructure of the nuclear envelope of amphibian oocytes: a reinvestigation. II. The immature oocyte and dynamic aspects. J Ultrastruct Res 30:317-27.

Franke WW, Scheer U (1974). Structures and Functions of the Nuclear Envelope. In: The Cell Nucleus Vol. 1 (H Busch, eds.), pp. 219-347. New York and London: Academic Press.

Frasch M, Paddy MR, Saumweber H (1988). Developmental and Mitotic Behavior of Two Novel Groups of Nuclear Envelope Antigens. J Cell Sci 90:247-264.

Fridell RA, Bogerd HP, Cullen BR (1996). Nuclear export of late HIV-1 mRNAs occurs via a cellular protein export pathway. Proc Natl Acad Sci U S A 93:4421-4.

Fridell RA, Fischer U, Luhrmann R, Meyer BE, Meinkoth JL, Malim MH, Cullen BR (1996). Amphibian transcription factor IIIA proteins contain a sequence element functionally equivalent to the nuclear export signal of human immunodeficiency virus type 1 Rev. Proc Natl Acad Sci U S A 93:2936-40.

Fridell RA, Truant R, Thorne L, Benson RE, Cullen BR (1997). Nuclear import of hnRNP A1 is mediated by a novel cellular cofactor related to karyopherin-beta. J Cell Sci 110:1325-31.

Fried HM, Warner JR (1981). Cloning of yeast gene for trichodermin resistance and ribosomal protein L3. Proc Natl Acad Sci U S A 78:238-242.

Fritz CC, Green MR (1996). HIV Rev uses a conserved cellular protein export pathway for the nucleocytoplasmic transport of viral RNAs. Curr Biol 6:848-54.

Fritz CC, Zapp ML, Green MR (1995). A human nucleoporin-like protein that specifically interacts with HIV Rev. Nature 376:530-3.

Fujiki Y, Hubbard AL, Fowler S, Lazarow PB (1982). Isolation of intracellular membranes by means of sodium carbonate treatment: application to endoplasmic reticulum. J Cell Biol 93:97-102.

Fukuda M, Asano S, Nakamura T, Adachi M, Yoshida M, Yanagida M, Nishida E (1997). CRM1 is responsible for intracellular transport mediated by the nuclear export signal. Nature 390:308-11.

Galfre G, Milstein C (1981). Preparation of monoclonal antibodies: strategies and procedures. Method Enzymol 73:3-46.

Georgatos SD, Maroulakou I, Blobel G (1989). Lamin A, lamin B, and lamin B receptor analogues in yeast. J Cell Biol 108:2069-2082.

Gerace L, Blobel G (1980). The nuclear envelope lamina is reversibly depolymerized during mitosis. Cell 19:277-87.

Gerace L, Blum A, Blobel G (1978). Immunocytochemical localization of the major polypeptides of the nuclear pore complex-lamina fraction. Interphase and mitotic distribution. J Cell Biol 79:546-66.

Goh PY, Kilmartin JV (1993). *NDC10*: a gene involved in chromosome segregation in *Saccharomyces cerevisiae*. J Cell Biol 121:503-12.

Goldberg M, Jenkins H, Allen T, Whitfield WG, Hutchison CJ (1995). *Xenopus* lamin B3 has a direct role in the assembly of a replication competent nucleus: evidence from cell-free egg extracts. J Cell Sci 108:3451-61.

Goldberg MW, Allen TD (1992). High resolution scanning electron microscopy of the nuclear envelope: demonstration of a new, regular, fibrous lattice attached to the baskets of the nucleoplasmic face of the nuclear pores. J Cell Biol 119:1429-40.

Goldberg MW, Allen TD (1996). The nuclear pore complex and lamina: three-dimensional structures and interactions determined by field emission in-lens scanning electron microscopy. J Mol Biol 257:848-65.

Goldberg MW, Wiese C, Allen TD, Wilson KL (1997). Dimples, pores, star-rings, and thin rings on growing nuclear envelopes: evidence for structural intermediates in nuclear pore complex assembly. J Cell Sci 110:409-20.

Goldfarb DS (1997). Whose finger is on the switch? Science 276:1814-6.

Goldstein AL, Snay CA, Heath CV, Cole CN (1996). Pleiotropic nuclear defects associated with a conditional allele of the novel nucleoporin *Rat9p/Nup85p*. Mol Biol Cell 7:917-34.

Gorlich D, Prehn S, Laskey RA, Hartmann E (1994). Isolation of a protein that is essential for the first step of nuclear protein import. Cell 79:767-778.

Gorlich D, Vogel F, Mills AD, Hartmann E, Laskey RA (1995). Distinct functions for the two importin subunits in nuclear protein import. Nature 377:246-8.

Gorsch LC, Dockendorff TC, Cole CN (1995). A conditional allele of the novel repeat-containing yeast nucleoporin RAT7/NUP159 causes both rapid cessation of mRNA export and reversible clustering of nuclear pore complexes. J Cell Biol 129:939-55.

Grandi P, Dang T, Pane N, Shevchenko A, Mann M, Forbes D, Hurt E (1997). Nup93, a vertebrate homologue of yeast Nic96p, forms a complex with a novel 205-kDa protein and is required for correct nuclear pore assembly. Mol Biol Cell 8:2017-38.

Grandi P, Doye V, Hurt EC (1993). Purification of NSP1 reveals complex formation with 'GLFG' nucleoporins and a novel nuclear pore protein NIC96. Embo J 12:3061-71.

Grandi P, Emig S, Weise C, Hucho F, Pohl T, Hurt EC (1995). A novel nuclear pore protein Nup82p which specifically binds to a fraction of Nsp1p. J Cell Biol 130:1263-73.

Grandi P, Schlaich N, Tekotte H, Hurt EC (1995). Functional interaction of Nic96p with a core nucleoporin complex consisting of Nsp1p, Nup49p and a novel protein Nup57p. Embo J 14:76-87.

Greco A, Pierotti MA, Bongarzone I, Pagliardini S, Lanzi C, Della Porta G (1992). TRK-T1 is a novel oncogene formed by the fusion of TPR and TRK genes in human papillary thyroid carcinomas. Oncogene 7:237-42.

Guan T, Muller S, Klier G, Pante N, Blevitt JM, Haner M, Paschal B, Aebi U, Gerace L (1995). Structural analysis of the p62 complex, an assembly of O-linked glycoproteins that localizes near the central gated channel of the nuclear pore complex. Mol Biol Cell 6:1591-603.

Guddat U, Bakken AH, Pieler T (1990). Protein-mediated nuclear export of RNA: 5S rRNA containing small RNPs in *Xenopus* oocytes. Cell 60:619-28.

Hansen W, Garcia PD, Walter P (1986). In vitro protein translocation across the yeast endoplasmic reticulum: ATP-dependent post-translational translocation of the prepro-α-factor. Cell 45:397-406.

Hardwick KG, Pelham RB (1992). *SED5* encodes a 39-kD integral membrane protein required for vesicular transport between the ER and the Golgi complex. J Cell Biol 119:513-521.

He DC, Nickerson JA, Penman S (1990). Core filaments of the nuclear matrix. J Cell Biol 110:569-80.

Heath CV, Copeland CS, Amberg DC, Del Priore V, Snyder M, Cole CN (1995). Nuclear pore complex clustering and nuclear accumulation of poly(A)+ RNA associated with mutation of the *Saccharomyces cerevisiae RAT2/NUP120* gene. J Cell Biol 131:1677-97.

Henriquez R, Blobel G, Aris JP (1990). Isolation and sequencing of NOP1. A yeast gene encoding a nucleolar protein homologous to a human autoimmune antigen. J Biol Chem 265:2209-15.

Henry M, Borland CZ, Bossie M, Silver PA (1996). Potential RNA binding proteins in *Saccharomyces cerevisiae* identified as suppressors of temperature-sensitive mutations in *NPL3*. Genetics 142:103-15.

Higgins D., Thompson J., T. G (1994). CLUSTAL W: improving the sensitivity of progressive multiple sequence alignment through sequence weighting, position-specific gap penalties and weight matrix choice. Nucleic Acids Res 22:4673-4680.

Hinshaw JE, Carragher BO, Milligan RA (1992). Architecture and design of the nuclear pore complex. Cell 69:1133-41.

Hoffman CS, Winston F (1987). A ten-minute DNA preparation from yeast efficiently releases autonomous plasmids for transformation of *Escherichia coli*. Gene 57:267-72.

Holm C (1982). Clonal lethality caused by the yeast plasmid 2 mu DNA. Cell 29:585-94.

Holt GD, Snow CM, Senior A, Haltiwanger RS, Gerace L, Hart GW (1987). Nuclear pore complex glycoproteins contain cytoplasmically disposed O-linked N-acetylglucosamine. J Cell Biol 104:1157-64.

Hu T, Guan T, Gerace L (1996). Molecular and functional characterization of the p62 complex, an assembly of nuclear pore complex glycoproteins. J Cell Biol 134:589-601.

Hurt EC (1988). A novel nucleoskeletal-like protein located at the nuclear periphery is required for the life cycle of *Saccharomyces cerevisiae*. Embo J 7:4323-34.

Hurwitz ME (1997). Nup82p, an Essential Yeast Nucleoporin on the Cytoplasmic Face of the Nuclear Pore Complex, is Required for poly(A)+ RNA export. Doctoral Thesis, The Rockefeller University, New York, NY.

Imamoto N, Shimamoto T, Takao T, Tachibana T, Kose S, Matsubae M, Sekimoto T, Shimonishi Y, Yoneda Y (1995). In vivo evidence for involvement of a 58 kDa component of nuclear pore- targeting complex in nuclear protein import. Embo J 14:3617-26.

Imamoto N, Tachibana T, Matsubae M, Yoneda Y (1995). A karyophilic protein forms a stable complex with cytoplasmic components prior to nuclear pore binding. J Biol Chem 270:8559-65.

Irniger S, Piatti S, Michaelis C, Nasmyth K (1995). Genes involved in sister chromatid separation are needed for B-type cyclin proteolysis in budding yeast. Cell 81:269-78.

Izaurralde E, Jarmolowski A, Beisel C, Mattaj IW, Dreyfuss G, Fischer U (1997). A role for the M9 transport signal of hnRNP A1 in mRNA nuclear export. J Cell Biol 137:27-35.

Izaurralde E, Lewis J, Gamberi C, Jarmolowski A, McGuigan C, Mattaj IW (1995). A cap-binding protein complex mediating U snRNA export. Nature 376:709-12.

Izaurralde E, Stepinski J, Darzynkiewicz E, Mattaj IW (1992). A cap binding protein that may mediate nuclear export of RNA polymerase II-transcribed RNAs. J Cell Biol 118:1287-95.

Jackson DA, Cook PR (1988). Visualization of a filamentous nucleoskeleton with a 23 nm axial repeat. Embo J 7:3667-77.

Jarmolowski A, Boelens WC, Izaurralde E, Mattaj IW (1994). Nuclear export of different classes of RNA is mediated by specific factors. J Cell Biol 124:627-35.

Jarnik M, Aebi U (1991). Toward a more complete 3-D structure of the nuclear pore complex. J Struct Biol 107:291-308.

Kadowaki T, Chen S, Hitomi M, Jacobs E, Kumagai C, Liang S, Schneiter R, Singleton D, Wisniewska J, Tartakoff AM (1994). Isolation and characterization of *Saccharomyces cerevisiae* mRNA transport-defective (mtr) mutants [published erratum appears in J Cell Biol 1994 Sep;126(6):1627]. J Cell Biol 126:649-59.

Kalland KH, Szilvay AM, Brokstad KA, Saetrevik W, Haukenes G (1994). The human immunodeficiency virus type 1 Rev protein shuttles between the cytoplasm and nuclear compartments. Mol Cell Biol 14:7436-44.

Kartenbeck J, Zentgraf H, Scheer U, Franke WW (1971). The nuclear envelope in freeze-etching. Ergeb Anat Entwicklungsgesch 45:3-55.

Kenna MA, Petranka JG, Reilly JL, Davis LI (1996). Yeast Nle3p/Nup170p is required for normal stoichiometry of FG nucleoporins within the nuclear pore complex. Mol Cell Biol 16:2025-36.

Kilmartin JV (1994). Genetic and biochemical approaches to spindle function and chromosome segregation in eukaryotic microorganisms. Curr Opin Cell Biol 6:50-54.

Kilmartin JV, Adams AE (1984). Structural rearrangements of tubulin and actin during the cell cycle of the yeast *Saccharomyces*. J Cell Biol 98:922-33.

Kilmartin JV, Dyos SL, Kershaw D, Finch JT (1993). A spacer protein in the *Saccharomyces cerevisiae* spindle poly body whose transcript is cell cycle-regulated. J Cell Biol 123:1175-84.

Kilmartin JV, Fogg J (1982). Partial purification of yeast spindle pole bodies. In: Microtubules and Microorganisms (P Cappucinelli , NR Morris, eds.), pp. 157-170. New York: Marcel Dekker Inc.

Kilmartin JV, Goh PY (1996). Spc110p: assembly properties and role in the connection of nuclear microtubules to the yeast spindle pole body. Embo J 15:4592-602.

Kiseleva E, Goldberg M, Allen T, Akey C (1998). Active nuclear pore complexes in *Chironomus*: visualization of transporter configurations related to mRNP export. J Cell Sci 111:223-36.

Kiseleva E, Goldberg MW, Daneholt B, Allen TD (1996). RNP export is mediated by structural reorganization of the nuclear pore basket. J Mol Biol 260:304-11.

Klein F, Laroche T, Cardenas ME, Hofmann JF, Schweizer D, Gasser SM (1992). Localization of RAP1 and topoisomerase II in nuclei and meiotic chromosomes of yeast. J Cell Biol 117:935-948.

Kolling R, Nguyen T, Chen EY, Botstein D (1993). A New Yeast Gene with a Myosin-Like Heptad Repeat Structure. Mol Gen Genet 237:359-369.

Kraemer D, Wozniak RW, Blobel G, Radu A (1994). The human CAN protein, a putative oncogene product associated with myeloid leukemogenesis, is a nuclear pore complex protein that faces the cytoplasm. Proc Natl Acad Sci U S A 91:1519-23.

Kraemer DM, Strambio-de-Castillia C, Blobel G, Rout MP (1995). The essential yeast nucleoporin NUP159 is located on the cytoplasmic side of the nuclear pore complex and serves in karyopherin-mediated binding of transport substrate. J Biol Chem In press.

Kudo N, Khochbin S, Nishi K, Kitano K, Yanagida M, Yoshida M, Horinouchi S (1997). Molecular cloning and cell cycle-dependent expression of mammalian CRM1, a protein involved in nuclear export of proteins. J Biol Chem 272:29742-51.

Kutay U, Bischoff FR, Kostka S, Kraft R, Gorlich D (1997). Export of importin alpha from the nucleus is mediated by a specific nuclear transport factor [see comments]. Cell 90:1061-71.

Latterich M, Schekman R (1994). The karyogamy gene *KAR2* and novel proteins are required for ER-membrane fusion. Cell 78:87-98.

Lee A, Tam R, Belhumeur P, DiPaolo T, Clark MW (1993). Prp20, the *Saccharomyces cerevisiae* homologue of the regulator of chromosome condensation, RCC1, interacts with double-stranded DNA through a multi-component complex containing GTP-binding proteins. J Cell Sci 106:287-98.

Lee MS, Henry M, Silver PA (1996). A protein that shuttles between the nucleus and the cytoplasm is an important mediator of RNA export. Genes Dev 10:1233-46.

Li O, Heath CV, Amberg DC, Dockendorff TC, Copeland CS, Snyder M, Cole CN (1995). Mutation or deletion of the *Saccharomyces cerevisiae* *RAT3/NUP133* gene causes temperature-dependent nuclear accumulation

of poly(A)+ RNA and constitutive clustering of nuclear pore complexes. Molecular Biology of the Cell 6:401-417.

Loeb JDJ, Davis LI, Fink GR (1993). NUP2, a novel yeast nucleoporin, has functional overlap with other proteins of the nuclear pore complex. Mol Biol Cell 4:209-222.

Loeb JDJ, Schlenstedt G, Pellman D, Kornitzer D, Silver PA, Fink GR (1995). The yeast nuclear import receptor is required for mitosis. Proc Natl Acad Sci USA 92:7647-7651.

Lupas AD, Van Dyke M, Stock J (1991). Predicting Coiled Coils from Protein Sequences. Science 252:1162-1164.

Macaulay C, Forbes DJ (1996). Assembly of the nuclear pore: biochemically distinct steps revealed with NEM, GTP gamma S, and BAPTA. J Cell Biol 132:5-20.

Macaulay C, Meier E, Forbes DJ (1995). Differential mitotic phosphorylation of proteins of the nuclear pore complex. J Biol Chem 270:254-62.

Mahajan R, Delphin C, Guan T, Gerace L, Melchior F (1997). A small ubiquitin-related polypeptide involved in targeting RanGAP1 to nuclear pore complex protein RanBP2. Cell 88:97-107.

Mahajan R, Gerace L, Melchior F (1998). Molecular characterization of the SUMO-1 modification of RanGAP1 and its role in nuclear envelope association. J Cell Biol 140:259-70.

Mann K, Mecke D (1982). The isolation of *Saccharomyces cerevisiae* nuclear membranes with nuclease and high-salt treatment. Biochim Biophys Acta 687:57-62.

Mann K, Mecke D (1982). The Triton X-100 and high salt resistant residue of *Saccharomyces cerevisiae* nuclear membranes. Biosciences 37:916-920.

Marschall LG, Stearns T (1997). Cytoskeleton: anatomy of an organizing center. Curr Biol 7:R754-6.

Marshall ICB, Wilson KL (1997). Nuclear Envelope Assembly After Mitosis. Trends Cell Bio 7:69-74.

Masuda H (1994). The formation and functioning of the yeast mitotic spindles. BioEssays 17:45-51.

Masuda H, Sevick M, Cande WZ (1992). *In vitro* microtubule-nucleating activity of spindle pole bodies in fission yeast *Schizosaccharomyces pombe*: Cell cycle dependent activation in *Xenopus* cell-free extracts. J Cell Biol 117:1055-1066.

Matunis MJ, Coutavas E, Blobel G (1996). A novel ubiquitin-like modification modulates the partitioning of the Ran-GTPase-activating protein RanGAP1 between the cytosol and the nuclear pore complex. J Cell Biol 135:1457-70.

Matunis MJ, Wu J, Blobel G (1998). SUMO-1 modification and its role in targeting the ran GTPase-activating protein, RanGAP1, to the nuclear pore complex. J Cell Biol 140:499-509.

McKeon F (1991). Nuclear lamin proteins: domains required for nuclear targeting, assembly, and cell-cycle-regulated dynamics. Curr Opin Cell Biol 3:82-6.

Meier UT, Blobel G (1992). Nopp140 shuttles on tracks between nucleolus and cytoplasm. Cell 70:127-38.

Meier UT, Blobel G (1994). NAP57, a mammalian nucleolar protein with a putative homologue in yeast and bacteria. J Cell Biol 127:1505-14.

Melchior F, Guan T, Yokoyama N, Nishimoto T. Gerace L (1995). GTP hydrolysis by Ran occurs at the nuclear pore complex in an early step of protein import. J Cell Biol 131:571-81.

Melchior F, Paschal B, Evans J, Gerace L (1993). Inhibition of nuclear protein import by nonhydrolyzable analogues of GTP and identification of the small GTPase Ran/TC4 as an essential transport factor. J Cell Biol 123:1649-1659.

Meyer BE, Malim MH (1994). The HIV-1 Rev trans-activator shuttles between the nucleus and the cytoplasm. Genes Dev 8:1538-47.

Michael WM, Choi M, Dreyfuss G (1995). A nuclear export signal in hnRNP A1: a signal-mediated, temperature- dependent nuclear protein export pathway. Cell 83:415-22.

Mirzayan C, Copeland CS, Snyder M (1992). The *NUF1* gene encodes an essential coiled-coil related protein that is a potential component of the yeast nucleoskeleton. J Cell Biol 116:1319-32.

Mitchell PJ, Cooper CS (1992). The Human *tpr* Gene Encodes a Protein of 2094 Amino Acids That Has Extensive Coiled-coil Regions and an Acidic C-terminal Domain. Oncogene 7:1319-1332.

Moir RD, Spann TP, Goldman RD (1995). The dynamic properties and possible functions of nuclear lamins. Int Rev Cytol 162B:141-82.

Monneron A, Bernhard W (1969). Fine structural organization of the interphase nucleus in some mammalian cells. J Ultrastruct Res 27:266-88.

Moore MS, Blobel G (1992). The two steps of nuclear import, targeting to the nuclear envelope and translocation through the nuclear pore, require different cytosolic factors. Cell 69:939-950.

Moore MS, Blobel G (1993). The GTP-binding protein Ran/TC4 is required for protein import into the nucleus. Nature 365:661-663.

Moore MS, Blobel G (1994). Purification of a Ran-interacting protein that is required for protein import into the nucleus. Proc Natl Acad Sci USA 91:10212-10216.

Mori K, Ma W, Gething M-J, Sambrook J (1993). A transmembrane protein with a *cdc2+/CDC28*-related kinase activity is required for signalling from the ER to the nucleus. Cell 74:743-756.

Moroianu J, Blobel G, Radu A (1995). Previously identified protein of uncertain function is karyopherin alpha and together with karyopherin beta docks import substrate at nuclear pore complexes. Proc Natl Acad Sci U S A 92:2008-11.

Moroianu J, Blobel G, Radu A (1997). RanGTP-mediated nuclear export of karyopherin alpha involves its interaction with the nucleoporin Nup153. Proc Natl Acad Sci U S A 94:9699-704.

Moroianu J, Hijikata M, Blobel G, Radu A (1995). Mammalian karyopherin alpha 1 beta and alpha 2 beta heterodimers: alpha 1 or alpha 2 subunit binds nuclear localization signal and beta subunit interacts with peptide repeat-containing nucleoporins. Proc Natl Acad Sci U S A 92:6532-6.

Mortimer RK, Johnson JR (1986). Genealogy of principal strains of the yeast genetic stock center. Genetics 113:35-43.

Murphy R, Watkins JL, Wente SR (1996). *GLE2*, a *Saccharomyces cerevisiae* homologue of the *Schizosaccharomyces pombe* export factor *RAE1*, is required for nuclear pore complex structure and function. Mol Biol Cell 7:1921-37.

Mutvei A, Dihlmann S, Herth W, Hurt EC (1992). NSP1 depletion in yeast affects nuclear pore formation and nuclear accumulation. Eur J Cell Biol 59:280-295.

Napier RM, Fowke LC, Hawes C, Lewis M, Pelham HR (1992). Immunological evidence that plants use both HDEL and KDEL for targeting proteins to the endoplasmic reticulum. J Cell Sci 102:261-271.

Nash RE, Puvion E, Bernhard W (1975). Perichromatin fibrils as components of rapidly labeled extranucleolar RNA. J Ultrastruct Res 53:395-405.

Nehrbass U, Blobel G (1996). Role of the nuclear transport factor p10 in nuclear import. Science 272:120-2.

Nehrbass U, Fabre E, Dihlmann S, Herth W, Hurt EC (1993). Analysis of nucleo-cytoplasmic transport in a thermosensitive mutant of nuclear pore protein NSP1. Eur J Cell Biol 62:1-12.

Nehrbass U, Kern H, Mutvei A, Horstmann H, Marshallsay B, Hurt EC (1990). NSP1: a yeast nuclear envelope protein localized at the nuclear pores exerts its essential function by its carboxy-terminal domain. Cell 61:979-989.

Nehrbass U, Rout MP, Maguire S, Blobel G, Wozniak RW (1996). The yeast nucleoporin Nup188p interacts genetically and physically with the core structures of the nuclear pore complex. J Cell Biol 133:1153-62.

Neville M, Stutz F, Lee L, Davis LI, Rosbash M (1997). The importin-beta family member Crm1p bridges the interaction between Rev and the nuclear pore complex during nuclear export. Curr Biol 7:767-75.

Newmeyer DD, Forbes DJ (1988). Nuclear import can be separated into distinct steps in vitro: nuclear pore binding and translocation. Cell 52:641-53.

Newmeyer DD, Forbes DJ (1990). An N-ethylmaleimide-sensitive cytosolic factor necessary for nuclear protein import: requirement in signal-mediated binding to the nuclear pore. J Cell Biol 110:547-57.

Newport J, Spann T (1987). Disassembly of the nucleus in mitotic extracts: membrane vesicularization, lamin disassembly, and chromosome condensation are independent processes. Cell 48:219-30.

Nickerson JA, Blencowe BJ, Penman S (1995). The architectural organization of nuclear metabolism. Int Rev Cytol 162A:67-123.

Nickerson JA, Krockmalnic G, He DC, Penman S (1990). Immunolocalization in three dimensions: immunogold staining of cytoskeletal and nuclear matrix proteins in resinless electron microscopy sections. Proc Natl Acad Sci U S A 87:2259-63.

Nigg EA (1993). Targets of cyclin-dependent protein kinases. Curr Opin Cell Biol 5:187-93.

Noguchi E, Hayashi N, Nakashima N, Nishimoto T (1997). Yrb2p, a Nup2p-related yeast protein, has a functional overlap with Rna1p, a yeast Ran-GTPase-activating protein. Mol Cell Biol 17:2235-46.

Normington K, Kohno K, Kozutsumi Y, Gething M-J, Sambrook J (1989). *S. cerevisiae* encodes an essential protein homologous in sequence and function to mammalian Bip. Cell 57:1223-1236.

Ohtsubo M, Kai R, Furuno N, Sekiguchi T, Sekiguchi M, Hayashida H, Kuma K, Miyata T, Fukushige S, Murotsu T, et al. (1987). Isolation and characterization of the active cDNA of the human cell cycle gene (RCC1) involved in the regulation of onset of chromosome condensation. Genes Dev 1:585-93.

Ohtsubo M, Okazaki H, Nishimoto T (1989). The RCC1 protein, a regulator for the onset of chromosome condensation locates in the nucleus and binds to DNA. J Cell Biol 109:1389-97.

Olson MV, Dutchik JE, Graham MY, Brodeur GM, Helms C, Frank M, MacCollin M, Scheinman R, Frank T (1986). Random-clone strategy for genomic restriction mapping in yeast. Proc Natl Acad Sci U S A 83:7826-30.

Ossareh-Nazari B, Bachelerie F, Dargemont C (1997). Evidence for a role of CRM1 in signal-mediated nuclear protein export. Science 278:141-4.

Pain D, Murakami H, Blobel G (1990). Identification of a receptor for protein import into mitochondria. Nature 347:444-449.

Palladino F, Laroche T, Gilson E, Axelrod A, Pillus L, Gasser SM (1993). *SIR3* and *SIR4* proteins are required for the positioning and integrity of yeast telomeres. Cell 75:543-555.

Park M, Dean M, Cooper CS, Schmidt M, O'Brien SJ, Blair DG, Vande-Woude GF (1986). Mechanism of met oncogene activation. Cell 45:895-904.

Parson WR, Lipman DJ (1988). Improved Tools for Biological Sequence Comparison. Proc Natl Acad Sci USA 85:2444-2448.

Paschal BM, Gerace L (1995). Identification of NTF2, a cytosolic factor for nuclear import that interacts with nuclear pore complex protein p62. J Cell Biol 129:925-37.

Paschal BM, Gerace L (1995). Identification of NTF2, a cytosolic factor for nuclear import that interacts with nuclear pore complex protein p62. J Cell Biol 129:925-37.

Pemberton LF, Rosenblum JS, Blobel G (1997). A distinct and parallel pathway for the nuclear import of an mRNA- binding protein. J Cell Biol 139:1645-53.

Pemberton LF, Rout MP, Blobel G (1995). Disruption of the nucleoporin gene NUP133 results in clustering of nuclear pore complexes. Proc Natl Acad Sci USA 92:1187-91.

Percipalle P, Clarkson WD, Kent HM, Rhodes D, Stewart M (1997). Molecular interactions between the importin alpha/beta heterodimer and proteins involved in vertebrate nuclear protein import. J Mol Biol 266:722-32.

Peter M, Nakagawa J, Doree M, Labbe JC, Nigg EA (1990). In vitro disassembly of the nuclear lamina and M phase-specific phosphorylation of lamins by cdc2 kinase. Cell 61:591-602.

Pfaller R, Newport JW (1995). Assembly/disassembly of the nuclear envelope membrane. Characterization of the membrane-chromatin interaction using partially purified regulatory enzymes. J Biol Chem 270:19066-72.

Pinol-Roma S, Dreyfuss G (1992). Shuttling of pre-mRNA binding proteins between nucleus and cytoplasm. Nature 355:730-2.

Pokrywka NJ, Goldfarb DS (1995). Nuclear export pathways of tRNA and 40 S ribosomes include both common and specific intermediates. J Biol Chem 270:3619-24.

Pollard VW, Michael WM, Nakielny S, Siomi MC, Wang F, Dreyfuss G (1996). A novel receptor-mediated nuclear protein import pathway. Cell 86:985-94.

Preuss D, Mulholland J, Kaiser CA, Orlean P, Albright C, Rose MD, Robbins PW, Botstein D (1991). Structure of the yeast endoplasmic reticulum: localization of ER proteins using immunofluorescence and immunoelectron microscopy. Yeast 7:891-911.

Radu A, Blobel G, Moore MS (1995). Identification of a protein complex that is required for nuclear protein import and mediates docking of import substrate to distinct nucleoporins. Proc Natl Acad Sci U S A 92:1769-73.

Radu A, Blobel G, Wozniak RW (1994). Nup107 is a novel nuclear pore complex protein that contains a leucine zipper. J Biol Chem 269:17600-5.

Radu A, Moore MS, Blobel G (1995). The peptide repeat domain of nucleoporin Nup98 functions as a docking site in transport across the nuclear pore complex. Cell 81:215-22.

Reichelt R, Holzenburg A, Buhle EL, Jr., Jarnik M, Engel A, Aebi U (1990). Correlation between structure and mass distribution of the nuclear pore complex and of distinct pore complex components. J Cell Biol 110:883-94.

Rexach M, Blobel G (1995). Protein import into nuclei: association and dissociation reactions involving transport substrate, transport factors, and nucleoporins. Cell 83:683-92.

Rexach MF, Latterich M, Scheckman RW (1994). Characteristics of Endoplasmic Reticulum-derived transport vesicles. J Cell Biol 126:1133-1148.

Richards SA, Carey KL, Macara IG (1997). Requirement of guanosine triphosphate-bound ran for signal-mediated nuclear protein export [see comments]. Science 276:1842-4.

Richardson WD, Mills AD, Dilworth SM, Laskey RA, Dingwall C (1988). Nuclear protein migration involves two steps: rapid binding at the nuclear envelope followed by slower translocation through nuclear pores. Cell 52:655-64.

Ris H (1989). Three-dimensional Imaging of Cell Ultrastructure with High Resolution Low Voltage SEM. Inst Phys Conf Ser 98:657-662.

Ris H (1991). The Three Dimensional Structure of the Nuclear Pore Complexes as Seen by High Voltage Electron Microscopy and High Resolution Low Voltage Scanning Electron Microscopy. EMSA Bull 21:54-56.

Ris H (1997). High-resolution field-emission scanning electron microscopy of nuclear pore complex. Scanning 19:368-75.

Ris H, Malecki M (1993). High-resolution field emission scanning electron microscope imaging of internal cell structures after Epon extraction from sections: a new approach to correlative ultrastructural and immunocytochemical studies. J Struct Biol 111:148-57.

Robinow CF, Marak J (1966). A fiber apparatus in the nucleus of yeast cells. J Cell Biol 29:129-151.

Rose MD, Misra LM, Vogel JP (1989). *KAR2*, a karyogamy gene, is the yeast homologue of the mammalian BiP/*GRP78* gene. Cell 57:1211-1221.

Rosenblum JS, Pemberton LF, Blobel G (1997). A nuclear import pathway for a protein involved in tRNA maturation. J Cell Biol 139:1655-61.

Rothblatt JA, Deshaies RJ, Sanders SL, Daum G, Schekman R (1989). Multiple genes are required for proper insertion of secretory proteins into the endoplasmic reticulum in yeast. J Cell Biol 109:2641-2652.

Rothblatt JA, Meyer DI (1986). Secretion in yeast: reconstitution of the translocation and glycosylation of α-factor and invertase in a homologous cell-free system. Cell 44:619-628.

Rothstein R (1990). Targeting, Disruption, Replacement and Allele Rescue: Integrative Transformation in Yeast. Methods Enzymol 194:281-301.

Rout MP, Blobel G (1993). Isolation of the nuclear pore complex. J Cell Biol 123:771-783.

Rout MP, Blobel G, Aitchison JD (1997). A distinct nuclear import pathway used by ribosomal proteins. Cell 89:715-25.

Rout MP, Kilmartin JV (1990). Components of the yeast spindle and spindle pole body. J Cell Biol 111:1913-1927.

Rout MP, Kilmartin JV (1991). Yeast spindle pole body components. In: Cold Spring Harbor Symposia on Quantitative Biology Vol. 56, pp. 687-692. Cold Spring Harbor, New York: Cold Spring Harbor Laboratory Press.

Rout MP, Kilmartin JV (1994). Preparation of yeast spindle pole bodies. In: Cell Biology: A Laboratory Handbook Vol. 1 (JE Celis, eds.), pp. 605-612. London: Academic Press.

Rout MP, Strambio-de-Castillia C (1998). Isolation of Yeast Nuclear Pore Complexes and Nuclear Envelopes. In: Cell Biology: A Laboratory Handbook Vol. 2 (JE Celis, eds.), pp. 143-151. London: Academic Press.

Rout MP, Wente SR (1994). Pores for thought: nuclear pore complex proteins. Trends Cell Biol 4:357-365.

Schlaich NL, Haner M, Lustig A, Aebi U, Hurt EC (1997). In vitro reconstitution of a heterotrimeric nucleoporin complex consisting of recombinant Nsp1p, Nup49p, and Nup57p. Mol Biol Cell 8:33-46.

Schlenstedt G, Wong DH, Koepp DM, Silver PA (1995). Mutants in a yeast Ran binding protein are defective in nuclear transport. Embo J 14:5367-78.

Schmidt-Zachmann MS, Dargemont C, Kuhn LC, Nigg EA (1993). Nuclear export of proteins: the role of nuclear retention. Cell 74:493-504.

Senior A, Gerace L (1988). Integral membrane proteins specific to the inner nuclear membrane and associated with the nuclear lamina. J Cell Biol 107:2029-2036.

Sherman F, Fink GR, Hicks JB (1986). Methods in Yeast Genetics. Cold Spring Harbor, NY: Cold Spring Harbor Press.

Shulga N, Roberts P, Gu Z, Spitz L, Tabb MM, Nomura M, Goldfarb DS (1996). In vivo nuclear transport kinetics in *Saccharomyces cerevisiae*: a role for heat shock protein 70 during targeting and translocation. J Cell Biol 135:329-39.

Simos G, Maison C, Georgatos SD (1996). Characterization of p18, a component of the lamin B receptor complex and a new integral membrane

protein of the avian erythrocyte nuclear envelope. J Biol Chem 271:12617-25.

Singleton DR, Chen S, Hitomi M, Kumagai C, Tartakoff AM (1995). A yeast protein that bidirectionally affects nucleocytoplasmic transport. J Cell Sci 108:265-72.

Siniossoglou S, Wimmer C, Rieger M, Doye V, Tekotte H, Weise C, Emig S, Segref A, Hurt EC (1996). A novel complex of nucleoporins, which includes Sec13p and a Sec13p homologue, is essential for normal nuclear pores. Cell 84:265-75.

Siomi H, Dreyfuss G (1995). A nuclear localization domain in the hnRNP A1 protein. J Cell Biol 129:551-60.

Siomi MC, Eder PS, Kataoka N, Wan L, Liu Q, Dreyfuss G (1997). Transportin-mediated nuclear import of heterogeneous nuclear RNP proteins. J Cell Biol 138:1181-92.

Smith V, Chou KN, Lashakari D, Botstein D, Brown PO (1996). Functional Analysis of the Genes of Yeast Chromosome V by Genetic Footprinting. Science 274:2069-2074.

Snyder M (1994). The spindle pole body of yeast. Chromosoma 103:369-380.

Sogaard M, Tani K, Ruby Ye R, Geromanos S, Tempst P, Kirchhausen T, Rothman JE, Sollner T (1994). A rab protein is required for the assembly of SNARE complexes in the docking transport vesicles. Cell 78:937-948.

Soman NR, Correa P, Ruiz BA, Wogan GN (1991). The TPR-MET oncogenic rearrangement is present and expressed in human gastric carcinoma and precursor lesions. Proc Natl Acad Sci U S A 88:4892-6.

Spann TP, Moir RD, Goldman AE, Stick R, Goldman RD (1997). Disruption of nuclear lamin organization alters the distribution of replication factors and inhibits DNA synthesis. J Cell Biol 136:1201-12.

Stade K, Ford CS, Guthrie C, Weis K (1997). Exportin 1 (Crm1p) is an essential nuclear export factor. Cell 90:1041-50.

Staufenbiel M, Deppert W (1984). Preparation of nuclear matrices from cultured cells: subfractionation of nuclei in situ. J Cell Biol 98:1886-94.

Stevens BJ, Swift H (1966). RNA transport from nucleus to cytoplasm in Chironomus salivary glands. J Cell Biol 31:55-77.

Stirling CJ, Rothblatt J, Hosobuchi M, Deshaies R, Schekman R (1992). Protein translocation mutants defective in the insertion of integral membrane proteins into the endoplasmic reticulum. Mol Biol Cell 3:129-142.

Strambio-de-Castillia C, Blobel G, Rout MP (1995). Isolation and Characterization of Nuclear Envelopes from the Yeast *Saccharomyces*. J Cell Biol 131:19-31.

Stutz F, Izaurralde E, Mattaj IW, Rosbash M (1996). A role for nucleoporin FG repeat domains in export of human immunodeficiency virus type 1 Rev protein and RNA from the nucleus. Mol Cell Biol 16:7144-50.

Stutz F, Neville M, Rosbash M (1995). Identification of a novel nuclear pore-associated protein as a functional target of the HIV-1 Rev protein in yeast. Cell 82:495-506.

Sukegawa J, Blobel G (1993). A nuclear pore complex protein that contains zinc finger motifs, binds DNA, and faces the nucleoplasm. Cell 72:29-38.

Sutter TR, Loper JC (1989). Disruption of the *Saccharomyces cerevisiae* gene for NADPH-cytochrome P450 reductase causes increased sensitivity to ketoconazole. Biochem Biophys Res Commun 160:1257-1266.

Szilvay AM, Brokstad KA, Kopperud R, Haukenes G, Kalland KH (1995). Nuclear export of the human immunodeficiency virus type 1 nucleocytoplasmic shuttle protein Rev is mediated by its activation domain and is blocked by transdominant negative mutants. J Virol 69:3315-23.

Tachibana T, Imamoto N, Seino H, Nishimoto T, Yoneda Y (1994). Loss of RCC1 leads to suppression of nuclear protein import in living cells. J Biol Chem 269:24542-5.

Taura T, Schlenstedt G, Silver PA (1997). Yrb2p is a nuclear protein that interacts with Prp20p, a yeast RCC1 homologue. J Biol Chem 272:31877-84.

Terns MP, Dahlberg JE, Lund E (1993). Multiple cis-acting signals for export of pre-U1 snRNA from the nucleus. Genes Dev 7:1898-908.

Thatcher JW, Shaw JM, Dickson WJ (1998). Marginal Fitness Contributions of Nonessential Genes in Yeast. Proc Natl Acad Sci USA 95:253-257.

Thomas B, Rothstein R (1989). Elevated Recombination Rates in Transcriptionally Active DNA. Cell 56:619-630.

Unwin PN, Milligan RA (1982). A large particle associated with the perimeter of the nuclear pore complex. J Cell Biol 93:63-75.

Visa N, Izaurralde E, Ferreira J, Daneholt B, Mattaj IW (1996). A nuclear cap-binding complex binds Balbiani ring pre-mRNA cotranscriptionally and accompanies the ribonucleoprotein particle during nuclear export. J Cell Biol 133:5-14.

Waters MG, Blobel G (1986). Secretory protein translocation in a yeast cell-free system can occur postranslationally and requires ATP hydrolysis. J Cell Biol 102:1543-1550.

Waters MG, Chirico WJ, Blobel G (1986). Protein translocation across the yeast microsomal membrane is stimulated by a soluble factor. J Cell Biol 103:2629-2636.

Waters MG, Evans EA, Blobel G (1988). Prepro-α-factor has a cleavable signal sequence. J Biol Chem 263:6209-6214.

Weighardt F, Biamonti G, Riva S (1995). Nucleo-cytoplasmic distribution of human hnRNP proteins: a search for the targeting domains in hnRNP A1. J Cell Sci 108:545-55.

Wen W, Meinkoth JL, Tsien RY, Taylor SS (1995). Identification of a signal for rapid export of proteins from the nucleus. Cell 82:463-73.

Wente SR, Blobel G (1993). A temperature-sensitive *NUP116* null mutant forms a nuclear envelope seal over the yeast nuclear pore complex thereby blocking nucleocytoplasmic traffic. J Cell Biol 123:275-284.

Wente SR, Blobel G (1994). *NUP145* encodes a novel yeast glycine-leucine-phenylalanine-glycine (GLFG) nucleoporin required for nuclear envelope structure. J Cell Biol 125:955-969.

Wente SR, Gasser SM, Caplan AJ (1998). The Nucleus and Nucleocytoplasmic Transport in *Saccharomyces cerevisae*. In: The Molecular and Cellular

Biology of the Yeast *Saccharomyces* In press (JR Broach, E Jones , J Pringle, eds.), Cold Spring Harbor, NY: Cold Spring Harbor Press.

Wente SR, Rout MP, Blobel G (1992). A new family of yeast nuclear pore complex proteins. J Cell Biol 119:705-723.

Wimmer C, Doye V, Grandi P, Nehrbass U, Hurt EC (1992). A new subclass of nucleoporins that functionally interact with nuclear pore protein NSP1. Embo J 11:5051-61.

Winey M, Hoyt MA, Chan C, Goetsch L, Botstein D (1993). NDC1: a nuclear periphery component required for yeast spindle pole body duplication. J Cell Biol 122:743-751.

Winey M, Mamay CL, O'Toole ET, Mastronarde DN, Giddings TH, Jr., McDonald KL, McIntosh JR (1995). Three-dimensional ultrastructural analysis of the *Saccharomyces cerevisiae* mitotic spindle. J Cell Biol 129:1601-15.

Winey M, Yarar D, Giddings TH, Jr., Mastronarde DN (1997). Nuclear pore complex number and distribution throughout the *Saccharomyces cerevisiae* cell cycle by three-dimensional reconstruction from electron micrographs of nuclear envelopes. Mol Biol Cell 8:2119-32.

Wolfe KD, Shields DC (1997). Molecular Evidence of an Ancient Duplication Event of the Entire Yeast Genome. Nature 387:708-713.

Wootton JC (1994). Non-globular domains in protein sequences: automated segmentation using complexity measures. Comput Chem 18:269-85.

Worman HJ, Evans CD, Blbel G (1990). The lamin B receptor of the nuclear envelope inner membrane: a polytopic protein with eight potential transmembrane domains. J Cell Biol 111:1535-1542.

Worman HJ, Yuan J, Blobel G, Georgatos SD (1988). A lamin B receptor in the nuclear envelope. Proc Natl Acad Sci U S A 85:8531-4.

Wotton D, Shore D (1997). A Novel Rap1p-Interacting Factor, Rif2p, Cooperates with Rif1p to regulate telomere length in *Saccharomyces cerevisiae*. Genes Dev 11:748-760.

Wozniak RW, Blobel G, Rout MP (1994). POM152 is an integral membrane protein of the pore membrane domain of the nuclear envelope. J Cell Biol 125:31-42.

Wozniak RW, Rout MP, Aitchison JD (1998). Karyopherins and Kissing Cousins. Trends Cell Biol in press:

Wu J, Matunis MJ, Kraemer D, Blobel G, Coutavas E (1995). Nup358, a cytoplasmically exposed nucleoporin with peptide repeats, Ran- GTP binding sites, zinc fingers, a cyclophilin A homologous domain, and a leucine-rich region. J Biol Chem 270:14209-13.

Xiao Z, McGrew JT, Schroeder AJ, Fitzgerald-Hayes M (1993). *CSE1* and *CSE2*, two new genes required for accurate mitotic chromosome segregation in *Saccharomyces cerevisiae*. Mol Cell Biol 13:4691-702.

Yabusaki Y, Murakami H, Ohkawa H (1988). Primary structure of *Saccharomyces cerevisiae* NADPH-Cytochrome P450 reductase deduced form nucleotide sequence of its cloned gene. J Biochem 103:1004-1010.

Yang Q, Rout MP, Akey CW (1998). Three-dimensional Architecture of the Isolated Yeast Nuclear Pore Complex: Functional and Evolutionary Implications. Mol Cell 1:223-234.

Yano R, Oakes ML, Tabb MM, Nomura M (1994). Yeast Srp1p has homology to armadillo/plakoglobin/beta-catenin and participates in apparently multiple nuclear functions including the maintenance of the nucleolar structure. Proc Natl Acad Sci U S A 91:6880-4.

Yaseen NR, Blobel G (1997). Cloning and characterization of human karyopherin β3. Proc Natl Acad Sci U S A 94:4451-6.

Yokoyama N, Hayashi N, Seki T, Pante N, Ohba T, Nishii K, Kuma K, Hayashida T, Miyata T, Aebi U, et al. (1995). A giant nucleopore protein that binds Ran/TC4. Nature 376:184-8.

Zabel U, Doye V, Tekotte H, Wepf R, Grandi P, Hurt EC (1996). Nic96p is required for nuclear pore formation and functionally interacts with a novel nucleoporin, Nup188p. J Cell Biol 133:1141-52.

Zachar Z, Kramer J, Mims IP, Bingham PM (1993). Evidence for channeled diffusion of pre-mRNAs during nuclear RNA transport in metazoans. J Cell Biol 121:729-42.

Zasloff M (1983). tRNA transport from the nucleus in a eukaryotic cell: carrier-mediated translocation process. Proc Natl Acad Sci U S A 80:6436-40.

Zimowska G, Aris JP, Paddy MR (1997). A Drosophila Tpr protein homolog is localized both in the extrachromosomal channel network and to nuclear pore complexes. J Cell Sci 110:927-44.